AN ABSTRACT OF THE DISSERTATION OF

Christopher Kekoa Hiroshi Guay for the degree of Doctor of Philosophy in Oceanography presented on July 30, 1999. Title: Geochemical Tracers of Arctic River Waters.

Abstract approved: Redacted for privacy

Kelly Kenison Falkner

The research presented in this dissertation examines the utility of naturally occurring geochemical signals for tracing the fluvial component of Arctic Ocean circulation. The dissertation comprises separate manuscripts that have been or will be submitted for publication in peer-reviewed journals.

An extensive survey of dissolved organic carbon (DOC) in the Arctic Ocean was achieved by means of a high-resolution, *in situ* UV fluorometer deployed on a nuclear submarine. Based on a strong linear correlation observed between fluorescence (320 nm excitation, 420 nm emission) and organic carbon concentrations determined directly by high-temperature combustion, a continuous record of DOC was produced at a keel depth of 58 m along a 2900-km transect north of the Beaufort, Chukchi, East Siberian and Laptev seas. The DOC record, combined with other physical and chemical measurements, identifies areas where river waters cross the shelves and enter the circulation of the interior Arctic Ocean. Fluvial sources were found to account for 12-56% of the total DOC in parts of the upper Makarov and Amundsen basins.

Distributions of temperature, salinity and barium are presented for the upper Laptev Sea and adjacent areas of the Nansen, Amundsen and Makarov basins during the summer in 1993, 1995 and 1996. Preliminary results of q-mode factor analysis captured the

Atlantic and fluvial end-members of a mixing model proposed for the Laptev Sea. Distributions of fluvial discharge inferred from the tracer measurements are consistent with local winds and suggest two principal pathways by which river waters can enter the interior Arctic Ocean from the Laptev Sea. When southerly to southeasterly wind conditions prevail, river waters are transported northwards beyond the shelf break and over the slope and adjacent basin areas. These waters can then enter the interior Arctic Ocean via upper layer flow aligned roughly along the Lomonosov Ridge. Under other wind conditions, river waters are steered primarily along the inner Laptev shelf and into the East Siberian Sea as part of the predominantly eastward coastal current system. These waters then appear to cross the shelf and enter the interior Arctic Ocean via upper layer flow aligned roughly along the Mendeleyev Ridge.

©Copyright by Christopher Kekoa Hiroshi Guay
July 30, 1999
All Rights Reserved

Geochemical Tracers of Arctic River Waters

by

Christopher Kekoa Hiroshi Guay

A DISSERTATION

submitted to

Oregon State University

in partial fulfillment of
the requirements for the
degree of

Doctor of Philosophy

Presented July 30, 1999
Commencement June 2000

Doctor of Philosophy dissertation of Christopher Kekoa Hiroshi Guay presented on July 30, 1999

APPROVED:

Redacted for privacy

Major Professor, representing Oceanography

Redacted for privacy

Dean of College of Oceanic and Atmospheric Sciences

Redacted for privacy

Dean of Graduate School

I understand that my dissertation will become a part of the permanent collection of Oregon State University libraries. My signature below authorizes release of my dissertation to any reader upon request.

Redacted for privacy

Christopher Kekoa Hiroshi Guay, Author

ACKNOWLEDGEMENTS

I would like to thank my major professor, Dr. Kelly Kenison Falkner, for the professional opportunities, guidance and support she provided me over the course of my graduate studies. Thanks also to the other members of my committee, Dr. Robert Collier, Dr. Kathryn Higley, Dr. Robin Muench and Dr. Clayton Paulson for contributing valuable insight and advice during the preparation of this dissertation. I would also like to acknowledge Dr. Jeff Ramsey, who served as my Graduate Council Representative up through my preliminary oral examination but could not be present at my final defense due to a scheduling conflict.

I gratefully acknowledge the United States Navy, in particular Commander Steve Kremer and the crew of the *USS Archerfish*, for their cooperation and support during the SCICEX-97 cruise. I would also like to thank the following people for providing data and technical assistance: Dr. Terry Whitledge (chief scientist, chlorophyll-*a* data), Dr. Gary Klinkhammer and F. Joseph Bussell (ZAPS fluorometry), Dr. Ronald Benner and Brenda Black (high-temperature combustion DOC measurements), Dr. Paula Coble and Robyn Conmy (excitation/emission matrices), and Dr. Muench and John Gunn (CTD data).

I thank Dr. Muench, Mr. Gunn, Dr. Ursula Schauer and the Alfred Wegener Institut für Polar- und Meeresforschung for enabling me to receive water samples from the ARK IX/4, ARK XI and ARK XII cruises onboard the *R/V Polarstern*. Oxygen isotope data from these cruises were made available to me by Dr. Reinhold Bayer, Manfred Mensch, Dr. Markus Frank and Wilhelm Stein. Dr. Ruth Preller and Pam Posey provided geostrophic wind data for the Arctic between 1993 and 1997.

Thanks to Adrian Avram, Andy Ungerer and Tim Wagner for assisting me with sample analyses at the Oregon State University ICP-MS facility. I greatly benefited from additional comments and ancillary data contributed by Dr. Tim Boyd, Dr. Rob Holman, Dr. Wieslaw Maslowski, Mark Ortermeyer, Dr. Nick Pisias, Dr. Andrey Proshutinsky, Ignatius Rigor, Dr. Michael Steele and Dr. Patricia Wheeler. This research was supported by grants from the National Science Foundation Office of Polar Programs (OPP-9707459, OPP-9622603, OPP-9424334) and the Office of Naval Research (YIP N00014-93-1-0318, AASERT N00014-93-1-1093).

CONTRIBUTION OF AUTHORS

For all of the chapters included in this dissertation, I wrote the initial drafts myself and subsequently incorporated suggestions and contributions from my co-authors. Dr. Kelly Kenison Falkner thoroughly reviewed all of the chapters and aided in interpretation of the data. For Chapter 2, Dr. Gary Klinkhammer, Dr. Ronald Benner and Dr. Paula Coble reviewed the manuscript drafts and provided comments. The ZAPS fluorometry data were provided by Dr. Klinkhammer and F. Joe Bussell. Analyses for DOC by high-temperature combustion were performed by Dr. Benner and Brenda Black. Excitation-emission matrices were produced by Dr. Coble and Robyn Conmy. Dr. Terry Whitledge acted as chief scientist during the SCICEX-97 cruise and made measurements of chlorophyll-*a*. Tim Wagner assisted with the Ba analyses by ICP-MS. For Chapter 3, Dr. Robin Muench reviewed the manuscript drafts and contributed comments. Dr. Muench also assisted in collecting CTD data and water samples during the cruises onboard the *R/V Polarstern* in 1993, 1995 and 1996. Dr. Reinhold Bayer, Manfred Mensch and Dr. Markus Frank contributed oxygen isotope data from these cruises. For Chapter 4, Dr. Rob Holman and Dr. Nick Pisias reviewed the manuscript, contributed comments and advice, and provided the original computer code for the q-mode factor analysis (I significantly modified the computer routines for the specific application presented in this chapter).

TABLE OF CONTENTS

TABLE OF CONTENTS (Continued)

LIST OF FIGURES

LIST OF FIGURES (Continued)

LIST OF TABLES

LIST OF APPENDIX FIGURES

I do not wish to expiate, but to live. My life is for itself and not for a spectacle. I much prefer that it should be of a lower strain, so it be genuine and equal, than that it should be glittering and unsteady. I wish it to be sound and sweet, and not to need diet and bleeding. I ask primary evidence that you are a man, and refuse this appeal from the man to his actions. I know that for myself it makes no difference whether I do or forbear those actions which are reckoned excellent. I cannot consent to pay for a privilege where I have intrinsic right. Few and mean as my gifts may be, I actually am, and do not need for my own assurance or the assurance of my fellows any secondary testimony.

What I must do is all that concerns me, not what the people think. This rule, equally arduous in actual and in intellectual life, may serve for the whole distinction between greatness and meanness. It is the harder because you will always find those who think they know what is your duty better than you know it. It is easy in the world to live after the world's opinion; it is easy in solitude to live after our own; but the great man is he who in the midst of the crowd keeps with perfect sweetness the independence of solitude.

* * * * *

The magnetism which all original action exerts is explained when we inquire the reason of self-trust. Who is the Trustee? What is the aboriginal Self, on which a universal reliance may be grounded? What is the nature and power of that science-baffling star, without parallax, without calculable elements, which shoots a ray of beauty even into trivial and impure actions, if the least mark of independence appear? The inquiry leads us to that source, at once the essence of genius, of virtue, and of life, which we call Spontaneity or Instinct. We denote this primary wisdom as Intuition, whilst all later teachings are tuitions. In that deep force, the last fact behind which analysis cannot go, all things find their common origin. For the sense of being which in calm hours rises, we know not how, in the soul, is not diverse from things, from space, from light, from time, from man, but one with them and proceeds obviously from the same source whence their life and being also proceed. We first share the life by which things exist and afterwards see them as appearances in nature and forget that we have shared their cause. Here is the fountain of action and thought. Here are the lungs of that inspiration which giveth man wisdom and which cannot be denied without impiety and atheism. We lie in the lap of immense intelligence, which makes us receivers of its truth and organs of its activity. When we discern justice, when we discern truth, we do nothing of ourselves, but allow a passage to its beams. If we ask whence this comes, if we seek to pry into the soul that causes, all philosophy is at fault. Its presence or its absence is all we can affirm. Every man discriminates between the voluntary acts of his mind and his involuntary perceptions, and knows that to his involuntary perceptions a perfect faith is due. He may err in the expression of them, but he knows that these things are so, like day and night, not to be disputed. My willful actions and acquisitions are but roving;--the idlest reverie, the faintest native emotion, command my curiosity and respect. Thoughtless people contradict as readily the statement of perceptions as of opinions, or rather much more readily; for they do not distinguish between perception and notion. They fancy that I choose to see this or that thing. But perception is not whimsical, but fatal. If I see a trait, my children will see it after me, and in course of time all mankind,--although it may chance that no one has seen it before me. For my perception of it is as much a fact as the sun.

— Ralph Waldo Emerson
(from "Self-Reliance")

And it is a strange thing that most of the feeling we call religious, most of the mystical outcrying which is one of the most prized and used and desired reactions of our species, is really the understanding and the attempt to say that man is related to the whole thing, related inextricably to all reality, known and unknowable. This is a simple thing to say, but the profound feeling of it made a Jesus, a St. Augustine, a St. Francis, a Roger Bacon, a Charles Darwin, and an Einstein. Each of them in his own tempo and with his own voice discovered and reaffirmed with astonishment the knowledge that all things are one thing and that one thing is all things--plankton, a shimmering phosphorescence on the sea and the spinning planets and an expanding universe, all bound together by the elastic string of time. It is advisable to look from the tide pool to the stars and then back to the tide pool again.

— John Steinbeck
(from *The Log from the Sea of Cortez*)

THE HISTORY OF SCIENCE

All fables of adventure stress
The need for courtesy and kindness:
Without the Helpers none can win
The flaxen-haired Princess.

They look the ones in need of aid,
Yet, thanks to them, the gentle-hearted
Third Brother beds the woken Queen,
While seniors who made

Cantankerous replies to crones
And dogs who begged to share their rations,
Must expiate their pride as daws
Or wind-swept bachelor stones.

Few of a sequel, though, have heard:
Uneasy pedagogues have censored
All written reference to a brother
Younger than the Third.

Soft-spoken as New Moon this Fourth,
A Sun of gifts to all he met with,
But when advised 'Go South a while!',
Smiled 'Thank You!' and turned North,

Trusting some map in his own head,
So never reached the goal intended
(His map, of course, was out) but blundered
On a wonderful instead,

A tower not circular but square,
A treasure not of gold but silver:
He kissed a shorter Sleeper's hand
And stroked her raven hair.

Dare sound Authority confess
That one can err his way to riches,
Win glory by mistake, his dear
Through sheer wrong-headedness?

— W. H. Auden

Geochemical Tracers of Arctic River Waters

1. INTRODUCTION

Approximately 10% (3500 $km^3\ yr^{-1}$) of the world's fluvial discharge flows into the Arctic Ocean, which accounts for roughly 3 % of the area and 1 % of the volume of the global oceans [*Menard and Smith*, 1966; Figures 1.1 and 1.2]. The disproportionately large fluvial discharge to the Arctic Ocean strongly influences its circulation and hydrologic structure. An ability to track Arctic river waters is therefore essential to understanding Arctic Ocean circulation and its links to global climate and assessing the transport and fate of pollutants released in the Arctic. Several physical and chemical tracers, including temperature, salinity, alkalinity, ^3He, tritium, halocarbons, Si, and $\delta^{18}O$, have been applied to studying circulation in the upper Arctic Ocean and have been used to estimate ages, residence times and ventilation rates for its different water masses [*Bauch et al.*, 1995; *Jones et al.*, 1991; *Östlund and Hut*, 1984; *Schlosser et al.*, 1994; *Wallace et al.*, 1992]. Such tracers have also been used with simple linear mixing models to distinguish the fluvial component from sea-ice meltwater, Pacific, and Atlantic components of Arctic Ocean waters. None of these tracers, however, can be used to distinguish between waters from different rivers within the Arctic.

The research presented in this dissertation is part of a program to investigate the utility of naturally occurring geochemical tracers for differentiating components of fluvial discharge within the Arctic Ocean. Individual Arctic rivers have distinct aqueous geochemical signatures (reflecting the unique distributions of rock types, vegetation, climate zones and landforms in their drainage basins) that in principle can be used to distinguish them from each other. The practical application of such an approach depends on the natural variability of the inorganic signals in Arctic rivers and the extent to which they remain detectable as river waters mix with oceanic waters. The tracers must be easy

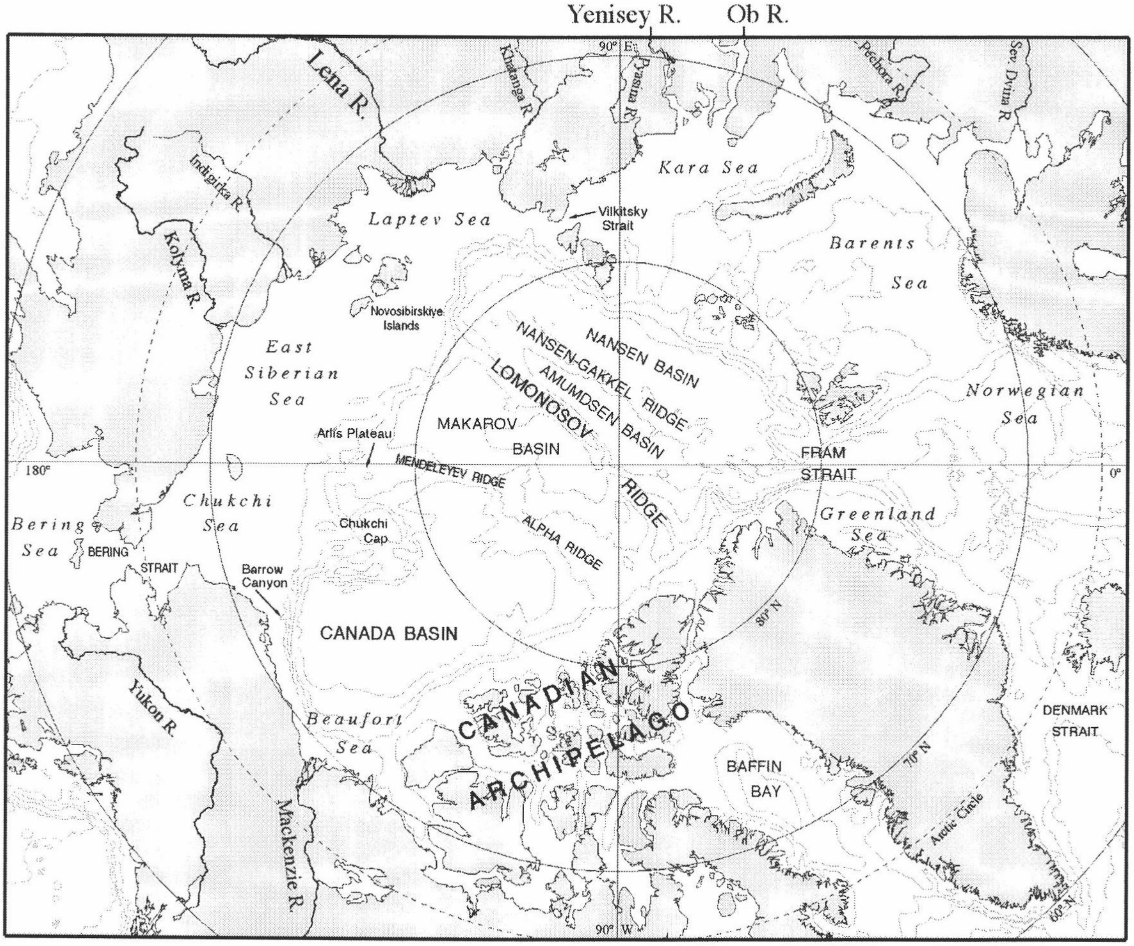

Figure 1.1 Bathymetry and major rivers of the Arctic.

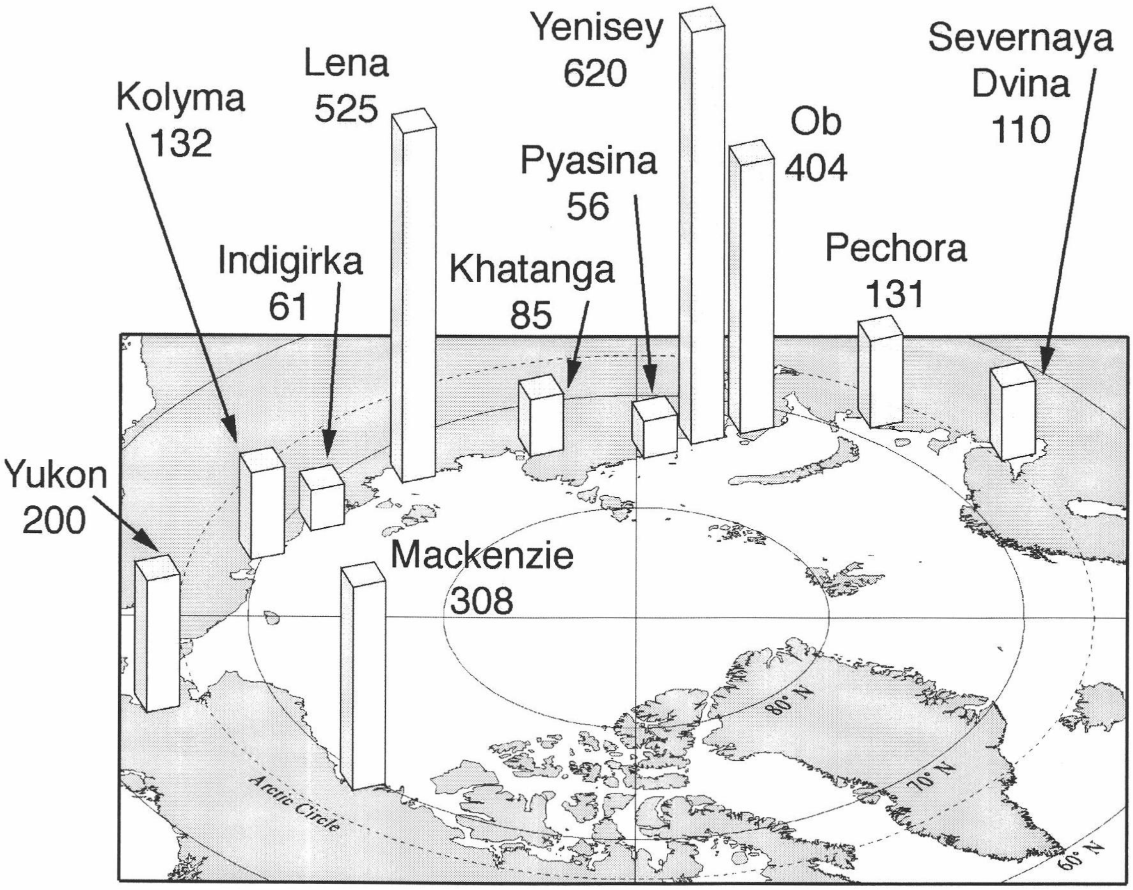

Figure 1.2 Mean annual discharge (km^3 yr^{-1}) of the ten largest rivers flowing directly into the Arctic Ocean and the Yukon River [values taken from *Meybeck and Ragu*, 1995].

enough to determine analytically so that extensive data bases can be generated that will allow mapping of circulation features. Work to date has focused on barium (Ba) and dissolved organic carbon (DOC) and their potential to serve as complementary tracers for distinguishing between contributions from North American and Eurasian rivers.

The principal external sources of Ba to the world's oceans are rivers [*Martin and Maybeck*, 1979] and hydrothermal venting at mid-ocean ridges [*Edmond et al.*, 1979; *Von Damm et al.*, 1985]; both sources tend to be elevated in Ba relative to the seawater into which they arrive. Although the extent to which hydrothermal activity occurs along the extremely slow-spreading Nansen-Gakkel Ridge and in other areas of the Arctic is not well known, most hydrothermal Ba is generally thought to precipitate inorganically as barite in the vicinity of hot spring sources [*Von Damm,* 1990]. Fluvial inputs, in contrast, tend to be enhanced in estuaries where Ba adsorbed onto riverborne clays becomes desorbed in exchange for the more abundant cations of seawater [*Carroll et al.*, 1993; *Edmond et al.*, 1978; *Hanor and Chan*, 1977; *Li and Chan*, 1979]. Complex cycling of Ba may occur in rivers and their estuaries under certain conditions, but its impact on net Ba fluxes to the ocean appears minimal [*Coffey et al.*, 1997; *Froelich et al.*, 1985; *Stecher*, 1999]. Recent work has suggested that brackish groundwater discharge also represents a significant source of Ba to coastal waters in some regions [*Moore*, 1997]. While this source should be less significant in the Arctic, where groundwater flow is limited by permafrost, it could be expected to play an increasing role in the event of rising global temperatures.

In general, Ba tends to be depleted in surface oceanic waters and enriched with depth and along advective flow lines, much like a hard-part nutrient such as alkalinity (which reflects $CaCO_3$ cycling) or Si [*Chan et al.*, 1977; *Falkner et al.*, 1993; *Lea*, 1990]. This has been attributed to uptake of Ba at the surface as the mineral barite ($BaSO_4$), which is formed in association with biological particulate matter [*Bishop*, 1988; *Collier and Edmond*, 1984; *Dehairs et al.*, 1980; *Dymond et al.*, 1992]; the exact mechanism by which

Ba is removed from surface oceanic waters remains the subject of research [e.g., *Bernstein et al.*, 1992; *Dehairs et al.*, 1987; *Fresnel et al.*, 1979]. There is clear evidence for the biologically associated removal of Ba from Arctic surface waters, particularly at the ice edge [*Falkner et al.*, 1994; *Guay and Falkner*, 1997; *Guay et al.*, 1999].

The Mackenzie River is highly elevated in Ba with respect to the other major rivers discharging directly into the Arctic [Figure 1.3; *Guay and Falkner*, 1998]. Effective riverine end-member concentrations of dissolved Ba (i.e., accounting for non-conservative behavior in the estuary; *Edmond et al.*, 1978) are 520 nmol Ba L^{-1} for the Mackenzie River and 90-150 nmol Ba L^{-1} for the major Eurasian Arctic rivers. In addition, values of [Ba] between 255 and 684 nmol Ba L^{-1} measured in the Yukon River between 1982 and 1996 indicate that the Yukon River is also elevated in Ba relative to Eurasian Arctic rivers [*United States Geological Survey*, 1982-1996].

Since the inorganic composition of surface waters in the Mackenzie River system is primarily controlled by the bedrock encountered by these waters during their residence in the drainage basin [*Reeder et al.*, 1972], the high Ba load of the Mackenzie River implies the existence of Ba-rich rocks in its watershed. The marine sedimentary rocks which occupy much of the drainage area of the Mackenzie River likely contain considerable amounts of biogenic Ba [*Bishop*, 1988; *Collier and Edmond*, 1984; *Dymond et al.*, 1992]. Economic deposits of barite have been documented in regions of British Columbia and the Yukon Territory drained by the Mackenzie River [*Dawson*, 1975; *Dawson*, 1977; *Morrow et al.*, 1978]. While the Mackenzie River is only the fourth largest Arctic river in terms of water discharge, it carries the highest suspended sediment load of the Arctic rivers (42 x 10^6 t yr^{-1}; *Meybeck and Ragu*, 1995). The high [Ba] observed in the Mackenzie River is consistent with observations of high [Ba] in low-latitude rivers bearing large suspended sediment loads, such as the Mississippi and Ganges-Brahmaputra [*Carroll et al.*, 1993; *Edmond et al.*, 1978; *Hanor and Chan*, 1977].

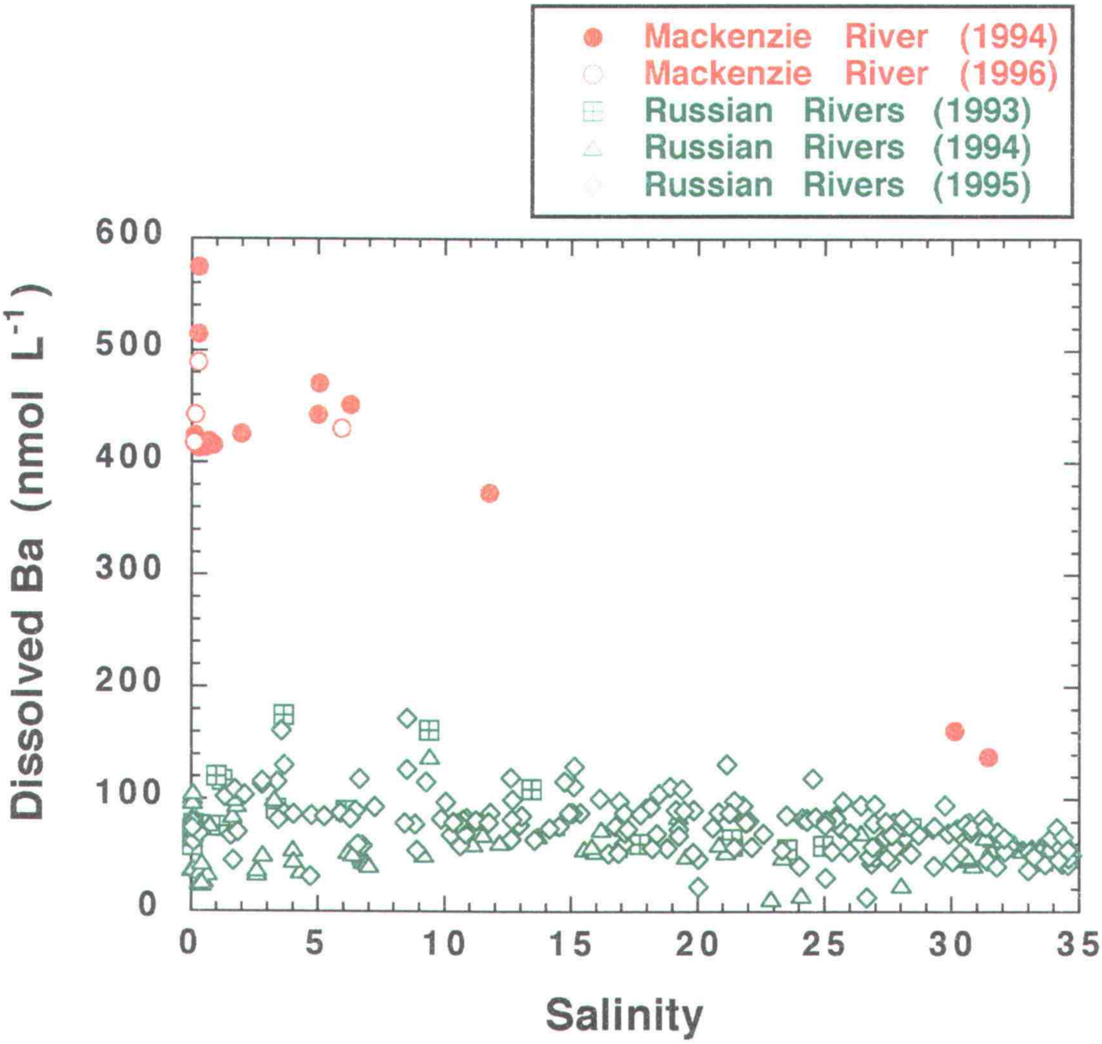

Figure 1.3 Composite plot of dissolved Ba versus salinity for 311 water samples collected between 1993 and 1996 from the estuaries of major Arctic rivers and adjacent seas.

Marine DOC is an actively cycling carbon species and constitutes the largest pool of reduced carbon in the oceans (700 Gt C; 1 Gt C = 10^{15} g C); this is comparable to the amounts of carbon contained in terrestrial biota (610 Gt C) and the atmosphere (600 Gt C) [values corrected to pre-industrial levels; *Siegenthaler and Sarmiento*, 1993]. Despite a growing appreciation of its significance to global carbon cycling [*Carlson et al.*, 1998], much remains unknown about the mechanisms by which DOC is created and destroyed in the oceans [*Hedges et al.*, 1997]. Primary sources of DOC to the Arctic Ocean include fluvial discharge, inflow from the North Atlantic and North Pacific and *in situ* production by phytoplankton and ice algae, but much uncertainty exists regarding the relative contributions from these sources and their geographical distributions [*Anderson et al.*, 1998; *Lundberg and Haugan*, 1996; *Wheeler et al.*, 1997]. Sinks include adsorption to particulate matter, microbial respiration [*Cota et al.*, 1996; *Rich et al.*, 1997] and photooxidation [*Vodacek et al.*, 1997].

The Lena, Yenisey and Ob rivers (the three largest Arctic rivers, which all enter from Eurasia and account for nearly half of the total fluvial discharge to the Arctic Ocean) have annual average DOC concentrations of 550-760 μmol C L^{-1}. In comparison, the Mackenzie River (the fourth largest Arctic river and the largest one entering from North America, accounting for nearly 10% of the total fluvial discharge to the Arctic Ocean) has an annual average DOC concentration of 430 μmol C L^{-1} [*Gordeev et al.*, 1996; *Meybeck and Ragu*, 1995; *Spitzy and Leenheer*, 1991; *Telang et al.*, 1991]. The high DOC in Eurasian rivers reflects the large areas of tundra, bogs, lakes and forests in their drainage basins [*Peake et al.*, 1972; *Telang et al.*, 1991].

While Eurasian Arctic rivers are low in Ba and the Mackenzie River is low in DOC with respect to each other, both sources of fluvial discharge are enriched in Ba and DOC relative to the marine waters into which they flow (Table 1.1). This suggests that Ba and DOC can serve as complimentary tracers to differentiate contributions from North American and Eurasian rivers and thus provide new information about circulation in the

Table 1.1 Concentration of Ba and DOC in source waters to the upper Arctic Ocean.

Source	Ba concentration (nmol Ba L^{-1})	DOC concentration (μmol C L^{-1})
Atlantic inflow	42-45*	60†
Pacific inflow	50-60*	54†
Mackenzie River	520*	430‡
Eurasian Arctic rivers	90-150*	550-760‡

*from *Guay and Falkner*, 1997.
†from *Wheeler et al.*, 1997.
‡from *Gordeev et al.*, 1996; *Meybeck and Ragu*, 1995; *Spitzy and Leenheer*, 1991; *Telang et al.*, 1991.

Arctic Ocean. It must be noted, however, that Ba and DOC can not be treated as strictly conservative tracers. Other processes besides mixing (e.g., biological activity, formation/melting of ice, etc.) can affect Ba and DOC in marine waters and must be considered when applying them as tracers of oceanic circulation. The effects of non-conservative processes are greatest in the dynamic estuarine and nearshore environments of the Arctic; they appear to be much less pronounced in the interior basins of the Arctic Ocean, where the perennial ice-cover severely limits sunlight and biological activity [*Falkner et al.*, 1994; *Guay and Falkner*, 1997].

In Chapter 2, results are presented from the SCICEX-97 cruise to the Arctic onboard the nuclear submarine *USS Archerfish*. A record of Ba and DOC was produced at a keel depth of 58 m along a 2900-km transect north of the Beaufort, Chukchi, East Siberian and Laptev seas. The tracer records identify areas where river waters cross the shelves and enter the interior Arctic Ocean, and the data provide further evidence of the utility of Ba and DOC for distinguishing between fluvial discharge from North American and Eurasian sources. The material in Chapter 2 was published in *Geophysical Research Letters* in April 1999 [*Guay et al.*, 1999]. In Chapter 3, results are presented from cruises to the

Laptev Sea and surrounding areas onboard the *R/V Polarstern* in the summer of 1993, 1995 and 1996. Areal distributions of fluvial discharge in the region are inferred from measurements of temperature, salinity, Ba and oxygen isotopes. The data highlight the large temporal variability characteristic of circulation over the Arctic marginal seas and indicate two principal pathways by which river waters can be transported from the Laptev Sea to the interior Arctic Ocean (one aligned roughly along the Lomonosov Ridge, and one aligned roughly along the Mendeleyev Ridge). The extent to which either pathway is favored in a given year is largely determined by local wind patterns during the summer months, when fluvial discharge is greatest and shelf waters are freshest. The material in Chapter 3 will be submitted for publication to the *Journal of Geophysical Research* in autumn 1999. In Chapter 4, factor analysis techniques are applied to a subset of the tracer data from the 1993 *Polarstern* cruise to test a mixing model that describes Laptev Sea waters as a combination of three primary end-members: Atlantic water, river discharge, and ice-melt. Overall conclusions and suggestions for future work are presented in Chapter 5.

2. HIGH-RESOLUTION MEASUREMENTS OF DISSOLVED ORGANIC CARBON IN THE ARCTIC OCEAN BY *IN SITU* FIBER-OPTIC SPECTROMETRY

Christopher K. H. Guay[1], Gary P. Klinkhammer[1], Kelly Kenison Falkner[1], Ronald Benner[2], Paula G. Coble[3], Terry E. Whitledge[2,4], Brenda Black[2], F. Joseph Bussell[1], and Tim A. Wagner[1]

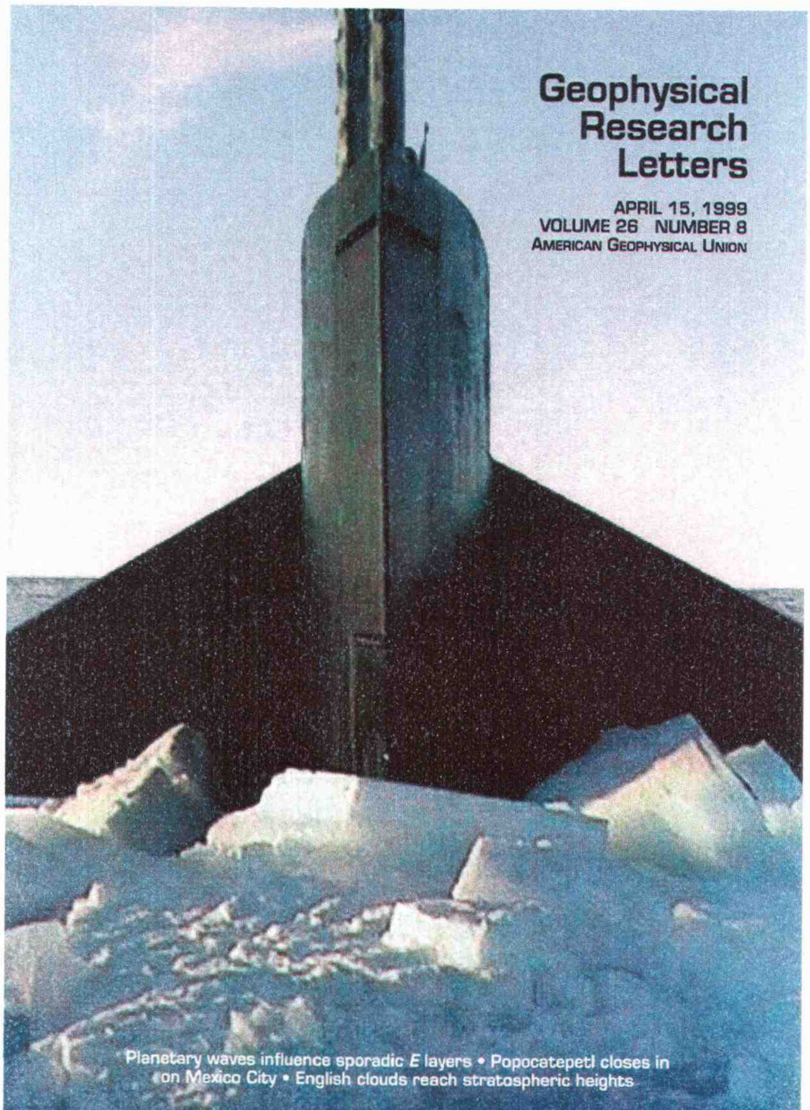

[1]College of Oceanic and Atmospheric Sciences, Oregon State University, Corvallis
[2]University of Texas Marine Science Institute, Port Aransas
[3]Department of Marine Science, University of South Florida, St. Petersburg
[4]Now at School of Fisheries and Ocean Sciences, University of Alaska, Fairbanks

Published in *Geophysical Research Letters*, Volume 26, Number 8, Pages 1007-1010, April 15, 1999. Copyright by the American Geophysical Union.

2.1 Abstract

Here we report results from an extensive survey of dissolved organic carbon (DOC) in the Arctic Ocean, which was achieved by means of a high-resolution, *in situ* UV fluorometer deployed on a nuclear submarine. Based on a strong linear correlation observed between fluorescence (320 nm excitation, 420 nm emission) and organic carbon concentrations determined directly by high-temperature combustion, a continuous record of DOC was produced at a keel depth of 58 m along a 2900-km transect north of the Beaufort, Chukchi, East Siberian and Laptev seas. The DOC record, combined with other physical and chemical measurements, identifies areas where river waters cross the shelves and enter the circulation of the Arctic interior. Fluvial sources were found to account for 12-56% of the total DOC in parts of the upper Makarov and Amundsen basins.

2.2 Introduction

Recent investigations of the Arctic Ocean [*Cota et al.*, 1996; *Wheeler et al.*, 1996] revealed larger and more active biological communities, higher levels of primary productivity and more dynamic carbon cycling than previously believed to exist in the region [*Apollonio*, 1959; *English*, 1961]. The large oceanic reservoir of dissolved organic carbon (DOC) in the Arctic remains poorly characterized despite its significance to the Arctic food web [*Rich et al.*, 1997] and global organic carbon cycling [*Lundberg and Haugan*, 1996; *Sarmiento et al.*, 1995]. Relatively few data exist for the interior Arctic Ocean due to its remoteness and the operational difficulties posed by its ice coverage and extreme weather conditions. Investigators working from drifting ice camps [*Gordon and Cranford*, 1985; *Kinney et al.*, 1971; *Melnikov and Pavlov*, 1978] and icebreakers [*Anderson et al.*, 1994; *Wheeler et al.*, 1997] observed high concentrations of DOC in the Eurasian and Canadian basins (typical values ranged from 65 to 125 μmol C L^{-1} at depths above 200 m and from 50 to 80 μmol C L^{-1} in deeper waters); much lower concentrations of particulate organic carbon (POC) were observed (0.2-0.8 μmol C L^{-1}, with values up to 3.6 μmol C L^{-1} occurring during periods of ice melt).

Primary sources of DOC to the Arctic Ocean include fluvial discharge, inflow from the North Atlantic and North Pacific and *in situ* production by phytoplankton and ice algae, but much uncertainty exists regarding the relative contributions from these sources and their geographical distributions [*Anderson et al.*, 1998; *Lundberg and Haugan*, 1996]. The outflow of water through Fram Strait results in a net export of DOC from the Arctic to the North Atlantic, which may play an important role in sustaining deep-ocean DOC gradients and turnover of the marine DOC pool [*Hansell and Carlson*, 1998].

2.3 Sample Collection

The SCICEX-97 cruise aboard the nuclear submarine *USS Archerfish* provided direct access to the ice-covered interior of the Arctic Ocean and allowed collection of quasi-synoptic data on an unprecedented scale and degree of resolution. The data reported in this paper were obtained between 12 and 21 September 1997, while the submarine maintained a keel depth of 58 m along an approximately 2900-km transect north of the Beaufort, Chukchi, East Siberian and Laptev seas (Figure 2.1).

Water samples for total organic carbon (TOC) and barium (Ba) analyses were collected from a sampling line inside the submarine supplied by an intake valve located 3 m above the keel (TOC samples were collected roughly every hour and Ba samples were collected roughly every 2 hours). *In situ* measurements of temperature, salinity and chlorophyll-*a* were obtained by a Seabird Electronics SBE-19 conductivity-temperature-depth (CTD) probe mounted in the sail of the submarine 15 m above the keel (sampling rate: 4 Hz). *In situ* measurements of fluorescence (320 nm excitation, 420 nm emission) were obtained by a zero angle photon spectrometer (ZAPS) [*Klinkhammer et al.*, 1997] installed in a compartment in the bow of the submarine located 8 m above the keel

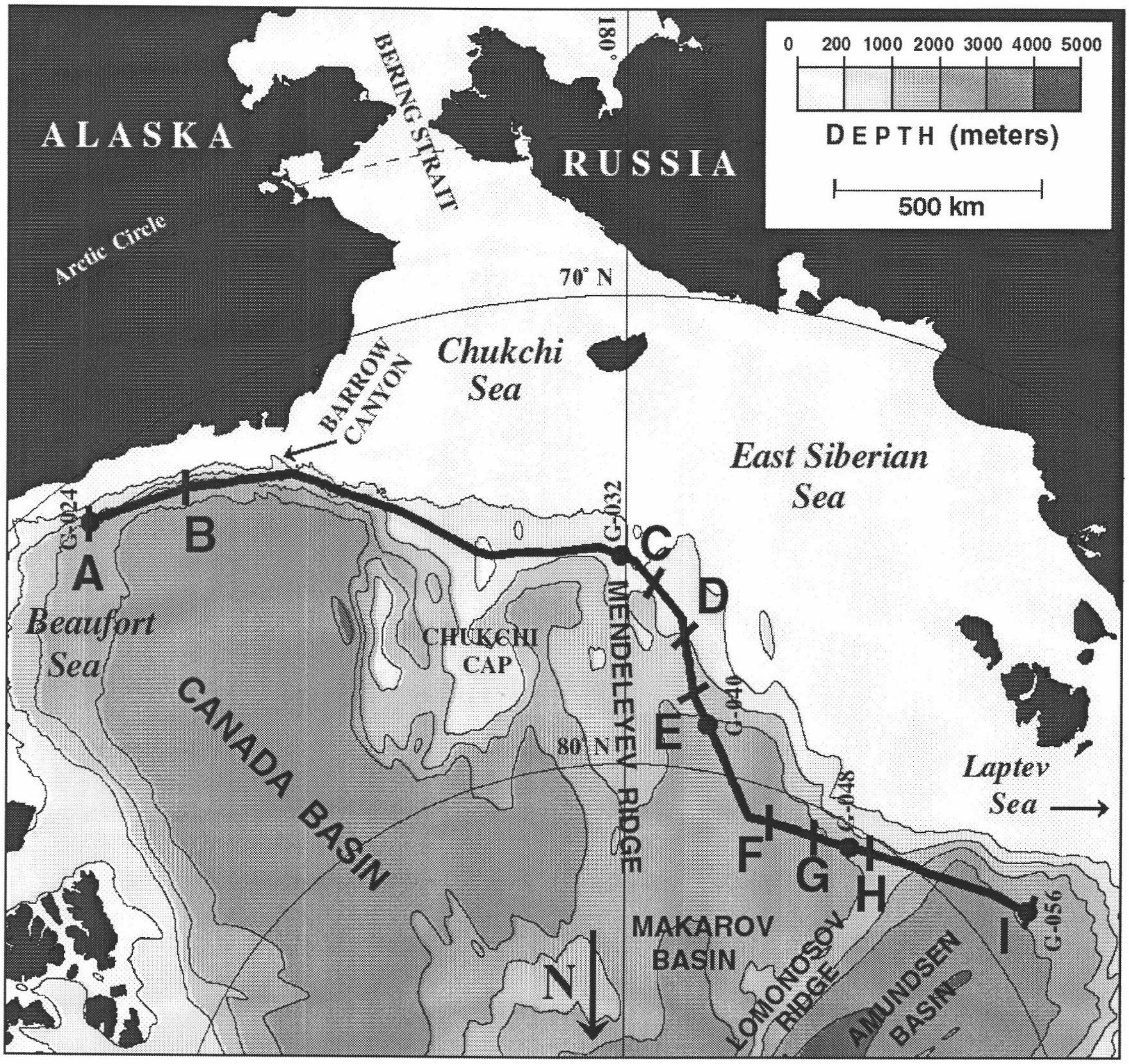

Figure 2.1 Transect occupied by the *USS Archerfish* from 12 to 21 September 1997. Letters A-I indicate points of reference discussed in the text. Black dots indicate locations of 5 samples for which excitation-emission matrices were constructed.

(sampling rate: 1.7 Hz). Previous work with the ZAPS instrument in mid-latitude coastal surface waters has shown that its response at these wavelengths is closely related to the humic-rich terrestrial component of dissolved organic matter.

In the following discussion, we have assumed that the difference in sampling heights for the various parameters is negligible. While this assumption may have resulted in some degree of uncertainty (particularly in areas of strong vertical gradients), it is not sufficient to invalidate our conclusions.

2.4 Results and Discussion

The SCICEX-97 expedition provided the first comparison between ZAPS response and direct measurements of organic carbon by high-temperature combustion [*Benner and Strom*, 1993]. A strong positive correlation ($r^2 = 0.84$, least-squares linear regression) was observed between ZAPS response and TOC along the transect (Figure 2.2). These results are contrary to the negative correlations between fluorescence (320 nm/420nm) and DOC documented in open ocean environments at lower latitudes [e.g., *Chen and Bada*, 1992], which were attributed to the combined effects of primary production, remineralization and photooxidation of organic material. Ice cover, seasonally limited insolation and low temperatures presumably diminish the influence of these processes in the Arctic Ocean. Our data are similar to observations made in estuaries and nearshore waters at lower latitudes [e.g., *Smart et al.*, 1976], consistent with the sizable fluvial discharge to the Arctic Ocean (roughly 10% of global river runoff and fluvial organic carbon flux enters the Arctic Ocean and its marginal seas).

Since particles accounted for a very small portion of the organic carbon in these samples (POC concentrations for 11 samples collected during the transect ranged from 1.1 to 3.4 μmol C L^{-1}, or ≤ 4.2% of TOC), TOC ≈ DOC and the concentration of DOC

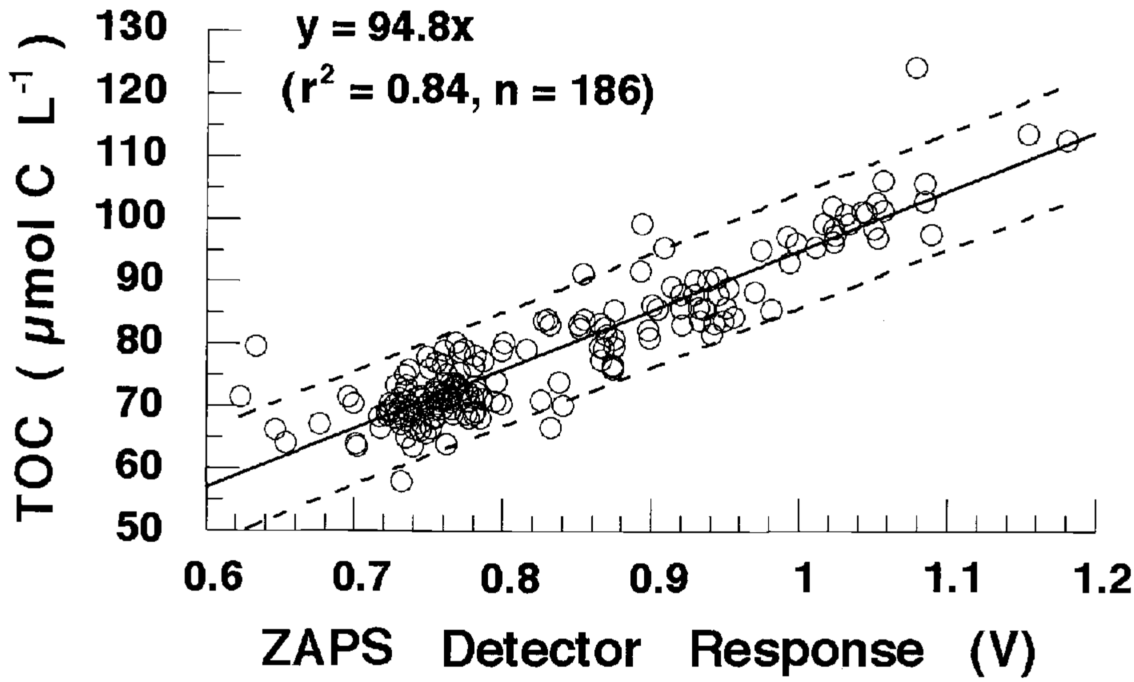

Figure 2.2 Calibration plot for the ZAPS instrument using TOC concentrations determined by high-temperature combustion. Dashed lines indicate the 95% prediction interval (± 9 µmol C L^{-1}). An empirically-derived correction factor of 0.5413 V was subtracted from the raw ZAPS detector response to account for reflectance from the walls of the compartment in which the ZAPS instrument was installed.

Table 2.1 Comparison of Organic Carbon Concentrations Measured by High-Temperature Combustion and the ZAPS Instrument to Total Integrated Fluorescence Signals (330 to 700 nm Emission) Produced by Excitation at 320 nm.

Sample Number	Julian Day	TOC (µmol C L^{-1})	DOC_{ZAPS_1} (µmol C L^{-1})	Integrated Fluorescence (ppb•nm)
G-024	255.840	80	82	1017
G-032	259.766	66	68	616
G-040	261.595	89	90	1209
G-048	263.218	81	83	1028
G-056	264.626	64	67	542

can be estimated from the response of the ZAPS instrument by the relation DOC_{ZAPS} = 94.8 x V, where DOC_{ZAPS} has units of μmol C L^{-1} and V is the voltage measured at the photomultiplier detector of the ZAPS instrument. Excitation-emission matrices [*Coble*, 1996] for 5 water samples collected along the transect showed that the peak signal occurred at or near the excitation/emission wavelengths selected by the ZAPS instrument. The total integrated fluorescence signals (emission wavelengths 330-700 nm) produced by excitation at 320 nm are positively linearly correlated with DOC_{ZAPS} concentrations (r^2 = 0.997; Table 2.1), further corroborating the ZAPS measurements based on detection at a single wavelength.

A plot of DOC_{ZAPS} versus salinity (Figure 2.3) reveals three distinct groups of data: (*i*) a complex regime in the Canada Basin and over the Chukchi Cap (points A-C on Fig. 1) suggestive of mixing between Pacific inflow, ice-melt and discharge from the Mackenzie River; (*ii*) a transition zone over the Mendeleyev Ridge (points C-D) corresponding to the front between waters of Pacific and Atlantic character; (*iii*) a linear (r^2 = 0.76) regime in the Makarov and Amundsen basins (points D-I) dominated by discharge from Eurasian Arctic rivers (fresh, high-DOC) and marine waters of Atlantic origin (saline, low-DOC). This latter trend is consistent with previous observations of a quasi-linear inverse relationship between fluorescence (320 nm/420 nm) and salinity in nearshore waters strongly influenced by terrestrial organic material [*Klinkhammer et al.*, 1997]. Ice melting and formation, phytoplankton production, microbial respiration and photooxidation likely account for much of the scatter in the data.

To a first-order approximation, the data from the Makarov and Amundsen basins suggest conservative mixing between Eurasian river discharge and Atlantic inflow. The zero-salinity intercept of the best-fit line (705 μmol C L^{-1}) is comparable to DOC concentrations reported for the major Eurasian Arctic rivers (550-760 μmol C L^{-1}) [*Gordeev et al.*, 1996]. Extrapolating to a salinity characteristic of the Atlantic layer in the Eurasian Basin (34.9) results in a value (58 μmol C L^{-1}) comparable to DOC

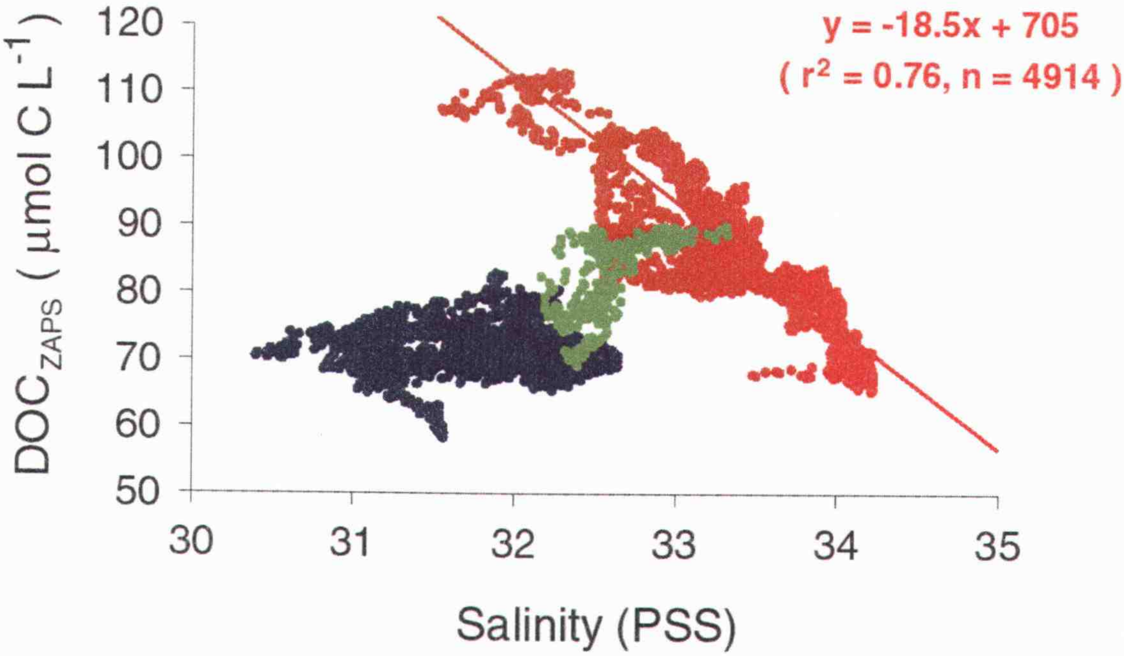

Figure 2.3 Relationship between DOC$_{ZAPS}$ and salinity for data collected along the transect. Blue symbols correspond to data from the Canada Basin and over the Chukchi Cap (points A-C), green symbols correspond to data from the transition zone over the Arlis Plateau (points C-D), and red symbols correspond to data from the Makarov and Amundsen basins (points D-I). The red line was fit to the data from the Makarov and Amundsen basins by least-squares linear regression.

concentrations reported for Atlantic source waters to the Arctic (50-60 μmol C L^{-1}) [*Wheeler et al.*, 1997].

Assuming linear combinations of these fluvial and marine end-members, the waters encountered along the transect on the Atlantic side of the front contain 90-99% Atlantic inflow and 1-10% fluvial discharge; these results are consistent with previous estimates of the fluvial component of upper waters (depth < 300 m) in the Eurasian Basin based on a salinity/^{18}O mass balance [*Bauch et al.*, 1995]. Between 12 and 56% of the total DOC in these waters is calculated to be derived from fluvial sources. The upper limit of this range is somewhat higher than other estimates of the relative fluvial DOC contribution to the Arctic based on a budget approach [*Wheeler et al.*, 1997] and measurements of terrestrial biomarkers [*R. Benner*, unpublished data]. This partly reflects the ability of high-resolution, *in situ* DOC measurements to capture narrow, intense fluvial features (see discussion below) that are not representative of the average composition of DOC in Arctic surface waters and would likely be missed by less densely sampled discrete bottle measurements.

Distributions of salinity, temperature, Ba, DOC_{ZAPS}, TOC and chlorophyll-*a* observed along the transect are consonant with known hydrographic features of the Arctic Ocean (Figure 2.4). The relatively low salinity (30.4-32.6) observed between the Beaufort Sea and Mendeleyev Ridge (points A-C on Fig. 1) is characteristic of surface waters in the Canada Basin, reflecting the influx of Pacific water through Bering Strait [*Carmack*, 1990]. Peaks in chlorophyll-*a* (3-6 μg L^{-1}) suggest local phytoplankton growth and/or advection of water from high-productivity regions over the Bering, Chukchi and Beaufort shelves [*Cota et al.*, 1996]. The high Ba concentrations (60-81 nmol Ba L^{-1}) encountered in this area are due to the influence of the Mackenzie River [*Guay and Falkner*, 1997].

The transect was punctuated by warm (T > 0 °C), relatively fresh (S < 32) waters over the slope north of Alaska. Particularly notable is the feature observed east of Barrow Canyon (point B) having an intense temperature maximum (5 °C) and local minima in

Figure 2.4 Distributions of salinity, temperature, Ba, DOC_{ZAPS}, TOC and chlorophyll-*a* along the transect at a keel depth of 58 m. Salinity, temperature and chlorophyll-*a* were measured by a Seabird Electronics SBE-19 conductivity-temperature-pressure (CTD) probe equipped with a Wet Star 95-1000-1 chlorophyll sensor (precision: ± 0.01, ± 0.01 °C, ± 0.03 μg L^{-1}, respectively). Analyses for Ba were conducted in the laboratory by isotope-dilution inductively coupled plasma quadrupole mass spectrometry (precision: ± 3 nmol Ba L^{-1} or better) [*Guay and Falkner*, 1997]. Analyses for TOC were conducted in the laboratory by high-temperature combustion (coefficient of variation: ≤ 2%) [*Benner and Strom*, 1993]. Values of DOC_{ZAPS} were determined from fluorescence measurements obtained by the ZAPS instrument as described in the text. Data obtained by the CTD and ZAPS instruments were averaged over 1-min time intervals. The data gap around Julian Day 261 corresponds to a 5.5 hour period when the submarine had surfaced through the ice and was not acquiring data.

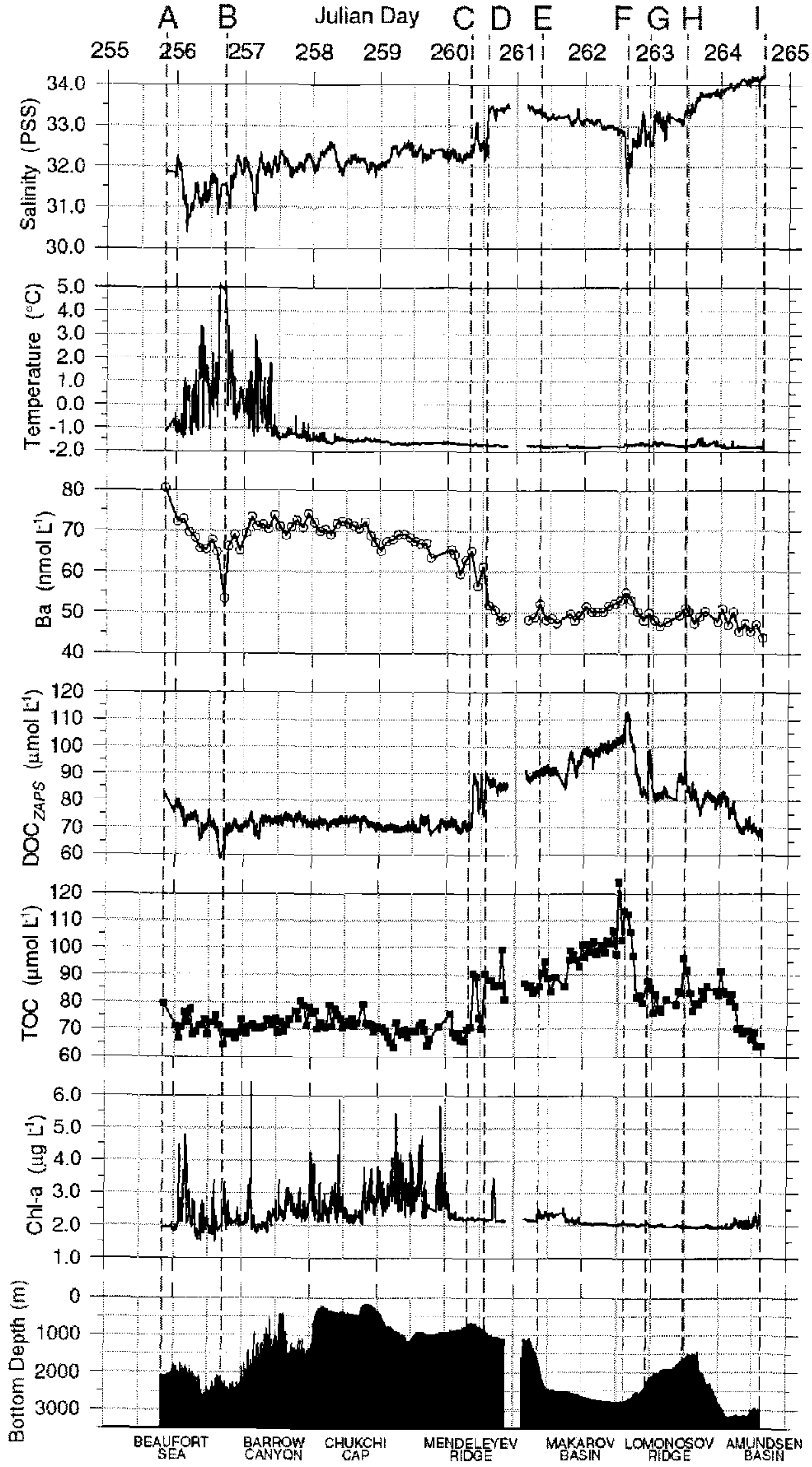
A B Julian Day C D E F G H I
255 256 257 258 259 260 261 262 263 264 265
Salinity (PSS)
Temperature (°C)
Ba (nmol L-1)
DOCZAPS (μmol L-1)
TOC (μmol L-1)
Chl-a (μg L-1)
Bottom Depth (m)
BEAUFORT SEA
BARROW CANYON
CHUKCHI CAP
MENDELEYEV RIDGE
MAKAROV BASIN
LOMONOSOV RIDGE
AMUNDSEN BASIN
CANADA BASIN

Figure 2.4

salinity (31.5), Ba (54 nmol Ba L^{-1}), DOC_{ZAPS} (62 μmol C L^{-1}) and TOC (64 μmol C L^{-1}). These features are associated with the Beaufort Undercurrent, a strong (≈10 cm s^{-1}), bathymetrically-steered mean eastward flow that typically extends from near-surface to the bottom between the 50-m and 2500-m isobaths in the southern Beaufort Sea [*Aagaard*, 1984]. The Beaufort Undercurrent is an extension of the Alaskan Coastal Current, which originates in the Bering Sea and becomes seasonally warmed by solar insolation and freshened by fluvial discharge and ice-melt during its northward transit through Bering Strait and the Chukchi Sea. The observed Ba minimum is a consequence of biological uptake occurring along the advective pathway of these waters in the summer [*Falkner et al.*, 1994]. The observed minima in DOC_{ZAPS} and TOC likely resulted from microbial respiration [*Rich et al.*, 1997] and/or photooxidation [*Vodacek et al.*, 1997].

The location of the hydrographic front separating waters of Pacific and Atlantic character (points C-D) is consistent with other studies indicating a recent (late 1980's) shift from its historical position over the Lomonosov Ridge to a position aligned along the Mendeleyev Ridge [*Morison et al.*, 1998]. The higher salinity (31.5-34.2) in the Makarov and Amundsen basins (points D-I) reflects source waters of Atlantic origin [Jones *et al.*, 1998], while the high concentrations of DOC_{ZAPS} (65-114 μmol C L^{-1}) and TOC (64-124 μmol C L^{-1}) observed in these waters reflect contributions from Eurasian Arctic rivers.

Eurasian Arctic rivers are low in Ba and the Mackenzie River is low in DOC with respect to each other, but both sources of fluvial discharge are enriched in DOC and Ba relative to the marine waters into which they flow [*Gordeev et al.*, 1996; *Guay and Falkner*, 1997]. Thus local minima in salinity coincident with local maxima in Ba, DOC_{ZAPS} and TOC (points A, E-H) indicate points along the transect strongly influenced by fluvial discharge and identify areas where river waters cross the shelves and enter the Arctic interior. The high Ba associated with the feature observed at point A and its location in the southern Beaufort Sea suggest that it is part of the Mackenzie River plume, while the high DOC_{ZAPS} associated with the features observed at points E-H and their locations over the Makarov Basin and the flanks of the Mendeleyev and Lomonosov ridges suggest that they are associated with discharge from Eurasian Arctic rivers. These fluvial features are accompanied by low chlorophyll-*a* concentrations (2.0-2.5 μg L^{-1}), which indicate low phytoplankton biomass and suggest that *in situ* productivity was not a major source of DOC in these waters.

The intensity of the observed fluvial signals is somewhat surprising, given that strong density stratification in the Arctic Ocean tends to inhibit vertical mixing and the depth occupied by the submarine was generally below the base of the summer surface mixed layer. The fact that these attenuated signals were still clearly detectable underscores the importance of Arctic fluvial inputs and illustrates the sensitivity of the high-resolution, optical DOC measurements. Our data suggest that DOC and Ba serve as complementary tracers for distinguishing between contributions from North American and Eurasian rivers and thus provide new information about circulation in the Arctic Ocean.

2.5 References

Aagaard, K., The Beaufort Undercurrent, in *The Alaskan Beaufort Sea: Ecosystems and Environments*, edited by P.W. Barnes, D. Schell, and E. Reimnitz, pp. 47-71, Academic Press, Inc., Orlando, Fla., 1984.

Anderson, L.G., G. Björk, O. Holby, E.P. Jones, G. Kattner, K.P. Koltermann, B. Liljeblad, R. Lindgren, B. Rudels, and J. Swift, Water masses and circulation in the Eurasian Basin: Results from the Oden 91 Expedition, *J. Geophys. Res.*, *99*, 3273-3283, 1994.

Anderson, L.G., K. Olsson, and M. Chierici, A carbon budget for the Arctic Ocean, *Global Biogeochem. Cycles, 12(3)*, 455-465, 1998.

Apollonio, S., Hydrobiological measurements on IGY Drifting Station Bravo, *Trans. Am. Geophys. Union*, *40*, 316-319, 1959.

Bauch, D., P. Schlosser, and R. Fairbanks, Freshwater balance and the sources of deep and bottom waters in the Arctic Ocean inferred from the distribution of $H_2{}^{18}O$, *Prog. Oceanog.*, *35*, 53-80, 1995.

Benner, R., and M. Strom, A critical evaluation of the analytical blank associated with DOC measurements by high-temperature catalytic oxidation, *Mar. Chem.*, *41*, 153-160, 1993.

Carmack, E.C., Large-scale physical oceanography of polar oceans, in *Polar Oceanography, Part A: Physical Science*, edited by W.O. Smith, pp. 171-222, Academic Press, San Diego, Calif., 1990.

Chen, R.F., and J.L. Bada, The fluorescence of dissolved organic matter in seawater, *Mar. Chem.*, *37*, 191-221, 1992.

Coble, P.G., Characterization of marine and terrestrial DOM in seawater using excitation-emission matrix spectroscopy, *Mar. Chem.*, *51*, 325-346, 1996.

Cota, G.F., L.R. Pomeroy, W.G. Harrison, E.P. Jones, F. Peters, W.M. Sheldon, and T.R. Weingartner, Nutrients, primary production and microbial heterotrophy in the southeastern Chukchi Sea: Arctic summer nutrient depletion and heterotrophy, *Mar. Ecol. Prog. Ser.*, *135*, 247-258, 1996.

English, T.S., Some biological observations in the central North Polar Sea, Drift Station Alpha, 1957-58, *Res. Pap. 13*, pp. 80, Arctic Institute of North America, Washington, DC, 1961.

Falkner, K.K., R.W. MacDonald, E.C. Carmack, and T. Weingartner, The potential of barium as a tracer of Arctic water masses, in *The Polar Oceans and Their Role in Shaping the Global Environment: The Nansen Centennial Volume, AGU Geophysical Monograph Series*, edited by O.M. Johannessen, R.D. Muench, and J.E. Overland, pp. 63-76, AGU Books, Washington, DC, 1994.

Gordeev, V., J. Martin, I. Sidorov, and M. Sidorova, A reassessment of the Eurasian river input of water, sediment, major elements, and nutrients to the Arctic Ocean, *Amer. J. Sci., 296*, 664-691, 1996.

Gordon, D.C., and P.J. Cranford, Detailed distribution of dissolved and particulate organic matter in the Arctic Ocean and comparison with other oceanic regions, *Deep-Sea Res., 32(10)*, 1221-1232, 1985.

Guay, C.K., and K.K. Falkner, Barium as a tracer of Arctic halocline and river waters, *Deep-Sea Res. II, 44(8)*, 1543-1569, 1997.

Hansell, D.A., and C.A. Carlson, Deep-ocean gradients in the concentration of dissolved organic carbon, *Nature, 395*, 263-266, 1998.

Jones, E.P., L.G. Anderson, and J.H. Swift, Distribution of Atlantic and Pacific waters in the upper Arctic Ocean: Implications for circulation, *Geophys. Res. Lett, 25(6)*, 765-768, 1998.

Kinney, P.J., T.C. Loder, and J. Groves, Particulate and dissolved organic matter in the Amerasian Basin of the Arctic Ocean, *Limnol. Oceanogr., 16*, 132-137, 1971.

Klinkhammer, G.P., C.S. Chin, C. Wilson, M.D. Rudnicki, and C.R. German, Distributions of dissolved manganese and fluorescent dissolved organic matter in the Columbia River estuary and plume as determined by in situ measurement, *Mar. Chem., 56*, 1-14, 1997.

Lundberg, L., and P.M. Haugan, A Nordic Seas-Arctic Ocean carbon budget from volume flows and inorganic carbon data, *Global Biogeochem. Cycles, 10(3)*, 493-510, 1996.

Melnikov, I.A., and G.L. Pavlov, Characteristics of organic carbon distribution in the water and ice of the Arctic Basin, *Oceanology, 18(2)*, 163-167, 1978.

Morison, J., M. Steele, and R. Andersen, Hydrography of the upper Arctic Ocean measured from the nuclear submarine *USS Pargo*, *Deep-Sea Res. I, 45*, 15-38, 1998.

Rich, J., M. Gosselin, E. Sherr, B. Sherr, and D.L. Kirchman, High bacterial production, uptake and concentrations of dissolved organic matter in the central Arctic Ocean, *Deep-Sea Res. II, 44(8)*, 1645-1663, 1997.

Sarmiento, J.L., R. Murnane, and C. Le Quéré, Air-sea CO_2 transfer and the carbon budget of the North Atlantic, *Phil. Trans. R. Soc. Lond. B, 348*, 211-219, 1995.

Smart, P.L., B.L. Finlayson, W.D. Rylands, and C.M. Ball, The relation of fluorescence to dissolved organic carbon in surface waters, *Water Res., 10*, 805-811, 1976.

Vodacek, A., N.V. Blough, M.D. DeGrandpre, E.T. Pelltzer, and R.K. Nelson, *Limnol. Oceanogr., 42(4)*, 674-686, 1997.

Wheeler, P.A., M. Gosselin, E. Sherr, D. Thibault, D.L. Kirchman, R. Benner, and T.E. Whitledge, Active recycling of organic carbon in the central Arctic Ocean, *Nature, 380*, 697-699, 1996.

Wheeler, P.A., J.M. Watkins, and R.L. Hansing, Nutrients, organic carbon and nitrogen in the upper water column of the Arctic Ocean: implications for the sources of dissolved organic carbon, *Deep-Sea Res. II, 44(8)*, 1571-1592, 1997.

3. OCEAN TRANSPORT PATHWAYS FOR EURASIAN ARCTIC RIVER DISCHARGE

Christopher K. H. Guay[1], Kelly Kenison Falkner[1], Robin D. Muench[2], Reinhold Bayer[3], Manfred Mensch[3], Markus Frank[3]

[1]College of Oceanic and Atmospheric Sciences, Oregon State University, Corvallis
[2]Earth and Space Research, Seattle, Washington
[3]Institut für Umweltphysik, Ruprecht-Karls-Universität, Heidelberg, Germany

Prepared for submission to the *Journal of Geophysical Research.*

3.1 Abstract

Distributions of temperature, salinity and barium are presented for the upper Laptev Sea and adjacent areas of the Nansen, Amundsen and Makarov basins during the summer in 1993, 1995 and 1996. The tracer data indicate that while fluvial discharge was largely confined to the shelf region of the Laptev Sea in the summer of 1993, surface waters containing a significant fluvial component extended beyond the shelf break and over the slope and basin areas north of the Laptev Sea in the summers of 1995 and 1996. These distributions of fluvial discharge are consistent with local winds and suggest two principal pathways by which river waters can enter the central Arctic basins from the Laptev Sea. When southerly to southeasterly wind conditions prevail, river waters are transported northwards beyond the shelf break and over the slope and adjacent basin areas. These waters can then enter the interior Arctic Ocean via upper layer flow aligned roughly along the Lomonosov Ridge. Under other wind conditions, river waters are steered primarily along the inner Laptev shelf and into the East Siberian Sea as part of the predominantly eastward coastal current system. These waters then appear to cross the shelf and enter the interior Arctic Ocean via upper layer flow aligned roughly along the Mendeleyev Ridge. The extent to which either pathway is favored in a given year is largely determined by local wind patterns during the summer months, when fluvial discharge is greatest and shelf waters are freshest.

3.2 Introduction

It has long been appreciated that the considerable fluvial discharge to the Arctic Ocean strongly influences its properties and circulation. Fluvial sources contribute to maintaining the cold Arctic halocline [*Rudels et al.*, 1996; *Steele and Boyd*, 1998], which insulates the perennial sea ice cover from heat contained in the underlying Atlantic layer. The export of fresh water from the Arctic through Fram Strait and the Canadian

Archipelago (of which fluvial discharge is a major component) affects water column stability in areas of deep convection in the North Atlantic and thereby influences global thermohaline circulation [*Aagaard and Carmack*, 1989]. Understanding the mechanisms by which river waters become incorporated into the circulation of the Arctic Ocean is therefore essential to investigating the links between the Arctic and global climate. Knowledge of the mixing pathways of fluvial discharge also provides information needed to assess the transport and fate of pollutants released to the Arctic Ocean [*Macdonald and Bewers*, 1996].

Exactly how and where river waters cross the broad shelves of the Arctic's marginal seas and enter the interior basins remains unclear. Based on physical and chemical tracer data, it appears that river waters flowing into the Eurasian Arctic seas are transported to the interior Arctic Ocean by surface flows roughly aligned along the Nansen-Gakkel, Lomonosov and Mendeleyev ridges [*Anderson et al.*, 1994; *Bauch et al.*, 1995; *Östlund and Hut*, 1984; *Guay and Falkner*, 1997; *Jones et al.*, 1991; *Wheeler et al.*, 1997]. Circulation models for the Arctic Ocean also tend to show water from Eurasian Arctic rivers entering the interior basins along these ridges [*Maslowski et al.*, 1998; *Proshutinsky and Johnson*, 1996]. These results are consistent with the conceptual depiction of mean circulation in the Nansen, Amundsen and Makarov basins as a group of basin-trapped cyclonic gyres (i.e., northward flow along the western flanks of the Nansen-Gakkel, Lomonosov and Mendeleyev ridges comprises the northward branches of the gyres occupying the Nansen, Amundsen and Makarov basins, respectively [*McLaughlin et al.*, 1996; *Rudels et al.*, 1994]).

The Laptev Sea (Figure 3.1) receives a large influx of fluvial discharge, as both direct runoff from rivers and as a component of shelf waters entering from the Kara Sea through Vilkitsky Strait and around the northern periphery of Severnaya Zemlya (Table 3.1). Here we present measurements of temperature, salinity and barium in the upper 50 m of the Laptev Sea and adjacent areas in three different years. The geographical distributions of

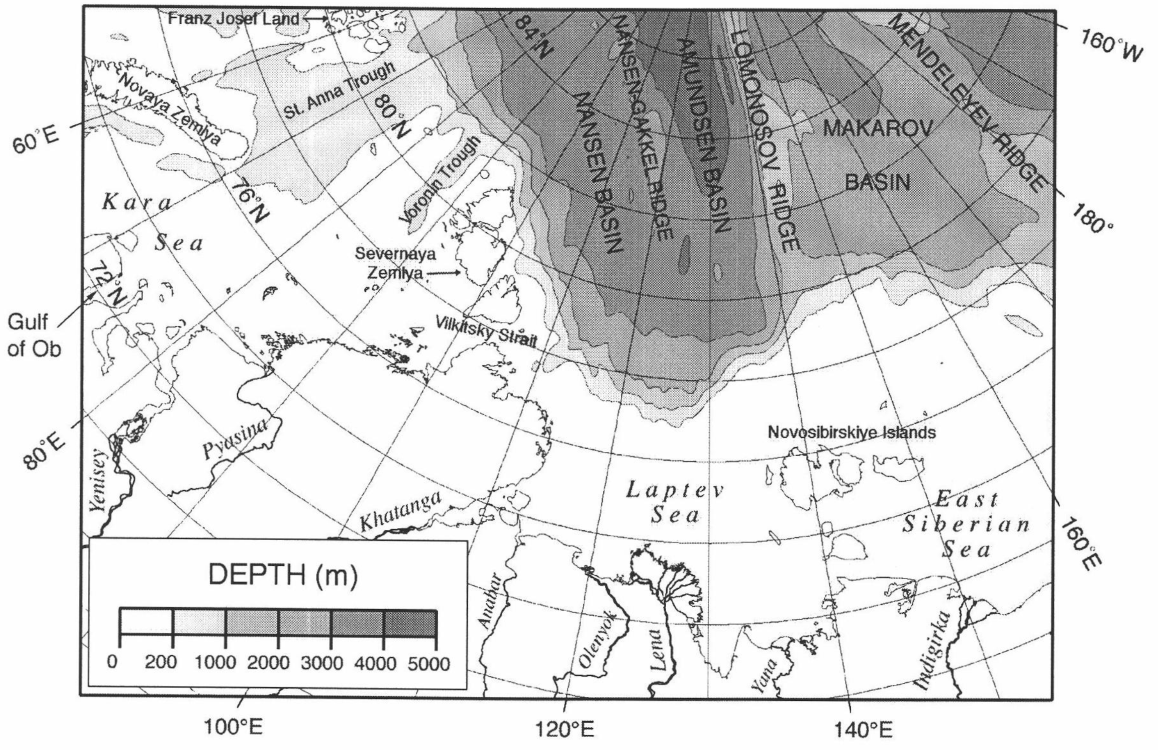

Figure 3.1 Map of the Laptev Sea and vicinity.

Table 3.1 Mean annual discharge of major rivers flowing into the Laptev and Kara seas [*Meybeck and Ragu*, 1995].

River	Annual Discharge ($km^3\ yr^{-1}$)
Laptev Sea	
Lena	525
Khatanga	85.3
Olenyok	35.8
Yana	34.3
Anabar	13.2
Omoloy	7.0
Kara Sea	
Yenisey	620
Ob	404
Pyasina	56.2
Taz	48.5
Taymyra	31.2
Pur	28.1
Nadym	14.8

these tracers suggest causes of interannual variability in the region and pathways by which discharge from Eurasian rivers transits the shelves and enters the interior Arctic Ocean.

3.3 Sample Collection and Analysis

The R/V *Polarstern* occupied 238 hydrographic stations in the Laptev Sea and adjacent areas of the Nansen and Amundsen basins (collectively referred to as the Eurasian Basin) and the Makarov Basin during three cruises in the summers of 1993, 1995 and 1996 (Table 3.2). At all of the stations, profiles of temperature and salinity were obtained using a conductivity-temperature-depth (CTD) instrument (NBIS Mark IV in 1993 and 1996, SeaBird SBE-911 in 1995). The CTD's were calibrated in the laboratory before and after each cruise. In addition, the CTD salinity data were calibrated against values of salinity determined onboard for discrete water samples collected during the hydrocasts. Accuracies are within 3 dbar for pressure, 0.005 °C for temperature and 0.005 for salinity. At 210 of the stations, water samples for Ba analysis were obtained from depths throughout the water column using a General Oceanics 24-bottle rosette sampler. Barium concentrations ([Ba]) were determined for the samples by isotope-dilution inductively coupled plasma mass spectrometry (ID-ICPMS) at Oregon State University on a Fisons PlasmaQuad II [*Guay and Falkner*, 1998]. The precision of the analytical procedure ranges from better than 5% at 10 nmol Ba L^{-1} to better than 3% at 100 nmol Ba L^{-1}.

Table 3.2 Cruises to the Laptev Sea and adjacent areas onboard the R/V *Polarstern* in 1993, 1995 and 1996.

Cruise	Year	Dates	Total number of stations	Stations with Ba samples
ARK IX/4	1993	26 Aug - 24 Sep	47	40
ARK XI	1995	19 Jul - 11 Sep	87	70
ARK XII	1996	16 Jul - 4 Sep	102	100

3.4 Results

At each station, mean values of temperature and salinity were calculated from all CTD measurements made at depths above 50 m. Mean values of [Ba] were calculated from all samples collected above 50 m (depth-weighted averages were calculated in order to minimize any bias created by non-uniform vertical spacing of samples). An averaging depth of 50 m was chosen because it includes the portion of the water column most strongly influenced by fluvial discharge and allows direct comparison between shallow shelf stations (bottom depth ≈ 50 m) and deeper stations over the slope and basin areas. Performing the calculations using a greater averaging depth (down to 200 m -- the maximum depth observed for the base of the halocline layer at these stations, below which river water would not be expected to penetrate [*Schauer et al.*, 1997]) yields results consistent with our conclusions based on an averaging depth of 50 m.

3.4.1 1993 Stations

Relatively high mean temperature (-0.42 °C), low mean salinity (30.12) and highest mean [Ba] (65 nmol Ba L^{-1}) were observed at the shallowest (bottom depth = 38 m), southernmost station over the Laptev shelf (Figures 3.2a, 3.3a and 3.4a). Warmer (mean T = -0.65 to 0.20 °C), fresher (mean S = 29.15 to 32.09) waters slightly elevated in Ba (mean [Ba] = 45 to 51 nmol Ba L^{-1}) were also observed in western Vilkitsky Strait. At the rest of the stations over the northern Laptev shelf and slope and adjacent areas of the Eurasian Basin, mean temperature ranged from -1.81 to -1.24 °C, mean salinity ranged from 31.04 to 33.70, and mean [Ba] ranged from 42 to 50 nmol Ba L^{-1}. Overall, temperature and [Ba] tended to decrease and salinity tended to increase moving offshore from shelf to basin.

3.4.2 1995 Stations

Mean temperature ranged from -1.80 to 1.14 °C, generally decreasing offshore from shelf to basin (Figure 3.2b). Highest temperatures were observed at stations over the northeastern Laptev shelf. Highest mean salinity (32.01 to 34.06) was observed at the stations in the western region of the sampling area (Figure 3.3b), with fresher waters occurring near the shelf break and more saline waters occurring over slope and basin areas. Mean [Ba] ranged from 43 to 60 nmol Ba L^{-1} at these stations, decreasing offshore from shelf to basin (Figure 3.4b). Relatively fresh waters (mean S = 30.88 to 32.55) moderately elevated in Ba (mean [Ba] = 48 to 58 nmol Ba L^{-1}) covered the northern Laptev shelf and extended over the southern Amundsen Basin and Lomonosov Ridge. Mean

Figure 3.2 Distributions of mean temperature in the upper 50 m of the water column in (a) 1993, (b) 1995, and (c) 1996.

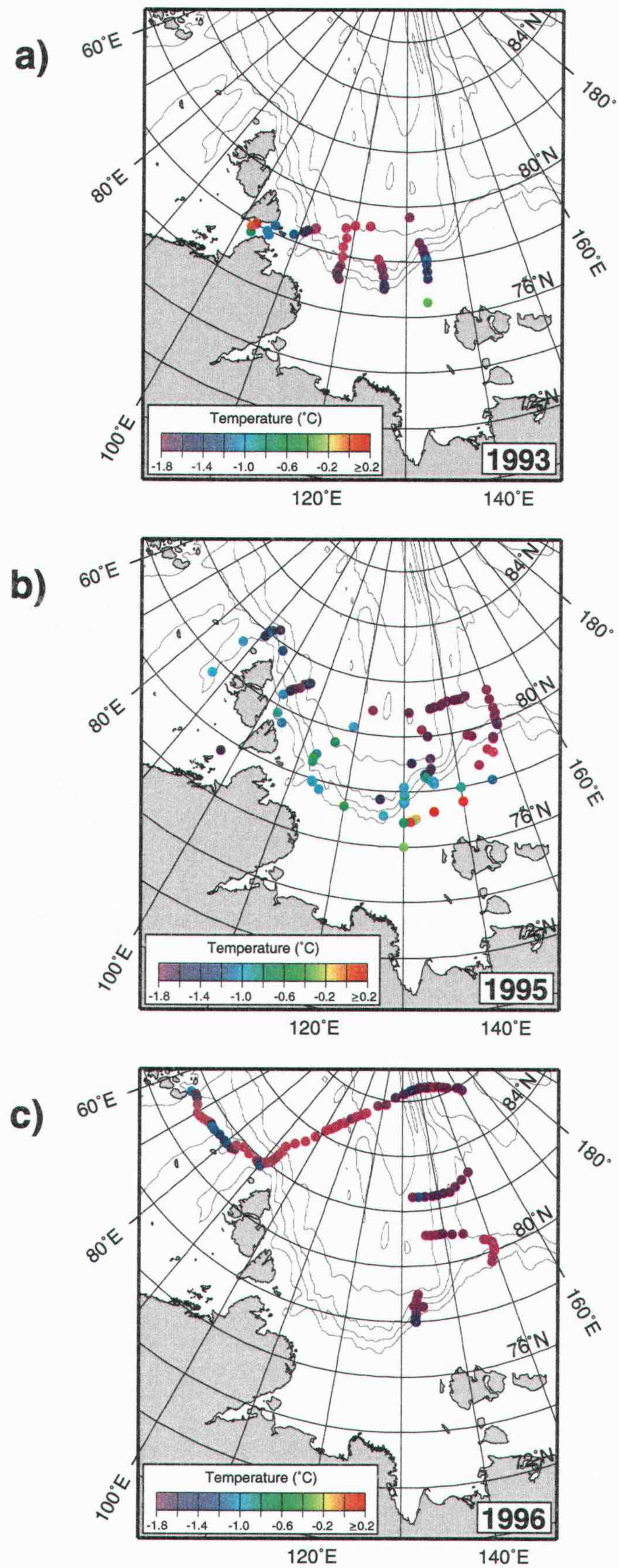
a)
60°E
80°E
100°E
120°E
140°E
180°
160°E
84°N
80°N
76°N
72°N
Temperature (°C)
-1.8 -1.4 -1.0 -0.6 -0.2 ≥0.2
1993
b)
60°E
80°E
100°E
120°E
140°E
180°
160°E
84°N
80°N
76°N
72°N
Temperature (°C)
-1.8 -1.4 -1.0 -0.6 -0.2 ≥0.2
1995
c)
60°E
80°E
100°E
120°E
140°E
180°
160°E
84°N
80°N
76°N
72°N
Temperature (°C)
-1.8 -1.4 -1.0 -0.6 -0.2 ≥0.2
1996

Figure 3.2

Figure 3.3 Distributions of mean salinity in the upper 50 m of the water column in (a) 1993, (b) 1995, and (c) 1996.

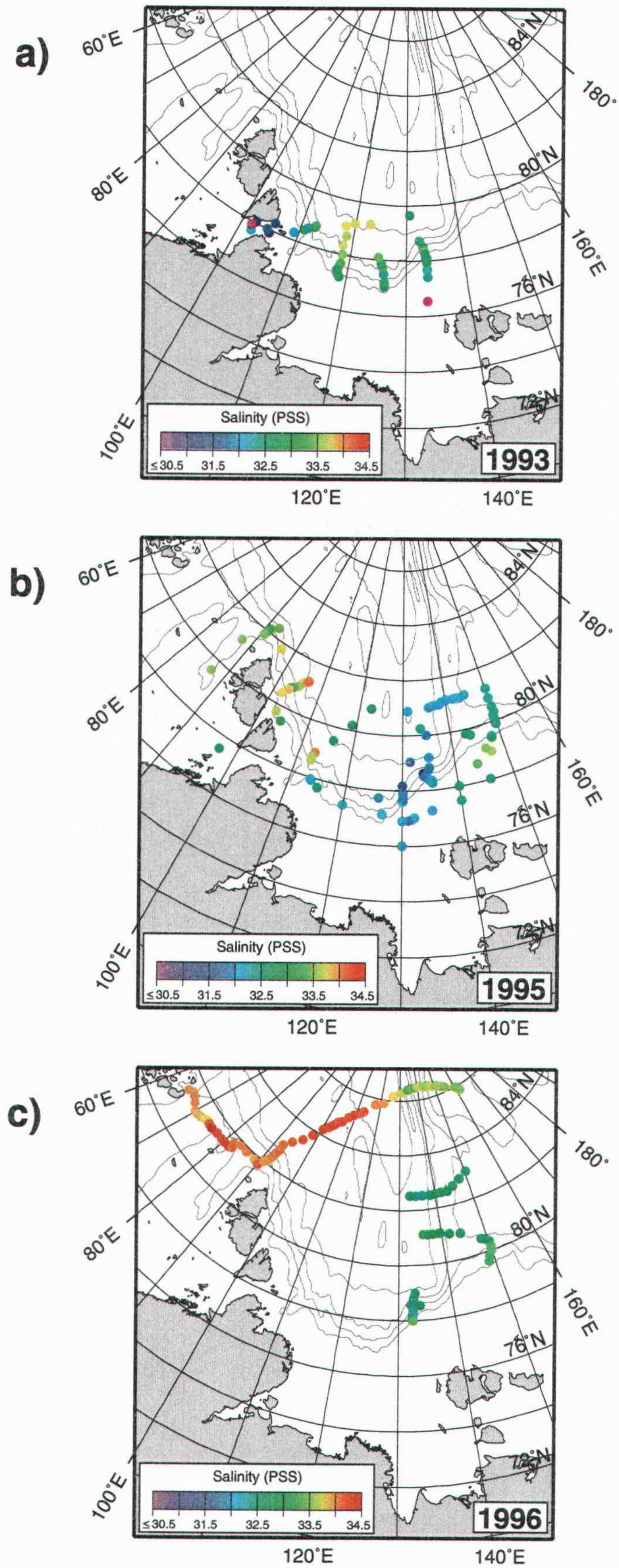
a)
60°E
80°E
100°E
84°N
180°
80°N
160°E
76°N
72°N
Salinity (PSS)
≤30.5
31.5
32.5
33.5
34.5
1993
120°E
140°E
b)
60°E
80°E
100°E
84°N
180°
80°N
160°E
76°N
72°N
Salinity (PSS)
≤30.5
31.5
32.5
33.5
34.5
1995
120°E
140°E
c)
60°E
80°E
100°E
84°N
180°
80°N
160°E
76°N
72°N
Salinity (PSS)
≤30.5
31.5
32.5
33.5
34.5
1996
120°E
140°E

Figure 3.3

Figure 3.4 Distributions of mean [Ba] in the upper 50 m of the water column in (a) 1993, (b) 1995, and (c) 1996.

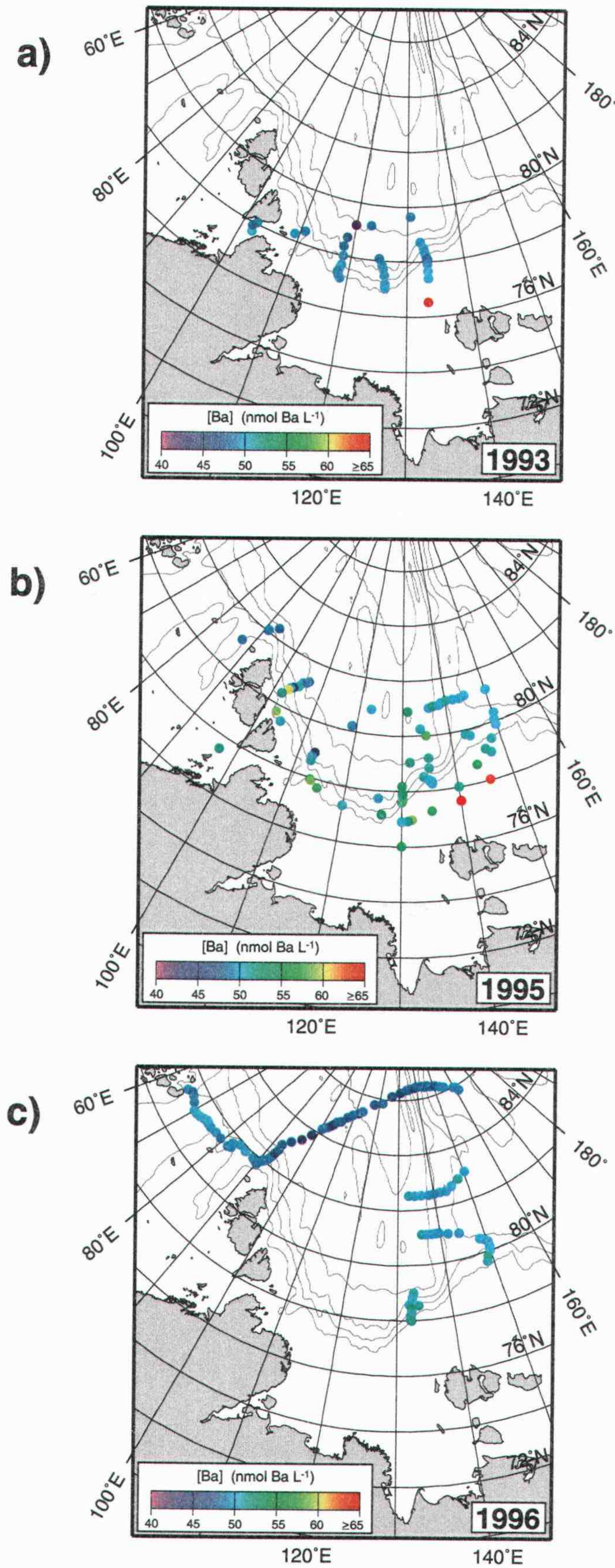
a)
60°E
80°E
100°E
84°N
80°N
76°N
72°N
180°
160°E
120°E
140°E
[Ba] (nmol Ba L-1)
40 45 50 55 60 ≥65
1993
b)
60°E
80°E
100°E
84°N
80°N
76°N
72°N
180°
160°E
120°E
140°E
[Ba] (nmol Ba L-1)
40 45 50 55 60 ≥65
1995
c)
60°E
80°E
100°E
84°N
80°N
76°N
72°N
180°
160°E
120°E
140°E
[Ba] (nmol Ba L-1)
40 45 50 55 60 ≥65
1996

Figure 3.4

salinity ranged from 32.50 to 33.48 at stations over the shelf north of the Novosibirskiye Islands and into the Makarov Basin. Mean [Ba] ranged from 49 to 56 nmol Ba L^{-1} at these stations except for two very high values (64 to 70 nmol Ba L^{-1}) observed at the southernmost, shallowest stations (bottom depths = 49 m and 33 m, respectively) in this area.

Individual profiles for the 1995 stations revealed 127 samples (out of 978 total samples) that had anomalously high [Ba] with respect to the other samples at that station and were not correlated with any features in temperature, salinity or $\delta^{18}O$ profiles [Figure 3.5; oxygen isotope data from these cruises are presented in detail by *Frank*, 1996; *Mensch et al.*, 1999; *Stein*, 1996]. Values of [Ba] were extremely high (between 240 and 800 nmol Ba L^{-1}) in 3 of these samples and ranged between 51 and 183 nmol Ba L^{-1} in the remainder. All 3 of the extreme samples and 37 of the other suspect samples were collected from the Niskin bottle in position 17 on the rosette, strongly suggesting that it was contaminated. The other anomalous samples suggest some degree of contamination from additional sources. Although we cannot be certain that these high [Ba] values do not represent contributions from some unidentified natural source, we opted for a conservative approach and excluded these suspect samples from the calculations of mean [Ba] for the 1995 stations. Note that [Ba] values for most of the 1995 samples are in agreement with values for the 1993 and 1996 samples having similar T-S properties, indicating that the entire 1995 Ba data set was not affected by contamination. While inferences based on the Ba data alone might still be regarded with uncertainty, our conclusions are reinforced by the combined tracer data set. A more complete discussion about the apparent contamination in these samples is presented in Appendix A.

Figure 3.5. ARK XI Station 44 (79.18° N, 135.06° E, occupied on August 17, 1995). Profiles of (a) temperature, (b) salinity, (c) [Ba], and (d) $\delta^{18}O$.

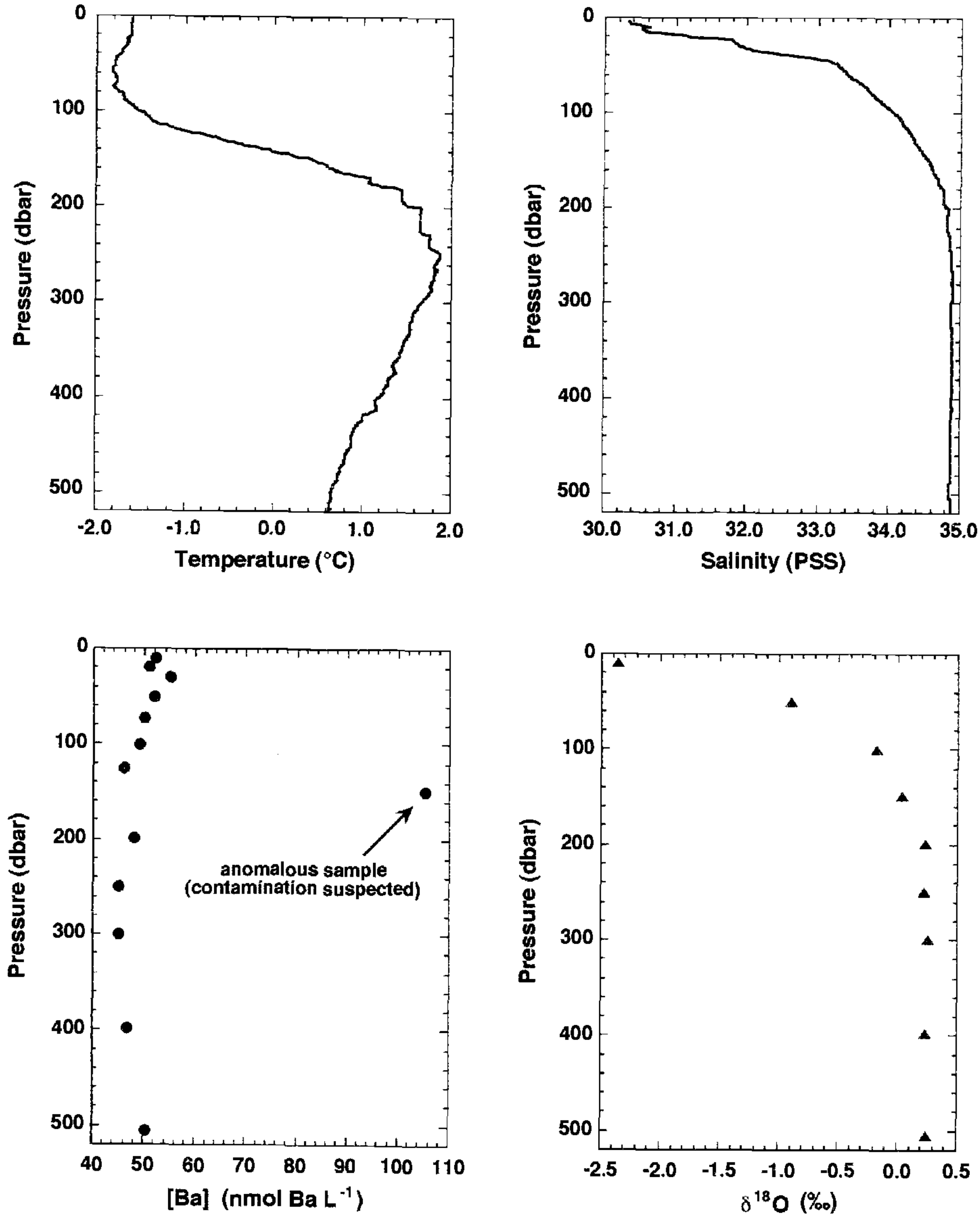

0
100
200
300
400
500
Pressure (dbar)
-2.0
-1.0
0.0
1.0
2.0
Temperature (°C)
30.0
31.0
32.0
33.0
34.0
35.0
Salinity (PSS)
40
50
60
70
80
90
100
110
[Ba] (nmol Ba L^-1)
anomalous sample
(contamination suspected)
-2.5
-2.0
-1.5
-1.0
-0.5
0.0
0.5
δ18O (‰)

Figure 3.5

3.4.3 1996 Stations

Mean temperature ranged from -1.82 to -1.34 °C, with highest values occurring near the shelf break and over the Lomonosov Ridge (Figure 3.2c). Lowest values occurred over the St. Anna and Voronin troughs and central Eurasian Basin. Mean salinity was highest (33.76 to 34.43) at stations between Franz Josef Land and Severnaya Zemlya and over the central Eurasian Basin (Figure 3.3c). Intermediate values (33.22 to 34.03) were observed over the St. Anna and Voronin troughs and along the northernmost stations over the Lomonosov Ridge. Mean salinity was lowest (32.42 to 33.61) along the more southerly transects across the Lomonosov Ridge and the slope north of the Laptev Sea and Novosibirskiye Islands. Mean [Ba] was highest (47 to 53 nmol Ba L^{-1}) at the southernmost stations over the Lomonosov Ridge and the slope north of the Laptev Sea and Novosibirskiye Islands (Figure 3.4c). Relatively high mean [Ba] (48 to 51 nmol Ba L^{-1}) was also observed over the St. Anna and Voronin troughs. Mean [Ba] ranged between 43 and 48 nmol Ba L^{-1} at the other stations.

3.5 Discussion

3.5.1 Distributions of Fluvial Discharge Inferred from Tracer Distributions

Eurasian Arctic rivers are much warmer and fresher ($T > 10$ °C, $S \approx 0$ during the summer) and fresher than the marine waters into which they flow. But temperature and salinity alone cannot be used as tracers of fluvial discharge because Arctic marine surface waters are affected by heat exchange with the atmosphere and ice melting/formation processes. Barium can be used as an additional fluvial tracer in the Arctic [*Guay and Falkner*, 1997; *Guay et al.*, 1999] due to its relative enrichment in Arctic rivers (effective end-member [Ba] = 100 to 200 nmol Ba L^{-1} for Eurasian Arctic rivers, [Ba] = 42 to 45 nmol Ba L^{-1} for North Atlantic source waters; *Guay and Falkner, 1998*). Thus in Figures

3.2-3.4, waters significantly influenced by fluvial discharge are indicated by relatively high temperature and low salinity coincident with high [Ba].

Fluvial discharge was largely confined to the Laptev shelf during the summer of 1993. The influence of the Lena River is evident at the southernmost station near the Novosibirskiye Islands. Stations in Vilkitsky Strait reflect the eastward flow of shelf waters from the Kara Sea, which contain a large fluvial component. Fluvial influence decreased over the slope and basin areas north of the shelf break.

Fluvial signals were most intense at the stations over the northeast Laptev shelf in the summer of 1995. In contrast to the situation observed in 1993, surface waters bearing a significant fluvial component extended beyond the shelf break into adjacent areas over the Amundsen and Makarov basins and the Lomonosov Ridge. The influence of river waters was also apparent near the shelf break in the vicinity of Severnaya Zemlya, indicating eastward flow from the Kara Sea and/or contributions from local sources.

Surface waters containing an appreciable fluvial component were observed over the slope north of the Laptev Sea and Novosibirskiye Islands in the summer of 1996. The influence of fluvial discharge was also evident at the stations over the Lomonosov Ridge, although it was much less pronounced along the northernmost transect across the ridge. Stations over the St. Anna and Voronin troughs suggest the outflow of river-influenced shelf waters from the Kara Sea. Fluvial signals were minimal at the stations in the central Eurasian Basin.

At the stations over the slope and basin north of the Laptev Sea (Figure 3.6; Table 3.3), vertically integrated Ba inventories for the upper 50 m of the water column were much higher in 1995 than in 1993 (two-sample t-test: $p = 2 \times 10^{-10}$, 2-sided). River water inventories calculated independently from a salinity-$\delta^{18}O$ mass balance [*Bauch et al.*, 1995; *Frank*, 1996; *Stein*, 1996] were also higher at the 1995 stations than at the 1993 stations (two-sample t-test: $p = 1 \times 10^{-5}$, 2-sided). While the data collected from this area

Figure 3.6 Stations over the slope and basin north of the Laptev Sea in (a) 1993, (b) 1995, and (c) 1996. The outlined area (79.7° N to 100 m depth contour, 110° E to 136° E) encloses all stations included in calculations of Ba and river water inventories.

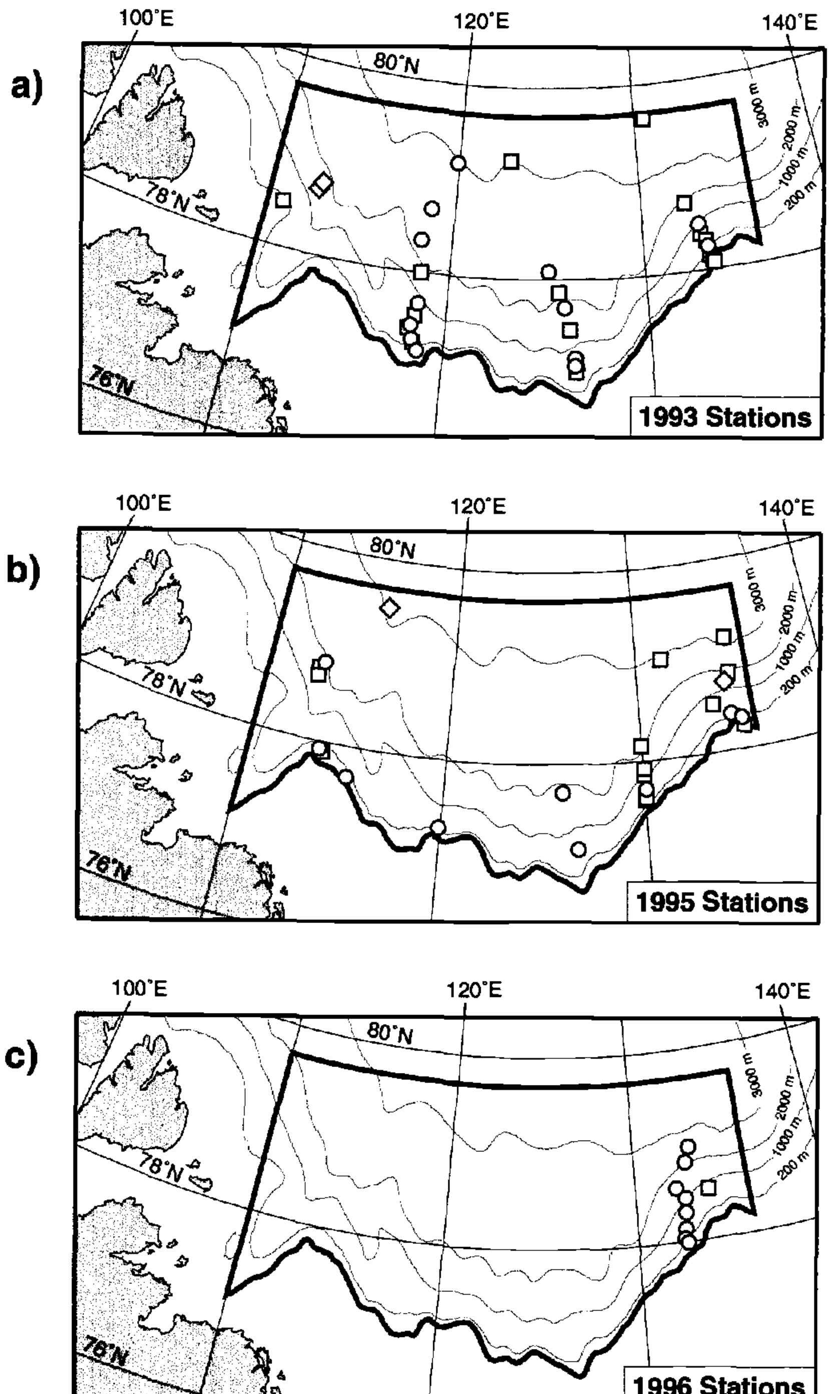
a)
100°E
120°E
140°E
80°N
78°N
76°N
3000 m
2000 m
1000 m
200 m
1993 Stations
b)
100°E
120°E
140°E
80°N
78°N
76°N
3000 m
2000 m
1000 m
200 m
1995 Stations
c)
100°E
120°E
140°E
80°N
78°N
76°N
3000 m
2000 m
1000 m
200 m
1996 Stations

Figure 3.6

Table 3.3 Comparison between Ba and river water inventories for the upper 50 m at stations north of the Laptev Sea (within the outlined area in Figure 3.6) in 1993, 1995 and 1996.

79.7° N to 100 m depth contour 110° E to 136° E,	1993 Stations	1995 Stations	1996 Stations
Ba Inventory			
Number of Stations with Ba Samples:	30	23	9
Mean Ba Inventory (mmol Ba m^{-2}):	2.34	2.62	2.60
Standard Deviation:	0.078	0.175	0.041
River Water Inventory (from salinity-$\delta^{18}O$ mass balance)			
Number of Stations with $\delta^{18}O$ samples:	19	16	1
Mean River Water Inventory (m):	2.80	4.40	4.04
Standard Deviation:	0.457	1.240	--

Figure 3.7 Stations over the Lomonosov Ridge and the slope and basin northeast of the Laptev Sea in (a) 1993, (b) 1995, and (c) 1996. The outlined area (81.3° N to 100 m contour, 129° E to 151° E) encloses all stations included in calculations of Ba and river water inventories.

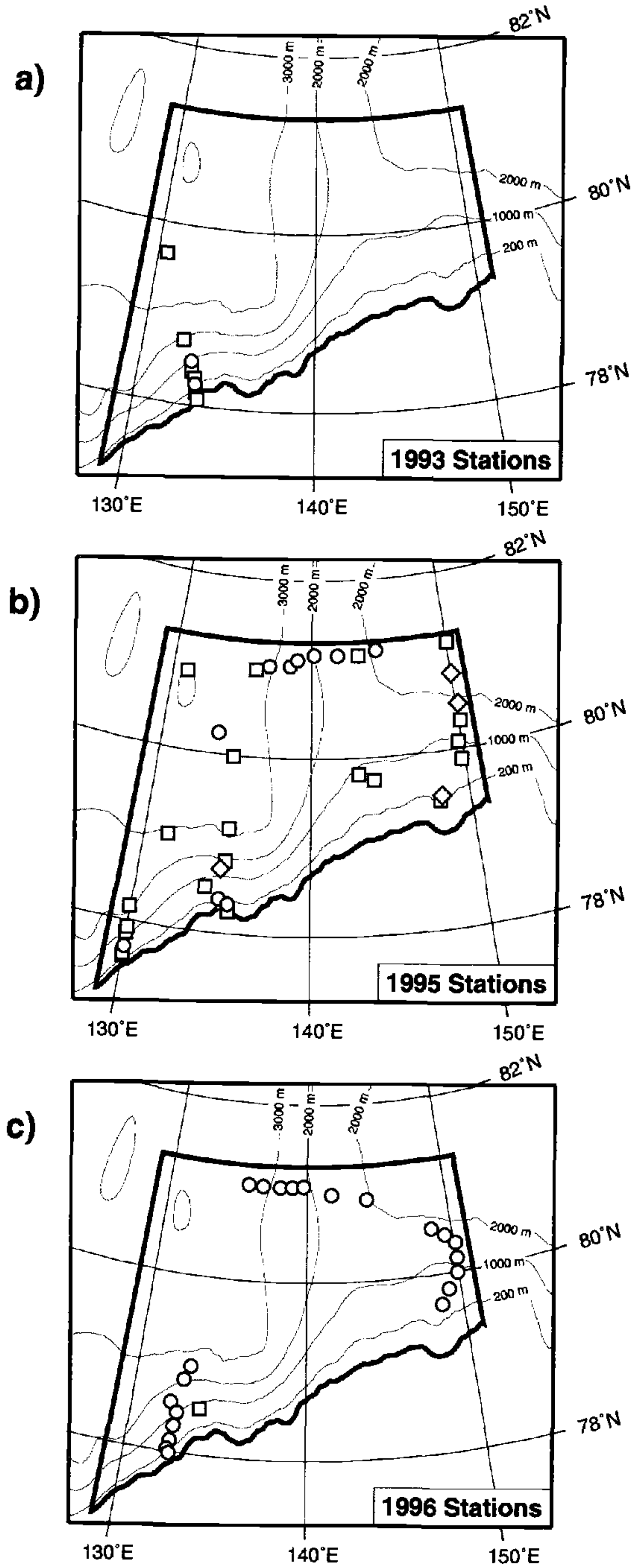
a)
82°N
80°N
78°N
3000 m
2000 m
2000 m
2000 m
1000 m
200 m
1993 Stations
130°E
140°E
150°E
b)
82°N
80°N
78°N
3000 m
2000 m
2000 m
2000 m
1000 m
200 m
1995 Stations
130°E
140°E
150°E
c)
82°N
80°N
78°N
3000 m
2000 m
2000 m
2000 m
1000 m
200 m
1996 Stations
130°E
140°E
150°E

Figure 3.7

Table 3.4. Comparison between Ba and river water inventories for the upper 50 m at stations over the southern end of the Lomonosov Ridge and the slope and basin northeast of the Laptev Sea (i.e., within the outlined area in Figure 3.7) in 1993, 1995 and 1996.

81.3° N to 100 m depth contour 129° E to 151° E	1993 Stations	1995 Stations	1996 Stations
Ba Inventory			
Number of Stations with Ba Samples:	9	32	23
Mean Ba Inventory (mmol Ba m^{-2}):	2.34	2.59	2.53
Standard Deviation:	0.063	0.117	0.090
River Water Inventory (from salinity-$\delta^{18}O$ mass balance)			
Number of Stations with $\delta^{18}O$ samples:	7	26	1
Mean River Water Inventory (m):	2.90	4.45	4.04
Standard Deviation:	0.293	0.884	--

in 1996 are insufficient to make statistically rigorous comparisons with data from other years, it appears that Ba and river water inventories were also higher in 1996 than in 1993.

At the stations over the southern end of the Lomonosov Ridge and the slope and basin northeast of the Laptev Sea (Figure 3.7, Table 3.4), vertically integrated Ba inventories for the upper 50 m of the water column were moderately higher in 1995 than in 1996 (two-sample t-test: $p = 0.047$, 2-sided). The mean river water inventory (based on salinity-$\delta^{18}O$ mass balance) for the 1995 stations was higher than the river water inventory at the single station in the area at which oxygen isotope data were collected in 1996. While the data collected from this area in 1993 are insufficient to make statistically meaningful comparisons with data from other years, it appears that Ba and river water inventories were lower in 1993 than in either 1995 or 1996.

These observations reflect the large interannual variability characteristic of surface circulation in the Laptev Sea [*Pavlov et al.*, 1996]. Despite the non-uniform distributions of sampling locations in the different years, the data suggest that more fluvial discharge flowed across the Laptev shelf and into the central Arctic basins during the summers of 1995 and 1996 than during the summer of 1993. The data also suggest, although less conclusively, that cross-shelf transport of river water from the Laptev Sea to the interior Arctic Ocean was somewhat greater in the summer of 1995 than in the summer of 1996.

3.5.2 Relationship Between Local Winds and Distributions of Fluvial Discharge

The majority of the total annual discharge of Arctic rivers occurs from June to September, when large amounts of snow and ice melt in their drainage basins (Figure 3.8). Forcing by local winds during these months in 1993, 1995 and 1996 is consistent with our inferred distributions of fluvial discharge in the Laptev Sea and surrounding areas (Figures 3.9, 3.11-3.12). The northerly and westerly winds prevalent during the summer of 1993 would have tended to cause onshore transport of the ice pack and surface waters

Figure 3.8 Mean monthly discharge for the (a) Lena River, (b) Ob River, and (c) Yenisey River. The locations at which discharge measurements were made appear in parentheses (data source: The Global Runoff Data Centre, D-56002, Koblenz, Germany).

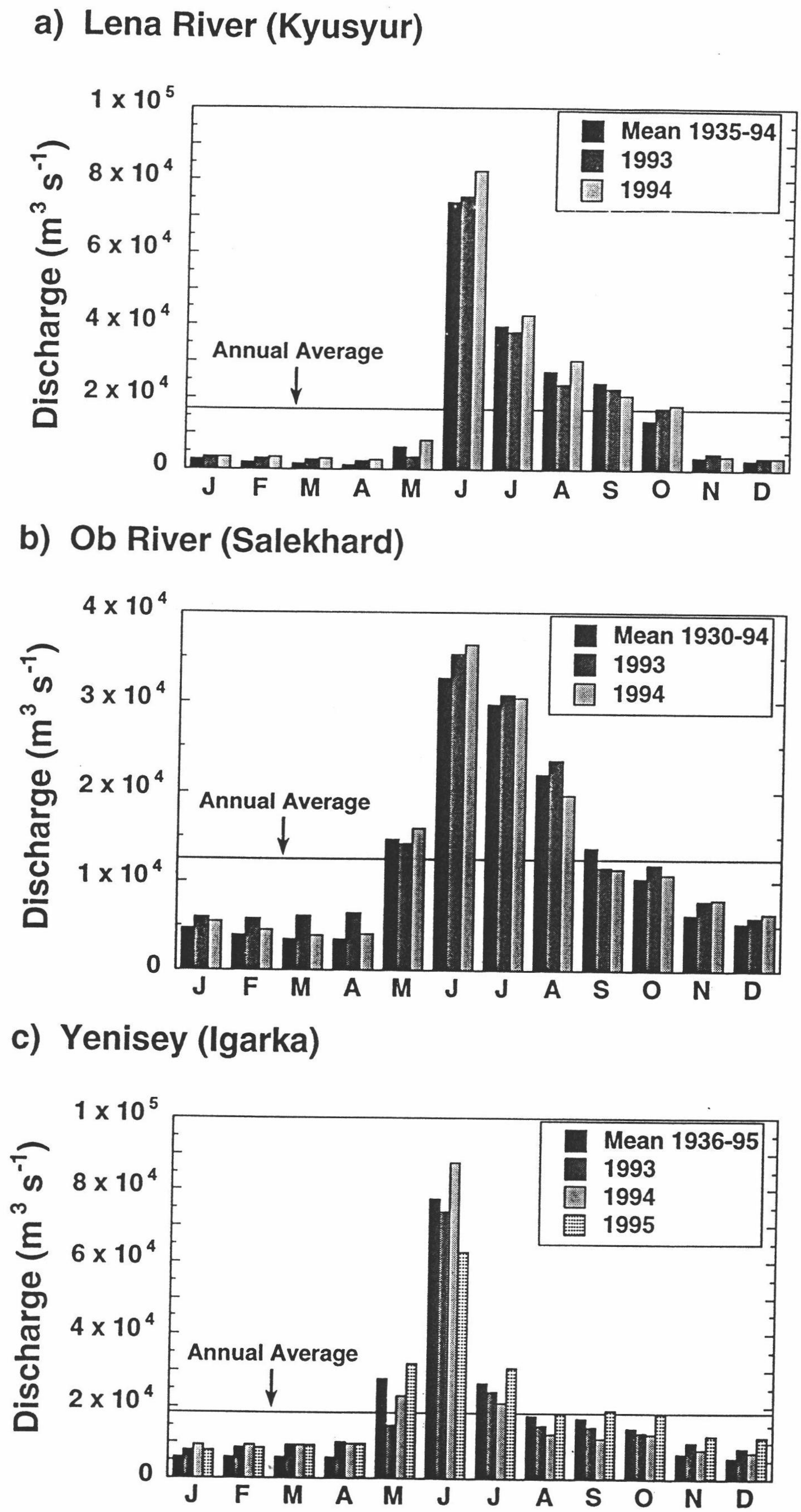
a) Lena River (Kyusyur)
Discharge (m^3 s^{-1})
1 x 10^5
8 x 10^4
6 x 10^4
4 x 10^4
2 x 10^4
0
Mean 1935-94
1993
1994
Annual Average
J F M A M J J A S O N D
b) Ob River (Salekhard)
Discharge (m^3 s^{-1})
4 x 10^4
3 x 10^4
2 x 10^4
1 x 10^4
0
Mean 1930-94
1993
1994
Annual Average
J F M A M J J A S O N D
c) Yenisey (Igarka)
Discharge (m^3 s^{-1})
1 x 10^5
8 x 10^4
6 x 10^4
4 x 10^4
2 x 10^4
0
Mean 1936-95
1993
1994
1995
Annual Average
J F M A M J J A S O N D

Figure 3.8

Figure 3.9 Monthly mean geostrophic winds in the Arctic for (a) Jun, (b) July, (c) Aug, and (d) Sep in 1993. Geostrophic winds were calculated from NOGAPS sea level pressure fields [*Hogan and Rosmond*, 1991]. Data courtesy of P. Posey and R. Preller, Naval Research Laboratory, Stennis Space Center.

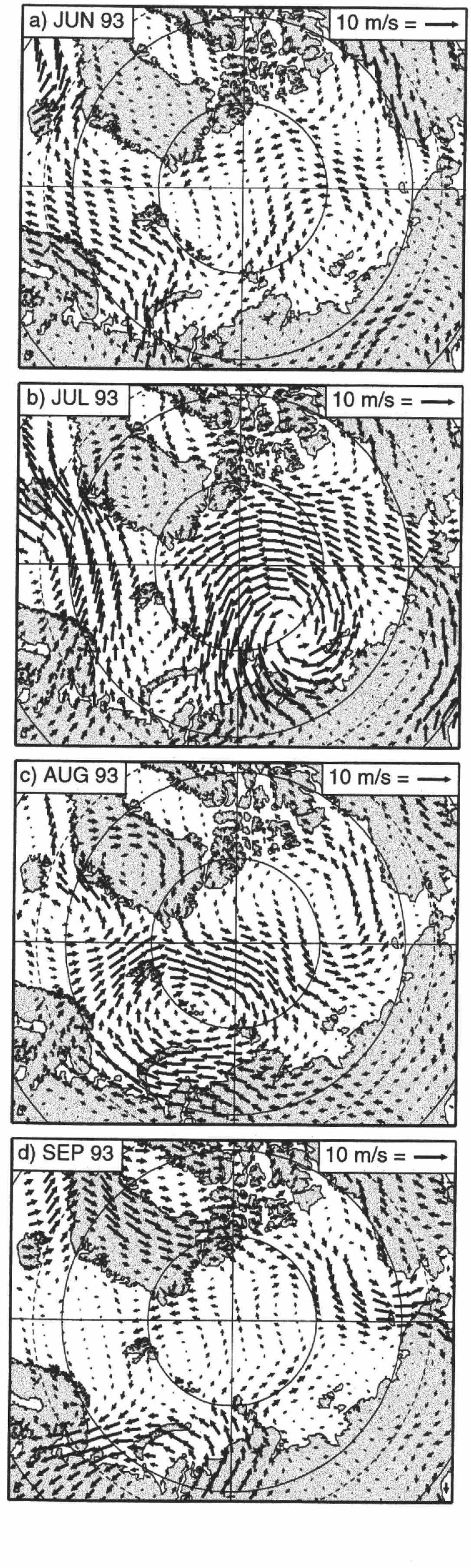

Figure 3.9

Figure 3.10 Monthly mean geostrophic winds in the Arctic for (a) Jun, (b) July, (c) Aug, and (d) Sep in 1994. Geostrophic winds were calculated from NOGAPS sea level pressure fields [*Hogan and Rosmond*, 1991]. Data courtesy of P. Posey and R. Preller, Naval Research Laboratory, Stennis Space Center.

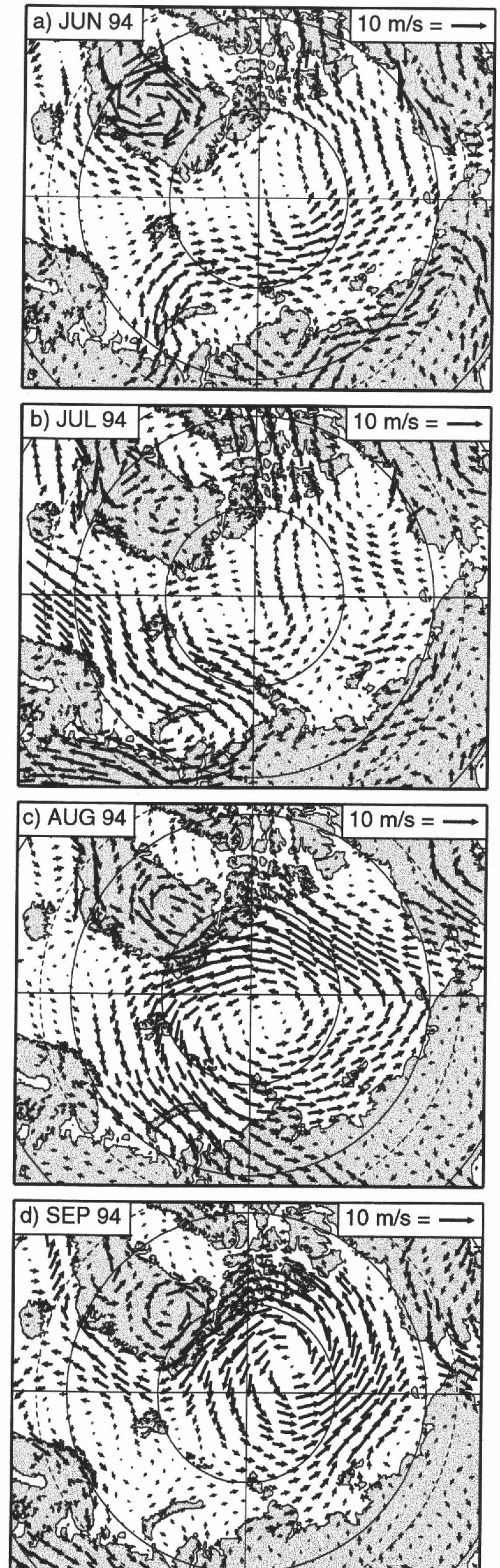

Figure 3.10

Figure 3.11 Monthly mean geostrophic winds in the Arctic for (a) Jun, (b) July, (c) Aug, and (d) Sep in 1995. Geostrophic winds were calculated from NOGAPS sea level pressure fields [*Hogan and Rosmond*, 1991]. Data courtesy of P. Posey and R. Preller, Naval Research Laboratory, Stennis Space Center.

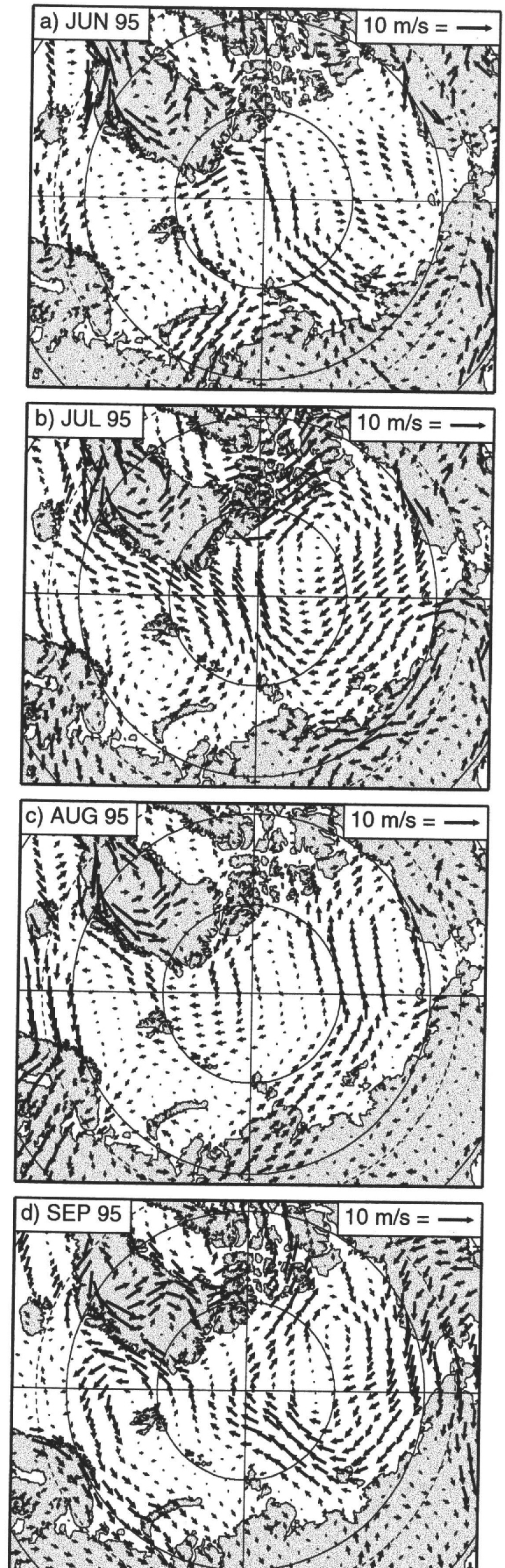

Figure 3.11

Figure 3.12 Monthly mean geostrophic winds in the Arctic for (a) Jun, (b) July, (c) Aug, and (d) Sep in 1996. Geostrophic winds were calculated from NOGAPS sea level pressure fields [*Hogan and Rosmond*, 1991]. Data courtesy of P. Posey and R. Preller, Naval Research Laboratory, Stennis Space Center.

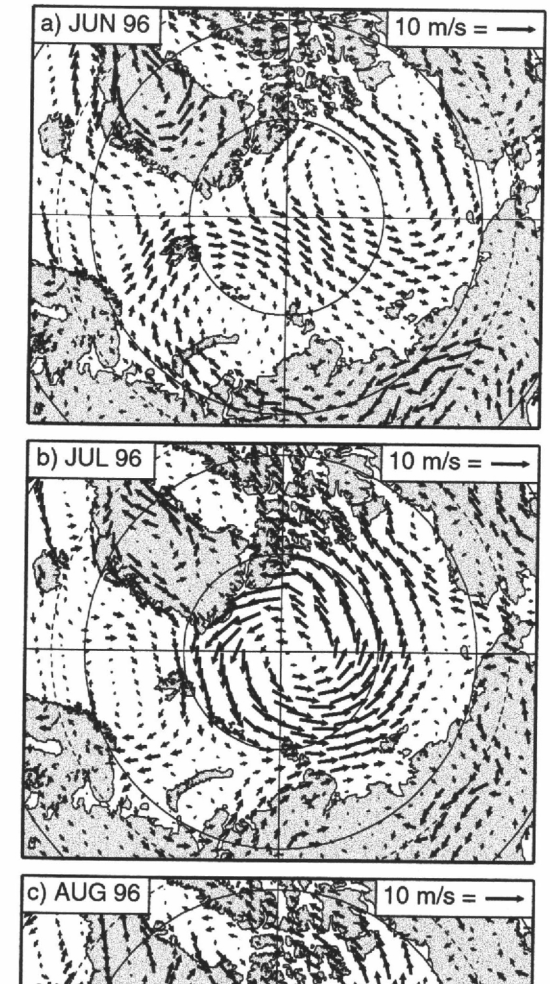

Figure 3.12

Figure 3.13 Monthly mean geostrophic winds in the Arctic for (a) Jun, (b) July, (c) Aug, and (d) Sep in 1997. Geostrophic winds were calculated from NOGAPS sea level pressure fields [*Hogan and Rosmond*, 1991]. Data courtesy of P. Posey and R. Preller, Naval Research Laboratory, Stennis Space Center.

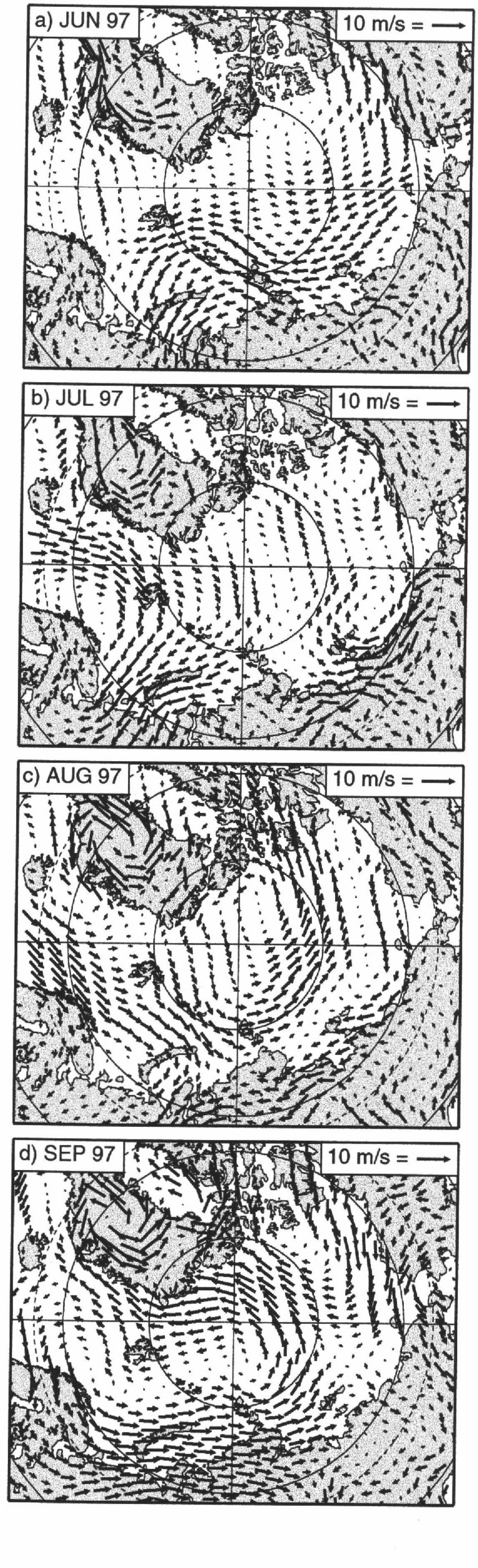

Figure 3.13

in this region. In contrast, the strong southerly to southeasterly winds present during the summer of 1995 would have tended to drive the ice pack and surface waters offshore from the Laptev shelf. Winds were mixed during the summer of 1996, but conditions associated with offshore transport prevailed in August and September (when all of the stations over the Laptev slope and southern Lomonosov Ridge were occupied).

These results indicate two principal pathways by which fluvial waters can enter the interior Arctic Ocean from the Laptev Sea. When southerly to southeasterly wind conditions prevail, shelf waters containing fluvial discharge are transported offshore beyond the Laptev shelf break and over the slope and adjacent basin areas. These waters can then be incorporated into northward surface flow aligned roughly along the Lomonosov Ridge. Under other wind conditions, fluvial discharge is steered primarily along the inner Laptev shelf and into the East Siberian Sea as part of the predominantly eastward coastal current system [*Pavlov et al.*, 1996]. These waters then appear to cross the shelf and enter the interior Arctic Ocean via upper layer flow aligned roughly along the Mendeleyev Ridge [*Guay and Falkner*, 1997; *Wheeler et al.*, 1997]. Circulation models indicate that fluvial discharge to the Kara and Laptev seas transits the shelves and enters the interior Arctic basins within a year of leaving the river mouths (W. Maslowski, personal communication). The extent to which either pathway is favored in a given year is largely determined by local wind patterns during the summer months, when fluvial discharge is greatest and shelf waters are freshest.

An understanding of the temporal variability in river water mixing pathways is relevant to investigations of the recent changes occurring in the Arctic system. From the late 1980's to the mid-1990's, a decrease in sea level pressure and a strengthening of the wintertime stratospheric polar vortex have been observed in the Arctic [*Thompson and Wallace*, 1998; *Walsh et al.*, 1996]. Changes in ocean circulation have also occurred over the same time period and appear to be related to changes in atmospheric forcing. The Beaufort Gyre has weakened, and waters of Atlantic origin have advanced farther into the

Arctic basin [*Carmack et al.*, 1997; *Carmack et al.*, 1995; *Morison et al.*, 1998]. As a result, the boundary between Atlantic and Pacific water masses and the axis of the Transpolar Drift have shifted from the Lomonosov Ridge to a position aligned roughly over the Mendeleyev Ridge [*Carmack et al.*, 1995; *McLaughlin et al.*, 1996; *Morison et al.*, 1998]. Decreases in Arctic sea ice cover have also been observed, which may be the result of divergent flow associated with these atmospheric and oceanic conditions [*Maslanik et al.*, 1996; *McPhee et al.*, 1998]. Whether these trends reflect a naturally occurring oscillation between two dominant circulation modes of the Arctic ice-ocean-atmosphere system [*Proshutinsky and Johnson*, 1997] and/or the effects of anthropogenic climate change [*Fyfe et al.*, 1999; *Shindell et al.*, 1999] remains unclear.

Data collected from the central Eurasian Basin during two submarine cruises in Aug-Sep 1993 and Apr-May 1995 show a salinification of the upper water column and a diminishing of the cold halocline layer relative to previous years [*Steele and Boyd*, 1998]. These observations were also attributed to the recent changes in Arctic atmospheric conditions, which were presumed to have shifted the primary insertion point of river-influenced Kara and Laptev shelf waters from the Amundsen Basin to the Makarov Basin since the late 1980's. Our tracer distributions and wind data for the summer of 1993 provide direct evidence in support of this mechanism. Further evidence is provided by tracer data from other cruises to the Arctic in 1993-1994 [*Guay and Falkner*, 1997; *Wheeler et al.*, 1997] suggesting the transport of Eurasian river water to the Arctic interior along the Mendeleyev Ridge (local winds during the season of maximum river discharge in 1994 would have also tended to oppose offshore transport from the Laptev shelf to adjacent areas of the Eurasian Basin, therefore favoring the Mendeleyev pathway over the Lomonosov pathway; Figure 3.10).

Our results further demonstrate, however, that cross-shelf transport of river water from the Laptev Sea to the interior Arctic Ocean resumed during the summers of 1995 and 1996. Although no tracer data were available for 1997, wind conditions associated with offshore transport from the Laptev shelf prevailed during most of the summer in this year as well (Figure 3.13). These observations suggest that discharge from Siberian rivers would have contributed to reestablishing the cold halocline layer in the Eurasian Basin in the years following the submarine cruise in the spring of 1995. Preliminary data from subsequent submarine cruises to the Arctic in 1996-1998 support this hypothesis (R. Muench, unpublished data). It therefore appears that the areal extent of fluvial influence and the formation of cold halocline water in the Eurasian Basin depends most strongly on the transport of shelf waters from the Laptev Sea to the interior Arctic Ocean along the Lomonosov Ridge pathway.

3.6 Conclusions

Because the areal distribution of fluvial discharge as well as the total amount of runoff ultimately determines its effect on Arctic Ocean circulation, it is important to understand the mechanisms governing the transport pathways of Eurasian Arctic river discharge and their temporal variability. Based on model results, observations of ice motion and a limited number of tracer measurements, it had previously been speculated that fluvial discharge to the Kara and Laptev seas enters the interior Arctic Ocean via surface flows aligned roughly along the Lomonosov and Mendeleyev ridges. Our data provide direct evidence of these transport pathways and indicate that they are driven primarily by atmospheric forcing. While recent investigations of variability in the Arctic system have focused on annually averaged large-scale atmospheric conditions, our data suggest that the extent to which either pathway is favored in a given year depends most strongly on local winds during the summer period of maximum runoff.

3.7 References

Aagaard, K., and E.C. Carmack, The role of sea ice and other fresh water in the Arctic circulation, *J. Geophys. Res.*, *94* (C10), 14,485-14,498, 1989.

Anderson, L.G., K. Olsson, and A. Skoog, Distribution of dissolved inorganic and organic carbon in the Eurasian Basin of the Arctic Ocean, in *The Polar Oceans and Their Role in Shaping the Global Environment*, edited by O.M. Johannessen, R.D. Muench, and J.E. Overland, pp. 255-262, Washington DC, 1994.

Bauch, D., P. Schlosser, and R. Fairbanks, Freshwater balance and the sources of deep and bottom waters in the Arctic Ocean inferred from the distribution of $H_2{}^{18}O$, *Prog. Oceanog.*, *35*, 53-80, 1995.

Carmack, E.C., K. Aagaard, J.H. Swift, R.W. Macdonald, F.A. McLaughlin, E.P. Jones, R.G. Perkin, J.N. Smith, K.M. Ellis, and L.R. Killius, Changes in temperature and tracer distributions within the Arctic Ocean: Results from the 1994 Arctic Ocean Section, *Deep-Sea Res. II*, *44* (8), 1487-1502, 1997.

Carmack, E.C., R.W. Macdonald, R.G. Perkin, F.A. McLaughlin, and R.J. Pearson, Evidence for warming of Atlantic water in the southern Canadian Basin of the Arctic Ocean: Results from the Larsen-93 expedition, *Geophys. Res. Lett.*, *22* (9), 1061-1064, 1995.

Frank, M., Spurenstoffuntersuchungen zur Zirkulation im Eurasischen Becken des Nordpolarmeeres, Erlangung der Doktorwürde thesis, Ruprecht-Karls-Universität, Heidelberg, 1996.

Fyfe, J.C., G.J. Boer, and G.M. Flate, The Arctic and Antarctic oscillations and their projected changes under global warming, *Geophys. Res. Lett.*, *26* (11), 1601-1604, 1999.

Guay, C.K., and K.K. Falkner, Barium as a tracer of Arctic halocline and river waters, *Deep-Sea Res. II*, *44* (8), 1543-1569, 1997.

Guay, C.K., and K.K. Falkner, A survey of dissolved barium in the estuaries of major Arctic rivers and adjacent seas, *Cont. Shelf Res.*, *18*, 859-882, 1998.

Guay, C.K., G.P. Klinkhammer, K.K. Falkner, R. Benner, P. Coble, T. Whitledge, B. Black, F.J. Bussell, and T.A. Wagner, High-resolution measurements of dissolved organic carbon in the Arctic Ocean by *in situ* fiber-optic spectrometry, *Geophys. Res. Lett.*, *26* (8), 1007-1010, 1999.

Hogan, T.F., and T.E. Rosmond, The description of the Navy Operational Global Atmospheric Prediction System, *Mon. Weather Rev.*, *119* (8), 1786-1815, 1991.

Jones, E.P., L.G. Anderson, and D.W.R. Wallace, Tracers of near-surface, halocline and deep waters in the Arctic Ocean: Implications for circulation, *J. Mar. Sys.*, *2*, 241-255, 1991.

Macdonald, R.W., and J.M. Bewers, Contaminants in the arctic marine environment: priorities for protection, *ICES J. Mar Sci.*, *53*, 537-563, 1996.

Maslanik, J.A., S.M. C., and R.G. Barry, Recent decreases in Arctic summer ice cover and linkages to atmospheric circulation anomalies, *Geophys. Res. Lett.*, *23* (13), 1677-1680, 1996.

Maslowski, W., Y. Zhang, and A.J. Semtner, Modeling fresh water sources, their distribution and sinks in the Arctic Ocean, in *ACSYS Conference on Polar Processes and Global Climate*, edited by K. Aagaard, D. Hartmann, V. Kattsov, D. Martinson, R. Stewart, and A. Weaver, pp. 159-161, World Climate Research Programme, Rosario, WA, USA, 1998.

McLaughlin, F.A., E.C. Carmack, R.W. Macdonald, and J.K.B. Bishop, Physical and geochemical properties across the Atlantic/Pacific water mass front in the southern Canadian Basin, *J. Geophys. Res.*, *101* (C1), 1183-1197, 1996.

McPhee, M.G., T.P. Stanton, J.H. Morison, and D.G. Martinson, Freshening of the upper ocean in the Arctic: Is perennial sea ice disappearing?, *Geophys. Res. Lett.*, *25* (10), 1729-1732, 1998.

Mensch, M., M. Frank, W. Stein, and R. Bayer, Distribution and circulation of water masses on the Eurasian shelves of the Arctic Ocean, *J. Geophys. Res.*, *in preparation*, 1999.

Meybeck, M., and A. Ragu, *River Discharges to the Oceans: An assessment of suspended solids, major ions and nutrients*, 245 pp., UNEP, Paris, 1995.

Morison, J., M. Steele, and R. Andersen, Hydrography of the upper Arctic Ocean measured from the nuclear submarine *USS Pargo*, *Deep-Sea Res. I*, *45*, 15-38, 1998.

Östlund, H.G., and G. Hut, Arctic Ocean water mass balance from isotope data, *J. Geophys. Res.*, *89*, 6373-6381, 1984.

Pavlov, V.K., L.A. Timokhov, G.A. Baskakov, M.Y. Kulakov, V.K. Kurazhov, P.V. Pavlov, S.V. Pivovarov, and V.V. Stanovoy, Hydrometeorological Regime of the Kara, Laptev, and East Siberian Seas, Applied Physics Laboratory, University of Washington, 1996.

Proshutinsky, A.Y., and M. Johnson, Two regimes of the Arctic Ocean circulation from ocean models and observations, *Eos, Trans. Am. Geophys. Union*, *76* (3), Abstract No. OS-29, 1996.

Proshutinsky, A.Y., and M.A. Johnson, Two circulation regimes of the wind-driven Arctic Ocean, *J. Geophys. Res.*, *102* (C6), 12,493-12,514, 1997.

Rudels, B., L.G. Anderson, and E.P. Jones, Formation and evolution of the surface mixed layer and halocline of the Arctic Ocean, *J. Geophys. Res.*, *101* (C4), 8807-8821, 1996.

Rudels, B., E.P. Jones, L.G. Anderson, and G. Kattner, On the intermediate depth waters of the Arctic Ocean, in *The Polar Oceans and Their Role in Shaping the Global Environment*, edited by O.M. Johannessen, R.D. Muench, and J.E. Overland, pp. 33-46, AGU Geophysical Monograph, Washington DC, 1994.

Schauer, U., R.D. Muench, B. Rudels, and L. Timokhov, Impact of eastern Arctic shelf waters on the Nansen Basin intermediate layers, *J. Geophys. Res.*, *102* (C2), 3371-3382, 1997.

Shindell, D.T., R.L. Miller, G.A. Schmidt, and L. Pandolfo, Simulation of recent northern winter climate trends by greenhouse-gas forcing, *Nature*, *3*, 452-455, 1999.

Steele, M., and T. Boyd, Retreat of the cold halocline layer in the Arctic Ocean, *J. Geophys. Res.*, *103* (C5), 10,419-10,435, 1998.

Stein, W., ^{18}O- und ^{3}H-Untersuchungen im Nordpolarmeer, Diplomarbeit, Ruprecht-Karls-Universität, Heidelberg, 1996.

Thompson, D.W.J., and J.M. Wallace, The Arctic Oscillation signature in the wintertime geopotential height and temperature fields, *Geophys. Res. Lett.*, *25* (9), 1297-1300, 1998.

Walsh, J.E., W.L. Chapman, and T.L. Shy, Recent decrease of sea level pressure in the central Arctic, *J. Climate*, *9*, 480-486, 1996.

Wheeler, P.A., J.M. Watkins, and R.L. Hansing, Nutrients, organic carbon and nitrogen in the upper water column of the Arctic Ocean: implications for the sources of dissolved organic carbon, *Deep-Sea Res. II*, *44* (8), 1571-1592, 1997.

4. FACTOR ANALYSIS OF TRACER DATA FROM THE LAPTEV SEA

4.1 Introduction

Factor analysis refers to a group of interrelated computational procedures that are used to simplify a set of multivariate observations and reveal its underlying structure [*Davis*, 1973]. All of the various methods of factor analysis involve the multiplication of a data matrix by its transpose, and the extraction of eigenvalues and eigenvectors from the resulting square matrix. Q-mode factor analysis investigates the relationships between individual observations within a data set and attempts to identify patterns in their arrangement in multivariate space.

This chapter describes a preliminary exploration of the utility of factor analysis for testing *a priori* assumptions about the nature of Arctic water mass composition. Q-mode factor analysis techniques were applied to a set of multivariate tracer data (salinity, oxygen isotopes and barium) collected from the Laptev Sea in 1993. This analysis was performed to test a mixing model that describes Laptev Sea waters as a combination of three primary end-members: Atlantic water, river discharge, and ice-melt. The properties of the factors returned by the q-mode analysis are compared to the given properties of the end-members specified in the model. The factor loadings are mapped to see if their spatial distribution is consistent with expected distributions for Atlantic water, river discharge and ice-melt in the Laptev Sea and adjacent areas.

4.2 Data and Analytical Procedure

The data presented here were collected during the ARK IX/4 cruise to the Laptev Sea onboard the R/V *Polarstern* in Aug-Sep 1993. Salinity, [Ba] and $\delta^{18}O$ data were collected at 12 stations in the vicinity of the northeastern Laptev Sea, along a 360-km transect running from shelf to basin (Figure 4.1). Vertical salinity profiles were obtained at each

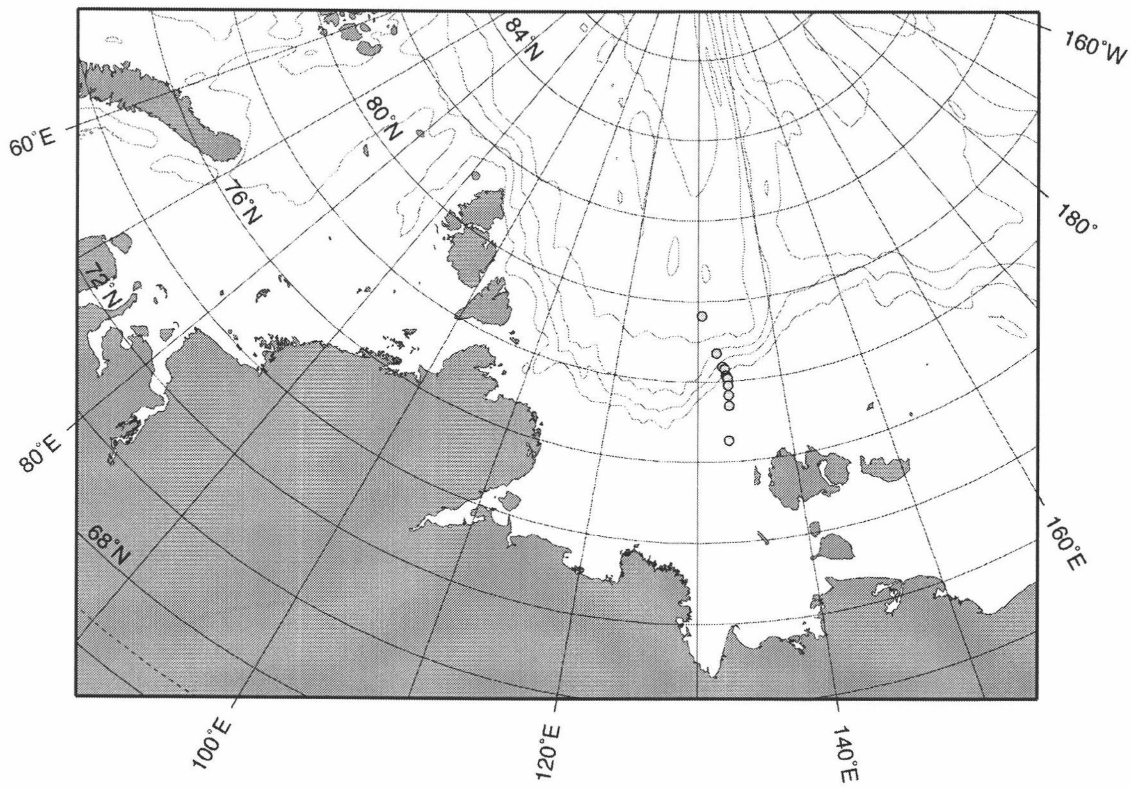

Figure 4.1 Transect in the vicinity of the northeastern Laptev Sea along which salinity, [Ba] and $\delta^{18}O$ data were collected during the ARK IX/4 *Polarstern* cruise in summer 1993.

station by CTD casts, and water samples for [Ba] and $\delta^{18}O$ analyses were collected at depths throughout the water column. Only the samples collected at depths shallower than 210 m (53 total samples) were included in the factor analysis.

4.3 Results

The results of the q-mode factor analysis, with varimax rotation, are shown in Table 4.1 (computational procedures are described in *Davis*, 1973). The first two eigenvalues of the similarity matrix accounted for nearly 100% of the observed variance. The factor composition scores were compared with the given properties of the Atlantic, fluvial and ice-melt end-members proposed for the three end-member mixing model (Table 4.2). Factor 2 matches the Atlantic end-member closely. Factor 1 matches the sense of the river end-member relative to the Atlantic end-member (i.e., lower salinity, higher [Ba] and more negative $\delta^{18}O$), but the factor composition scores do not exactly match the values given for the river end-member. Applying non-orthogonal rotation techniques may make the factor composition scores more closely match the actual salinity, [Ba] and $\delta^{18}O$ values of the end-members.

The factor 1 loadings are highest over the shelf, steadily decreasing in an offshore direction over the slope and basin areas north of the shelf break (Figure 4.2a). The geographical distribution of the factor 1 loadings is consistent with its interpretation as a river end-member. The factor 2 loadings are high over the basin and slope, decreasing in an onshore direction to maximum values over the shelf (Figure 4.2b). The geographical distribution of the factor 2 loadings is consistent with its interpretation as an Atlantic end-member. These results partially support the three end-member mixing model proposed for the Laptev Sea. While the factor analysis did a fair to good job capturing the Atlantic and river end-members, it did not successfully capture the expected ice-melt end-member. This is not surprising in light of the minimal influence of ice melting and formation

Table 4.1 Results of q-mode factor analysis and varimax rotation for the 1993 *Polarstern* data from the Laptev Sea.

Table 4.1

Variable Number	Variable	Means	Variance
1	Salinity (PSS)	33.35	1.85
2	[Ba] (nmol L^{-1})	47.0	22.4
3	$\delta^{18}O$ (‰)	-0.75	0.80

Constant Means Transform

Eigenvalues	Percent Variance	Cum.Variance
43.466	82.01	82.01
9.514	17.95	99.96

Factor Loadings Matrix

Station Number	Depth (m)	Factor 1	Factor 2	Communality
31	13	0.6978	-0.7156	0.9989
31	30	0.7818	-0.6229	0.9992
31	33	0.7852	-0.6185	0.9990
43	4	0.7057	-0.7083	0.9998
43	14	0.81	-0.5864	1.0000
43	29	0.949	-0.313	0.9986
43	48	0.9369	-0.3493	0.9998
42	11	0.7745	-0.6308	0.9977
42	22	0.9122	-0.4095	0.9999
42	37	0.9738	-0.2227	0.9980
42	57	0.9845	-0.1726	0.9990
41	9	0.8281	-0.5592	0.9985
41	49	0.9971	-0.0738	0.9997
40	15	0.9437	-0.3295	0.9992
40	49	0.9979	-0.0637	0.9998
40	74	0.9889	0.1483	1.0000
40	124	0.8927	0.4504	0.9998
40	174	0.7896	0.613	0.9992
40	209	0.7538	0.6571	1.0000
39	11	0.8957	-0.4416	0.9974
39	73	0.9919	0.1255	0.9996
39	99	0.9587	0.2845	1.0000
38	9	0.9467	-0.322	1.0000
38	18	0.9407	-0.3389	0.9998
38	32	0.9769	-0.2129	0.9997
38	59	0.9935	0.1138	1.0000
38	107	0.8524	0.5228	0.9998

Table 4.1 (continued)

Station Number	Depth (m)	Factor 1	Factor 2	Communality
38	122	0.8572	0.5148	0.9999
38	171	0.7716	0.636	1.0000
36	10	0.9386	-0.3449	1.0000
36	46	0.9998	0.0209	1.0000
36	96	0.9096	0.4154	1.0000
36	196	0.8274	0.5616	0.9999
35	14	0.9426	-0.334	1.0000
35	50	0.9993	0.0363	1.0000
35	99	0.9634	0.2681	1.0000
34	102	0.9729	0.2308	0.9999
34	203	0.8103	0.586	1.0000
32	12	0.9421	-0.3352	1.0000
32	22	0.9361	-0.3517	1.0000
32	47	0.9997	-0.0252	1.0000
32	98	0.9495	0.3127	0.9993
32	147	0.8463	0.5326	1.0000
32	198	0.7938	0.6082	1.0000
33	12	0.8996	-0.4366	0.9998
33	24	0.9398	-0.3416	1.0000
33	48	0.9994	0.0307	0.9998
33	74	0.9974	0.0713	0.9999
33	97	0.9867	0.1624	0.9999
33	127	0.9173	0.3982	0.9999
33	146	0.8797	0.4755	0.9999
33	170	0.8462	0.5329	1.0000
33	197	0.7992	0.6011	1.0000
	Percent Info:	82.0116	17.9511	
	Cumulative Info:	82.0116	99.9627	

Principal Factor Scores Matrix

Variable Number	Variable	Factor 1	Factor 2
1	Salinity (PSS)	0.6396	0.3633
2	[Ba] (nmol L^{-1})	0.6239	0.2694
3	$\delta^{18}O$ (‰)	0.4491	-0.8918

Scaled Factor Scores Matrix

Variable Number	Variable	Factor 1	Factor 2
1	Salinity (PSS)	1.1079	0.6293
2	[Ba] (nmol L^{-1})	1.0806	0.4667
3	$\delta^{18}O$ (‰)	0.7778	-1.5447

Table 4.1 (continued)

Factor Composition Scores

Variable Number	Variable	Factor 1	Factor 2
1	Salinity (PSS)	33.75	37.90
2	[Ba] (nmol L^{-1})	46.4	39.6
3	$\delta^{18}O$ (‰)	-0.53	2.10

Varimax Factor Loadings Matrix

Station Number	Depth (m)	Factor 1	Factor 2	Communality
31	13	0.9991	-0.0270	0.9989
31	30	0.9948	0.0980	0.9992
31	33	0.9941	0.1035	0.9990
43	4	0.9998	-0.0163	0.9998
43	14	0.9896	0.1438	1.0000
43	29	0.8988	0.4367	0.9986
43	48	0.9154	0.4023	0.9998
42	11	0.995	0.0873	0.9977
42	22	0.9397	0.3419	0.9999
42	37	0.8537	0.5188	0.9980
42	57	0.8264	0.5622	0.9990
41	9	0.9836	0.1759	0.9985
41	49	0.7666	0.6419	0.9997
40	15	0.9065	0.4212	0.9992
40	49	0.7601	0.6497	0.9998
40	74	0.606	0.7955	1.0000
40	124	0.3265	0.9451	0.9998
40	174	0.1392	0.9899	0.9992
40	209	0.0828	0.9966	1.0000
39	11	0.9502	0.3074	0.9974
39	73	0.6240	0.7812	0.9996
39	99	0.4894	0.8721	1.0000
38	9	0.9034	0.4287	1.0000
38	18	0.9109	0.4124	0.9998
38	32	0.8491	0.5280	0.9997
38	59	0.6333	0.7739	1.0000
38	107	0.2471	0.9689	0.9998
38	122	0.2561	0.9666	0.9999

Table 4.1 (continued)

Station Number	Depth (m)	Factor 1	Factor 2	Communality
38	171	0.1103	0.9939	1.0000
36	10	0.9135	0.4067	1.0000
36	46	0.7025	0.7117	1.0000
36	96	0.3629	0.9318	1.0000
36	196	0.2022	0.9793	0.9999
35	14	0.9088	0.4172	1.0000
35	50	0.6915	0.7224	1.0000
35	99	0.5042	0.8636	1.0000
34	102	0.537	0.8435	0.9999
34	203	0.1729	0.9849	1.0000
32	12	0.9093	0.4161	1.0000
32	22	0.9165	0.4000	1.0000
32	47	0.7346	0.6785	1.0000
32	98	0.4631	0.8859	0.9993
32	147	0.2359	0.9718	1.0000
32	198	0.1456	0.9893	1.0000
33	12	0.9494	0.3137	0.9998
33	24	0.9121	0.4099	1.0000
33	48	0.6955	0.7184	0.9998
33	74	0.6657	0.7461	0.9999
33	97	0.5945	0.8040	0.9999
33	127	0.3805	0.9247	0.9999
33	146	0.2996	0.9540	0.9999
33	170	0.2356	0.9718	1.0000
33	197	0.1544	0.988	1.0000
	Percent Info	50.9079	49.0548	
	Cumulative Info	50.9079	99.9627	

Varimax Principal Factor Scores Matrix

Variable Number	Variable	Factor 1	Factor 2
1	Salinity (PSS)	0.2056	0.7063
2	[Ba] (nmol L^{-1})	0.2597	0.6280
3	$\delta^{18}O$ (‰)	0.9435	-0.3268

Table 4.1 (continued)

Varimax Scaled Factor Scores Matrix

Variable Number	Variable	Factor 1	Factor 2
1	Salinity (PSS)	0.3561	1.2234
2	[Ba] (nmol L^{-1})	0.4499	1.0876
3	$\delta^{18}O$ (‰)	1.6343	-0.5660

Variable Number	Variable	Factor 1	Factor 2
1	Salinity (PSS)	29.74	35.17
2	[Ba] (nmol L^{-1})	52.9	44.0
3	$\delta^{18}O$ (‰)	-3.07	0.37

Figure 4.2 Distributions along the transect of factor loadings from the q-mode analysis with varimax rotation: (a) Factor 1 and (b) Factor 2. Black dots indicate locations of samples.

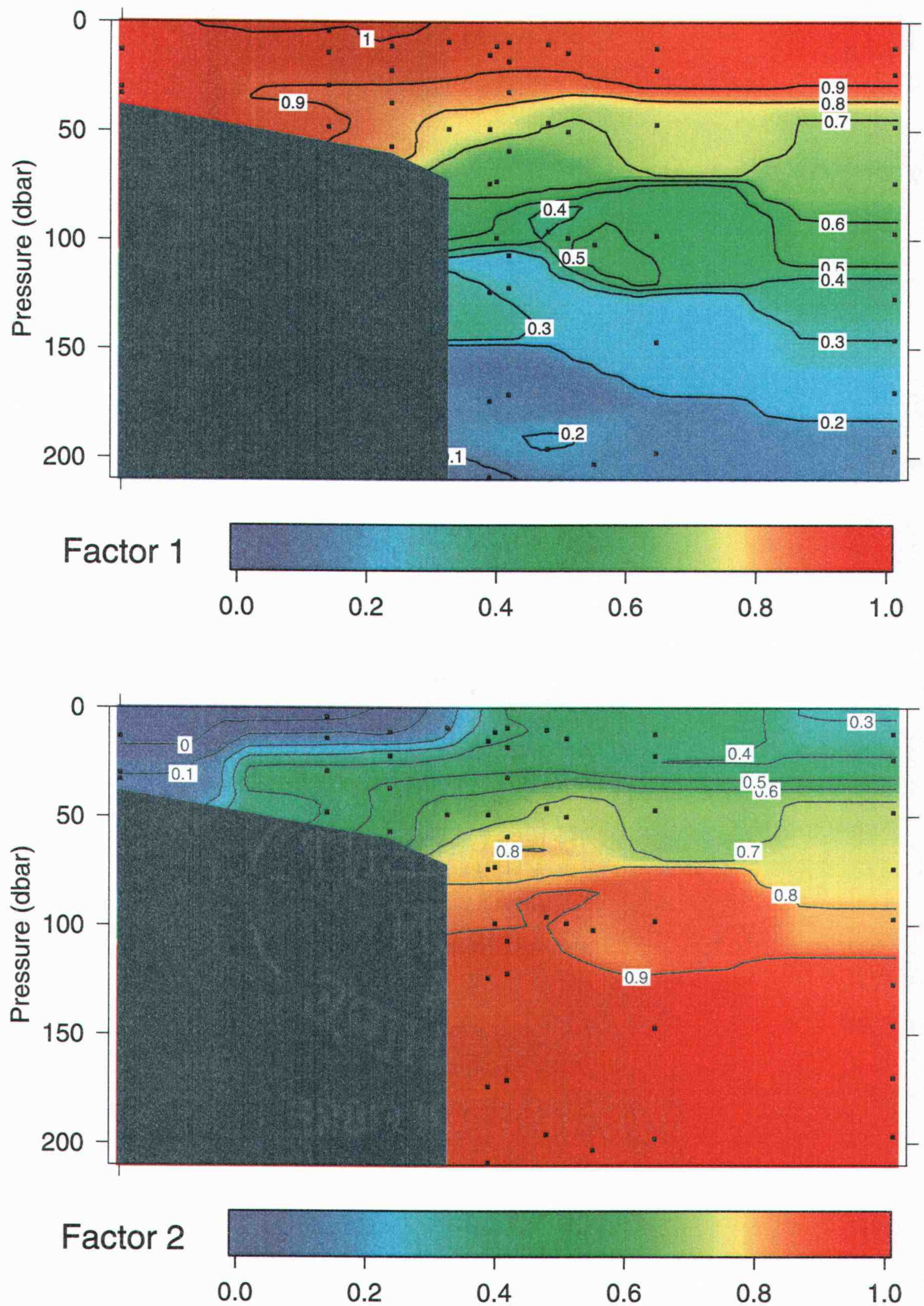
Pressure (dbar)
0
50
100
150
200
1
0.9
0.8
0.7
0.6
0.5
0.4
0.3
0.2
.1
Factor 1
0.0
0.2
0.4
0.6
0.8
1.0
Pressure (dbar)
0
50
100
150
200
0
0.1
0.3
0.4
0.5
0.6
0.7
0.8
0.9
Factor 2
0.0
0.2
0.4
0.6
0.8
1.0

Figure 4.2

Table 4.2 Comparison between varimax factor composition scores for the 1993 *Polarstern* data and the given properties of the proposed Atlantic, river and ice-melt end-members.

Variable	Factor 1	Factor 2	Atlantic end-member	River end-member	Ice-Melt end-member
Salinity (PSS)	29.7	35.2	34.9	0	3
[Ba] (nmol L^{-1})	53	44	42 - 45	100 - 200	≤ 5
$\delta^{18}O$ (‰)	-3.07	0.37	0.32	-20	-0.63 to 2.42

processes along this particular transect. A salinity-$\delta^{18}O$ mass balance showed that samples collected along the transect contained less than 2% ice-melt (except for three samples from the shallowest station over the shelf, which contained 4-6% ice-melt; *Bauch et al.*, 1995; *Frank*, 1996; *Stein*, 1996). If the samples had been more strongly influenced by ice melting and formation processes, the factor analysis would have been more likely to resolve a third factor corresponding to the ice-melt end-member of the mixing model.

It must be noted that this was a preliminary exercise performed on a limited subset of the available data. Future analyses on a more complete data set (i.e., one that includes our data from other cruises to the Arctic since 1993) will result in a fuller description of mixing in the upper Arctic Ocean. Expanding the data set to include other tracers (alkalinity, DOC, nutrients, etc.) will allow additional end-members to be considered (e.g., the factor corresponding to fluvial discharge could be resolved into two separate factors corresponding to discharge from North American and Eurasian rivers). Further insight will be gained by applying r-mode factor analysis techniques, which investigates the relationships between variables within a set of multivariate observations.

5. CONCLUSIONS

The research described in this dissertation illustrates the utility of geochemical signals for tracing the fluvial component of Arctic Ocean circulation. Combined with measurements of other physical and chemical tracers, Ba and DOC distributions identify areas where river waters cross the broad shelves of the Arctic's marginal seas and enter the interior basins. The data demonstrate that Ba and DOC serve as complementary tracers for distinguishing between contributions from North American and Eurasian rivers and thus provide new information about circulation in the Arctic Ocean.

Longer time series and data collected from different periods throughout the year will result in a more complete assessment of Ba and DOC concentrations in Arctic rivers and their ranges of interannual and seasonal variability. Additional surveys will also improve our understanding of how fluvial Ba and DOC signals are altered by non-conservative processes; it will be particularly important to further test the assumption that Ba and DOC behave virtually conservatively under the Arctic ice cover. More observations from the interior Arctic Ocean are necessary to determine the extent to which fluvial tracer signals remain detectable as river waters mix with oceanic waters.

Because the areal distribution of fluvial discharge as well as the total amount of runoff ultimately determines its effect on Arctic Ocean circulation, it is important to understand the mechanisms governing the transport pathways of Eurasian Arctic river discharge and their temporal variability. Based on model results, observations of ice motion and a limited number of tracer measurements, it had previously been speculated that Eurasian river discharge enters the interior Arctic Ocean via surface flows aligned roughly along the Lomonosov and Mendeleyev ridges. Our data provide direct evidence of these transport pathways and indicate that they are driven primarily by atmospheric forcing While recent investigations of variability in the Arctic system have focused on annually averaged large-scale atmospheric conditions, our data suggest that the extent to which either pathway is favored in a given year depends most strongly on local winds during the summer period of maximum runoff.

Future studies should be designed to collect samples from the area encompassing the Lomonosov and Mendeleyev ridges during multiple years. This would allow a direct assessment of the consistency between local wind patterns and the relative amounts of fluvial transport along these ridges in a given year. Additional observations from the interior Arctic Ocean are needed to further investigate the influence of fluvial discharge on the properties of upper Eurasian Basin waters. Examination of data from the SCICEX cruises in 1996-1999, for example, will determine whether the cold halocline was reestablished in the Eurasian Basin following the resumption of offshore transport from the Laptev shelf in the summers of 1995-1997.

Preliminary results of the q-mode factor analysis support the three end-member mixing model proposed for the Laptev Sea. The factor analysis did a fair to good job capturing the Atlantic and river end-members, although it did not appear to successfully capture the expected ice-melt end-member. This is likely the result of the minor contribution by ice melt to the subset of samples used for this exercise. Future analyses on a more complete data set (i.e., one that includes our data from other cruises to the Arctic since 1993) will result in a fuller description of mixing in the upper Arctic Ocean. Expanding the data set to include other tracers (alkalinity, DOC, nutrients, etc.) will allow additional end-members to be considered (e.g., the factor corresponding to fluvial discharge could be resolved into two separate factors corresponding to discharge from North American and Eurasian rivers).

Due to the remoteness of the Arctic Ocean and the operational difficulties posed by its ice coverage and extreme weather conditions, new technology and sampling techniques will be essential to obtaining longer tracer records with more seasonal resolution and areal coverage. Timed water samplers are currently being deployed on Arctic moorings to obtain tracer records with improved temporal resolution (K. Falkner, personal communication). More complete data sets will be provided by optical *in situ* sensors that can be deployed from autonomous oceanographic platforms (i.e., conventional platforms such as moorings and drifters, as well as next-generation platforms such as the SOLO profiling float [*Sherman and Davis*, 1995] and the remotely navigated underwater glider (SPRAY) being jointly developed at the Scripps Institution of Oceanography and the Woods Hole Oceanographic Institution). The ship-based ZAPS instrument can be adapted to create an autonomous sensor for *in situ* measurement of DOC in the upper Arctic Ocean (the main challenge will lie in reducing the power requirements of the xenon flash lamp or developing an alternative low-power light source capable of comparable performance). An instrument for making fluorescence-based *in situ* measurements of Ba in seawater is presently in the initial stages of development (K. Falkner, personal communication). Such sensors will produce long-term, high-resolution data records encompassing the diurnal to monthly variability that is an important feature of marine biogeochemical processes, especially in the upper ocean. Autonomous sensors will also enable data to be collected on more extensive spatial scales than possible using ship-based sampling methods and allow work to be conducted in harsh environments and remote areas otherwise impractical or impossible to access.

BIBLIOGRAPHY

Aagaard, K., The Beaufort Undercurrent, in *The Alaskan Beaufort Sea: Ecosystems and Environments*, edited by P.W. Barnes, D. Schell, and E. Reimnitz, pp. 47-71, Academic Press, Inc., Orlando, Fla., 1984.

Aagaard, K., and E.C. Carmack, The role of sea ice and other fresh water in the Arctic circulation, *J. Geophys. Res.*, *94* (C10), 14,485-14,498, 1989.

Anderson, L.G., G. Björk, O. Holby, E.P. Jones, G. Kattner, K.P. Koltermann, B. Liljeblad, R. Lindgren, B. Rudels, and J. Swift, Water masses and circulation in the Eurasian Basin: Results from the Oden 91 Expedition, *J. Geophys. Res.*, *99*, 3273-3283, 1994.

Anderson, L.G., K. Olsson, and A. Skoog, Distribution of dissolved inorganic and organic carbon in the Eurasian Basin of the Arctic Ocean, in *The Polar Oceans and Their Role in Shaping the Global Environment*, edited by O.M. Johannessen, R.D. Muench, and J.E. Overland, pp. 255-262, Washington DC, 1994.

Anderson, L.G., K. Olsson, and M. Chierici, A carbon budget for the Arctic Ocean, *Global Biogeochem. Cycles*, *12* (3), 455-465, 1998.

Apollonio, S., Hydrobiological measurements on IGY Drifting Station Bravo, *Trans. Am. Geophys. Union*, *40*, 316-319, 1959.

Bauch, D., P. Schlosser, and R. Fairbanks, Freshwater balance and the sources of deep and bottom waters in the Arctic Ocean inferred from the distribution of $H^2{}_{18}O$, *Prog. Oceanog.*, *35*, 53-80, 1995.

Benner, R., and M. Strom, A critical evaluation of the analytical blank associated with DOC measurements by high-temperature catalytic oxidation, *Mar. Chem.*, *41*, 153-160, 1993.

Bernstein, R.E., R.H. Byrne, P.R. Betzer, and A.M. Greco, Morphologies and transformations of celestite in seawater: The role of acantharia in strontium and barium geochemistry, *Geochim. Cosmochim. Acta*, *56*, 3273-3279, 1992.

Bishop, J.K.B., The barite-opal-organic carbon association in oceanic particulate matter, *Nature*, *332*, 341-343, 1988.

Carlson, C.A., H.W. Ducklow, D.A. Hansell, and W.O. Smith, Organic carbon partitioning during spring phytoplankton blooms in the Ross Sea polynya and the Sargasso Sea, *Limnol. Oceanogr.*, *43* (3), 375-386, 1998.

Carmack, E.C., Large-scale physical oceanography of polar oceans, in *Polar Oceanography, Part A: Physical Science*, edited by W.O. Smith, pp. 171-222, Academic Press, San Diego, Calif., 1990.

Carmack, E.C., K. Aagaard, J.H. Swift, R.W. Macdonald, F.A. McLaughlin, E.P. Jones, R.G. Perkin, J.N. Smith, K.M. Ellis, and L.R. Killius, Changes in temperature and tracer distributions within the Arctic Ocean: Results from the 1994 Arctic Ocean Section, *Deep-Sea Res. II*, *44* (8), 1487-1502, 1997.

Carmack, E.C., R.W. Macdonald, R.G. Perkin, F.A. McLaughlin, and R.J. Pearson, Evidence for warming of Atlantic water in the southern Canadian Basin of the Arctic Ocean: Results from the Larsen-93 expedition, *Geophys. Res. Lett.*, *22* (9), 1061-1064, 1995.

Carroll, J., K.K. Falkner, E.T. Brown, and W.S. Moore, The role of sediments in maintaining high dissolved ^{226}Ra and Ba in the Ganges-Bramaputra mixing zone, *Geochim. Cosmochim. Acta*, *57*, 2981-2990, 1993.

Chan, L.H., D. Drummond, J.M. Edmond, and B. Grant, On the barium data from the Atlantic GEOSECS Expedition, *Deep-Sea Res.*, *24*, 613-649, 1977.

Chen, R.F., and J.L. Bada, The fluorescence of dissolved organic matter in seawater, *Mar. Chem.*, *37*, 191-221, 1992.

Coble, P.G., Characterization of marine and terrestrial DOM in seawater using excitation-emission matrix spectroscopy, *Mar. Chem.*, *51*, 325-346, 1996.

Coffey, M., F. Dehairs, O. Collete, G. Luther, T. Church, and T. Jickells, The behaviour of dissolved barium in estuaries, *Estuarine, Coastal Shelf Sci.*, *45*, 113-121, 1997.

Collier, R., and J. Edmond, The trace element geochemistry of marine biogenic particulate matter, *Prog. Oceanog.*, *13*, 113-199, 1984.

Cota, G.F., L.R. Pomeroy, W.G. Harrison, E.P. Jones, F. Peters, W.M. Sheldon, and T.R. Weingartner, Nutrients, primary production and microbial heterotrophy in the southeastern Chukchi Sea: Arctic summer nutrient depletion and heterotrophy, *Mar. Ecol. Prog. Ser.*, *135*, 247-258, 1996.

Davis, J.C., *Statistics and Data Analysis in Geology*, 646 pp., John Wiley and Sons, New York, 1973.

Dawson, K.R., Barite, Fluorite, and Celestite Deposits and Occurrences, in *Report of Activities, Part A*, Geological Survey of Canada, Paper 75-1A, pp. 257-259, 1975.

Dawson, K.R., Regional Metallogeny of the Northern Cordillera, in *Report of Activities, Part A*, Geological Survey of Canada, Paper 77-1A, pp. 1-4, 1977.

Dehairs, F., R. Chesselet, and J. Jedwab, Discrete suspended particles of barite and the barium cycle in the open ocean, *Earth Planet. Sci. Lett.*, *49*, 528-550, 1980.

Dehairs, F., C.E. Lambert, R. Chesselet, and N. Risler, The biological production of marine suspended barite and the barium cycle in the Western Mediterranean Sea, *Biogeochem.*, *4*, 119-139, 1987.

Dymond, J., E. Suess, and M. Lyle, Barium in deep-sea sediment: A geochemical proxy for paleoproductivity, *Paleoceanogr.*, *7* (2), 163-181, 1992.

Edmond, J.M., E.D. Boyle, D. Drummond, B. Grant, and T. Mislick, Desorption of barium in the plume of the Zaire (Congo) River, *Neth. J. Sea Res.*, *12*, 324-328, 1978.

Edmond, J.M., C. Measures, R.E. McDuff, L.H. Chan, R. Collier, B. Grant, L.I. Gordon, and J.B. Corliss, Ridge crest hydrothermal activity and the balances of the major and minor elements in the ocean: The Galapagos data, *Earth Planet. Sci. Lett.*, *46*, 1-18, 1979.

English, T.S., Some biological observations in the central North Polar Sea, Drift Station Alpha, 1957-58, *Res. Pap. 13*, pp. 80, Arctic Institute of North America, Washington, DC, 1961.

Falkner, K.K., G. Klinkhammer, T.S. Bowers, J.F. Todd, B. Lewis, W. Landing, and J.M. Edmond, The behavior of Ba in anoxic marine waters, *Geochim. Cosmochim. Acta*, *57* (3), 537-554, 1993.

Falkner, K.K., R.W. MacDonald, E.C. Carmack, and T. Weingartner, The potential of barium as a tracer of Arctic water masses, in *The Polar Oceans and Their Role in Shaping the Global Environment: The Nansen Centennial Volume, AGU Geophys. Monograph Series*, edited by O.M. Johannessen, R.D. Muench, and J.E. Overland, pp. 63-76, AGU Books, Washington DC, 1994.

Frank, M., Spurenstoffuntersuchungen zur Zirkulation im Eurasischen Becken des Nordpolarmeeres, Erlangung der Doktorwürde thesis, Ruprecht-Karls-Universität, Heidelberg, 1996.

Fresnel, J., P. Galle, and P. Gayral, Resultats de la microanalyse des cristaux vacuolaires chez deux Chromophytes unicellulaires marines: Exanthemachrysis gayraliae, Pavlova sp. (Prymnesiophycees, Pavlovacees), *C. R. Acad. Sc. Paris*, *288* (Serie D), 823-825, 1979.

Froelich, P.N., L.W. Kaul, J.T. Byrd, M.O. Andreae, and K.K. Roe, Arsenic, barium, germanium, tin, dimethylsulfide and nutrient biogeochemistry in Charlotte Harbor, Florida, a phosphorus-enriched estuary, *Estuarine, Coastal Shelf Sci.*, *20*, 239-264, 1985.

Fyfe, J.C., G.J. Boer, and G.M. Flate, The Arctic and Antarctic oscillations and their projected changes under global warming, *Geophys. Res. Lett.*, *26* (11), 1601-1604, 1999.

Gordeev, V.V., J.M. Martin, I.S. Sidorov, and M.V. Sidorova, A reassessment of the Eurasian river input of water, sediment, major elements, and nutrients to the Arctic Ocean, *Amer. J. Sci.*, *296*, 664-691, 1996.

Gordon, D.C., and P.J. Cranford, Detailed distribution of dissolved and particulate organic matter in the Arctic Ocean and comparison with other oceanic regions, *Deep-Sea Res.*, *32(10)*, 1221-1232, 1985.

Guay, C.K., and K.K. Falkner, Barium as a tracer of Arctic halocline and river waters, *Deep-Sea Res. II*, *44* (8), 1543-1569, 1997.

Guay, C.K., and K.K. Falkner, A survey of dissolved barium in the estuaries of major Arctic rivers and adjacent seas, *Cont. Shelf Res.*, *18*, 859-882, 1998.

Guay, C.K., G.P. Klinkhammer, K.K. Falkner, R. Benner, P. Coble, T. Whitledge, B. Black, F.J. Bussell, and T.A. Wagner, High-resolution measurements of dissolved organic carbon in the Arctic Ocean by *in situ* fiber-optic spectrometry, *Geophys. Res. Lett.*, *26* (8), 1007-1010, 1999.

Hanor, J.S., and L.H. Chan, Non-conservative behavior of barium during mixing of Mississippi River and Gulf of Mexico waters, *Earth Planet. Sci. Lett.*, *37*, 242-250, 1977.

Hansell, D.A., and C.A. Carlson, Deep-ocean gradients in the concentration of dissolved organic carbon, *Nature*, *395*, 263-266, 1998.

Hedges, J.I., R.G. Keil, and R. Benner, What happens to terrestrial organic matter in the ocean?, *Org. Geochem.*, *27* (5/6), 195-212, 1997.

Hogan, T.F., and T.E. Rosmond, The description of the Navy Operational Global Atmospheric Prediction System, *Mon. Weather Rev.*, *119* (8), 1786-1815, 1991.

Jones, E.P., L.G. Anderson, and D.W.R. Wallace, Tracers of near-surface, halocline and deep waters in the Arctic Ocean: Implications for circulation, *J. Mar. Sys.*, *2*, 241-255, 1991.

Jones, E.P., L.G. Anderson, and J.H. Swift, Distribution of Atlantic and Pacific waters in the upper Arctic Ocean: Implications for circulation, *Geophys. Res. Lett*, *25(6)*, 765-768, 1998.

Kinney, P.J., T.C. Loder, and J. Groves, Particulate and dissolved organic matter in the Amerasian Basin of the Arctic Ocean, *Limnol. Oceanogr.*, *16*, 132-137, 1971.

Klinkhammer, G.P., C.S. Chin, C. Wilson, M.D. Rudnicki, and C.R. German, Distributions of dissolved manganese and fluorescent dissolved organic matter in the Columbia River estuary and plume as determined by in situ measurement, *Mar. Chem.*, *56*, 1-14, 1997.

Lea, D.W., Foraminiferal and coralline barium as paleoceanographic tracers, PhD thesis, Massachussetts Institute of Technology and Woods Hole Oceanographic Institution, WHOI-90-06, Cambridge, MA, 1990.

Li, Y.H., and L.H. Chan, Desorption of Ba and ^{226}Ra from riverborne sediments in the Hudson Estuary, *Earth Planet. Sci. Lett.*, *43*, 343-350, 1979.

Lundberg, L., and P.M. Haugan, A Nordic Seas-Arctic Ocean carbon budget from volume flows and inorganic carbon data, *Global Biogeochem. Cycles*, *10* (3), 493-510, 1996.

Macdonald, R.W., and J.M. Bewers, Contaminants in the arctic marine environment: priorities for protection, *ICES J. Mar Sci.*, *53*, 537-563, 1996.

Martin, J.-M., and M. Maybeck, Elemental mass-balance of material carried by major world rivers, *Mar. Chem.*, *7*, 173-206, 1979.

Maslanik, J.A., S.M. C., and R.G. Barry, Recent decreases in Arctic summer ice cover and linkages to atmospheric circulation anomalies, *Geophys. Res. Lett.*, *23* (13), 1677-1680, 1996.

Maslowski, W., Y. Zhang, and A.J. Semtner, Modeling fresh water sources, their distribution and sinks in the Arctic Ocean, in *ACSYS Conference on Polar Processes and Global Climate*, edited by K. Aagaard, D. Hartmann, V. Kattsov, D. Martinson, R. Stewart, and A. Weaver, pp. 159-161, World Climate Research Programme, Rosario, WA, USA, 1998.

McLaughlin, F.A., E.C. Carmack, R.W. Macdonald, and J.K.B. Bishop, Physical and geochemical properties across the Atlantic/Pacific water mass front in the southern Canadian Basin, *J. Geophys. Res.*, *101* (C1), 1183-1197, 1996.

McPhee, M.G., T.P. Stanton, J.H. Morison, and D.G. Martinson, Freshening of the upper ocean in the Arctic: Is perennial sea ice disappearing?, *Geophys. Res. Lett.*, *25* (10), 1729-1732, 1998.

Melnikov, I.A., and G.L. Pavlov, Characteristics of organic carbon distribution in the water and ice of the Arctic Basin, *Oceanology*, *18(2)*, 163-167, 1978.

Menard, H.W., and S.M. Smith, Hypsometry of ocean basin provinces, *J. Geophys. Res.*, *71* (18), 4305-4325, 1966.

Mensch, M., M. Frank, W. Stein, and R. Bayer, Distribution and circulation of water masses on the Eurasian shelves of the Arctic Ocean, *J. Geophys. Res.*, *in preparation*, 1999.

Meybeck, M., and A. Ragu, *River Discharges to the Oceans: An assessment of suspended solids, major ions and nutrients*, 245 pp., UNEP, Paris, 1995.

Moore, W.S., High fluxes of radium and barium from the mouth of the Ganges-Brahmaputra River during low river discharge suggest a large groundwater source, *Earth Planet. Sci. Lett.*, *150* (1-2), 141-150, 1997.

Morison, J., M. Steele, and R. Andersen, Hydrography of the upper Arctic Ocean measured from the nuclear submarine *USS Pargo*, *Deep-Sea Res. I*, *45*, 15-38, 1998.

Morrow, D.W., H.R. Krouse, E.D. Ghent, G.C. Taylor, and K.R. Dawson, A hypothesis concerning the origin of barite in Devonian carbonate rocks of northeastern British Columbia, *Can. J. Earth Sci.*, *15* (9), 1391-1406, 1978.

Östlund, H.G., and G. Hut, Arctic Ocean water mass balance from isotope data, *J. Geophys. Res.*, *89*, 6373-6381, 1984.

Pavlov, V.K., L.A. Timokhov, G.A. Baskakov, M.Y. Kulakov, V.K. Kurazhov, P.V. Pavlov, S.V. Pivovarov, and V.V. Stanovoy, Hydrometeorological Regime of the Kara, Laptev, and East Siberian Seas, Applied Physics Laboratory, University of Washington, 1996.

Peake, E., B.L. Baker, and G.W. Hodgson, Hydrogeochemistry of the surface waters of the Mackenzie River drainage basin, Canada—II. The contribution of amino acids, hydrocarbons and chlorins to the Beaufort Sea by the Mackenzie River system, *Geochim. Cosmochim. Acta*, *36*, 867-883, 1972.

Proshutinsky, A.Y., and M. Johnson, Two regimes of the Arctic Ocean circulation from ocean models and observations, *Eos, Trans. Am. Geophys. Union*, *76* (3), Abstract No. OS-29, 1996.

Proshutinsky, A.Y., and M.A. Johnson, Two circulation regimes of the wind-driven Arctic Ocean, *J. Geophys. Res.*, *102* (C6), 12,493-12,514, 1997.

Reeder, S.W., B. Hitchon, and A.A. Levinson, Hydrogeochemistry of the surface waters of the Mackenzie River drainage basin, Canada-I. Factors controlling the inorganic composition, *Geochim. Cosmochim. Acta*, *36*, 825-865, 1972.

Rich, J., M. Gosselin, E. Sherr, B. Sherr, and D.L. Kirchman, High bacterial production, uptake and concentrations of dissolved organic matter in the central Arctic Ocean, *Deep-Sea Res. II*, *44* (8), 1645-1663, 1997.

Rudels, B., L.G. Anderson, and E.P. Jones, Formation and evolution of the surface mixed layer and halocline of the Arctic Ocean, *J. Geophys. Res.*, *101* (C4), 8807-8821, 1996.

Rudels, B., E.P. Jones, L.G. Anderson, and G. Kattner, On the intermediate depth waters of the Arctic Ocean, in *The Polar Oceans and Their Role in Shaping the Global Environment*, edited by O.M. Johannessen, R.D. Muench, and J.E. Overland, pp. 33-46, AGU Geophysical Monograph, Washington DC, 1994.

Sarmiento, J.L., R. Murnane, and C. Le Quéré, Air-sea CO_2 transfer and the carbon budget of the North Atlantic, *Phil. Trans. R. Soc. Lond. B*, *348*, 211-219, 1995.

Schauer, U., R.D. Muench, B. Rudels, and L. Timokhov, Impact of eastern Arctic shelf waters on the Nansen Basin intermediate layers, *J. Geophys. Res.*, *102* (C2), 3371-3382, 1997.

Schlosser, P., D. Bauch, R. Fairbanks, and G. Bönisch, Arctic river runoff: mean residence time on the shelves and in the halocline, *Deep-Sea Res. I*, *41*, 1053-1068, 1994.

Sherman, J.T., and R.E. Davis, Observations of Temperature Microstructure in NATRE, *J. Phys. Oceanogr.*, *25*, 1913-1929, 1995.

Shindell, D.T., R.L. Miller, G.A. Schmidt, and L. Pandolfo, Simulation of recent northern winter climate trends by greenhouse-gas forcing, *Nature*, *3*, 452-455, 1999.

Siegenthaler, U., and J.L. Sarmiento, Atmospheric carbon dioxide and the ocean, *Nature*, *365*, 119-125, 1993.

Smart, P.L., B.L. Finlayson, W.D. Rylands, and C.M. Ball, The relation of fluorescence to dissolved organic carbon in surface waters, *Water Res.*, *10*, 805-811, 1976.

Spitzy, A., and J. Leenheer, Dissolved Organic Carbon in Rivers, in *Biogeochemistry of Major World Rivers*, edited by E.T. Degens, S. Kempe, and J.E. Richey, pp. 213-232, John Wiley and Sons Ltd, Chichester, 1991.

Stecher, H.A., Rapid barium removal in the Deleware estuary, *Geochim. Cosmochim. Acta*, *63* (7-8), 1003-1012, 1999.

Steele, M., and T. Boyd, Retreat of the cold halocline layer in the Arctic Ocean, *J. Geophys. Res.*, *103* (C5), 10,419-10,435, 1998.

Stein, W., ^{18}O- und ^{3}H-Untersuchungen im Nordpolarmeer, Diplomarbeit, Ruprecht-Karls-Universität, Heidelberg, 1996.

Telang, S.A., R. Pocklington, A.S. Naidu, E.A. Romankevich, I.I. Gitelson, and M.I. Gladyshev, Carbon and Mineral Transport in Major North American, Russian Arctic, and Siberian Rivers: the St Lawrence, the Mackenzie, the Yukon, the Arctic Alaskan Rivers, the Arctic Basin Rivers in the Soviet Union, and the Yenisei, in *Biogeochemistry of Major World Rivers*, edited by E.T. Degens, S. Kempe, and J.E. Richey, pp. 75-104, John Wiley and Sons Ltd, Chichester, 1991.

Thompson, D.W.J., and J.M. Wallace, The Arctic Oscillation signature in the wintertime geopotential height and temperature fields, *Geophys. Res. Lett.*, *25* (9), 1297-1300, 1998.

United States Geological Survey, *U. S. Geological Survey Water Data Reports, Water resources data, Alaska-water years 1982-1996*, Anchorage, 1982-1996.

Vodacek, A., N.V. Blough, M.D. DeGrandpre, E.T. Peltzer, and R.K. Nelson, Seasonal variation of CDOM and DOC in the Middle Atlantic Bight: Terrestrial inputs and photooxidation, *Limnol. Oceanogr.*, *42* (4), 674-686, 1997.

Von Damm, K.L., Seafloor hydrothermal activity: Black smoker chemistry and chimneys, *Annu. Rev. Earth Planet. Sci.*, *18*, 173-204, 1990.

Von Damm, K.L., J.M. Edmond, B. Grant, C.I. Measures, B. Walden, and R.F. Weiss, Chemistry of submarine hydrothermal solutions at 21°N, East Pacific Rise, *Geochim. Cosmochim. Acta*, *49*, 2197-2220, 1985.

Wallace, D.W.R., P. Schlosser, M. Krysell, and G. Bönisch, Halocarbon and tritium/^{3}He dating of water masses in the Nansen Basin of the Arctic Ocean, *Deep-Sea Res.*, *39*, S435-S458, 1992.

Walsh, J.E., W.L. Chapman, and T.L. Shy, Recent decrease of sea level pressure in the central Arctic, *J. Climate*, *9*, 480-486, 1996.

Wheeler, P.A., M. Gosselin, E. Sherr, D. Thibault, D.L. Kirchman, R. Benner, and T.E. Whitledge, Active recycling of organic carbon in the central Arctic Ocean, *Nature*, *380*, 697-699, 1996.

Wheeler, P.A., J.M. Watkins, and R.L. Hansing, Nutrients, organic carbon and nitrogen in the upper water column of the Arctic Ocean: implications for the sources of dissolved organic carbon, *Deep-Sea Res. II*, *44* (8), 1571-1592, 1997.

APPENDICES

APPENDIX A: APPARENT CONTAMINATION OF BARIUM SAMPLES FROM THE ARK XI CRUISE IN 1995

The distribution of [Ba] in the samples collected during the ARK XI cruise in 1995 is strongly skewed towards higher values and has a greater variance than the distributions for samples collected during the ARK IX/4 and ARK XII cruises in 1993 and 1996, respectively (Figure A.1). Individual profiles for the 1995 stations identified 127 samples (out of 978 total samples) that had anomalously high [Ba] with respect to the other samples at that station and were not correlated with any features in temperature, salinity or $\delta^{18}O$ profiles (See Figure 3.5). Values of [Ba] were extremely high (between 240 and 800 nmol Ba L^{-1}) in 3 of these samples and ranged between 51 and 183 nmol Ba L^{-1} in the remainder. A plot of [Ba] versus salinity for the ARK XI samples and 55 additional water samples collected onboard the *R/V Yakov Smirnitsky* from the inner Laptev shelf in the summer of 1995 [*Guay and Falkner*, 1998] further suggest that the suspect samples were anomalously high in Ba relative to other samples collected from the same area during the same period of time (Figure A.2).

All 3 of the extreme samples and 37 of the other suspect samples were collected from the Niskin bottle in position 17 on the rosette (Figure A.3), strongly suggesting that it was contaminated (while it is conceivable that some or all of the high [Ba] values could be real, it is highly unlikely that so many of them would be associated with a single Niskin bottle if there were no contamination involved). The other anomalous samples suggest some degree of contamination from additional sources. If the suspect samples (i.e., all samples collected from Niskin bottle number 17 and the samples identified as anomalously high based on examination of individual station profiles) are excluded, the distribution of [Ba] in the 1995 samples appears similar to the distributions for the 1993 and 1996 samples (Figure A.4).

Figure A.1 The distributions of [Ba] for the samples collected during the 1993, 1995 and 1996 *Polarstern* cruises. For each distribution, the box represents the inner quartile range (the middle 50% of the data -- i.e., the lower and upper ends of the box correspond to the 25th and 75th percentiles, respectively) and the horizontal line through the box indicates the median. The whiskers extend through all values whose distance from the box is within 1.5 times the inner quartile range. Values further than 1.5 times the inner quartile range of the box are plotted as individual symbols. Note the different scales for the upper and lower portions of the y-axis (this was done to accommodate the three extreme samples in the 1995 distribution).

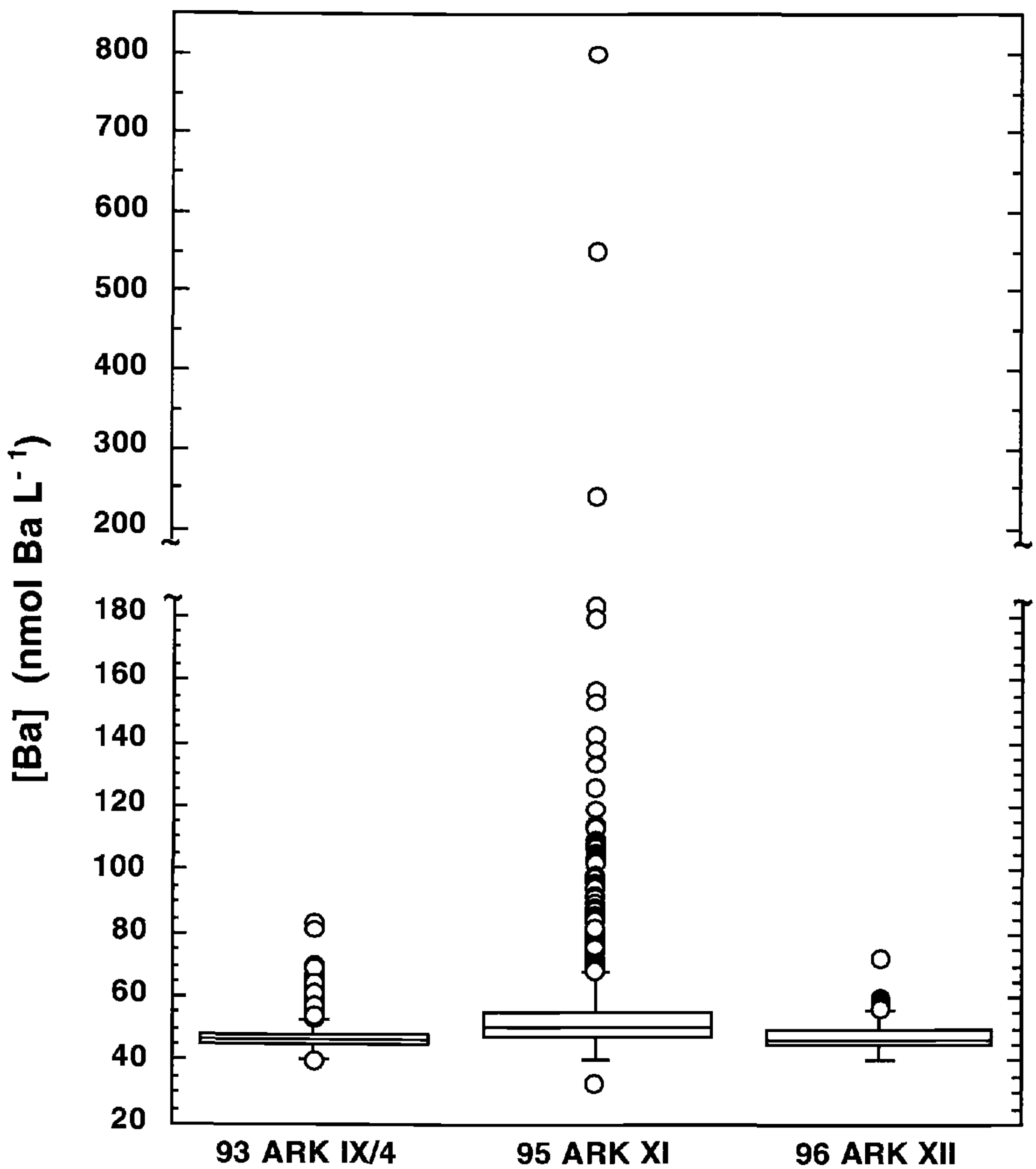

800
700
600
500
400
300
200
180
160
140
120
100
80
60
40
20
[Ba] (nmol Ba L-1)
93 ARK IX/4
95 ARK XI
96 ARK XII

Figure A.1

Figure A.2 Barium-salinity relationship for the 1995 *Polarstern* samples and 55 additional samples collected from the inner Laptev Sea in the summer of 1995 onboard the *R/V Yakov Smirnitsky*. Note the different scales for the upper and lower portions of the y-axis.

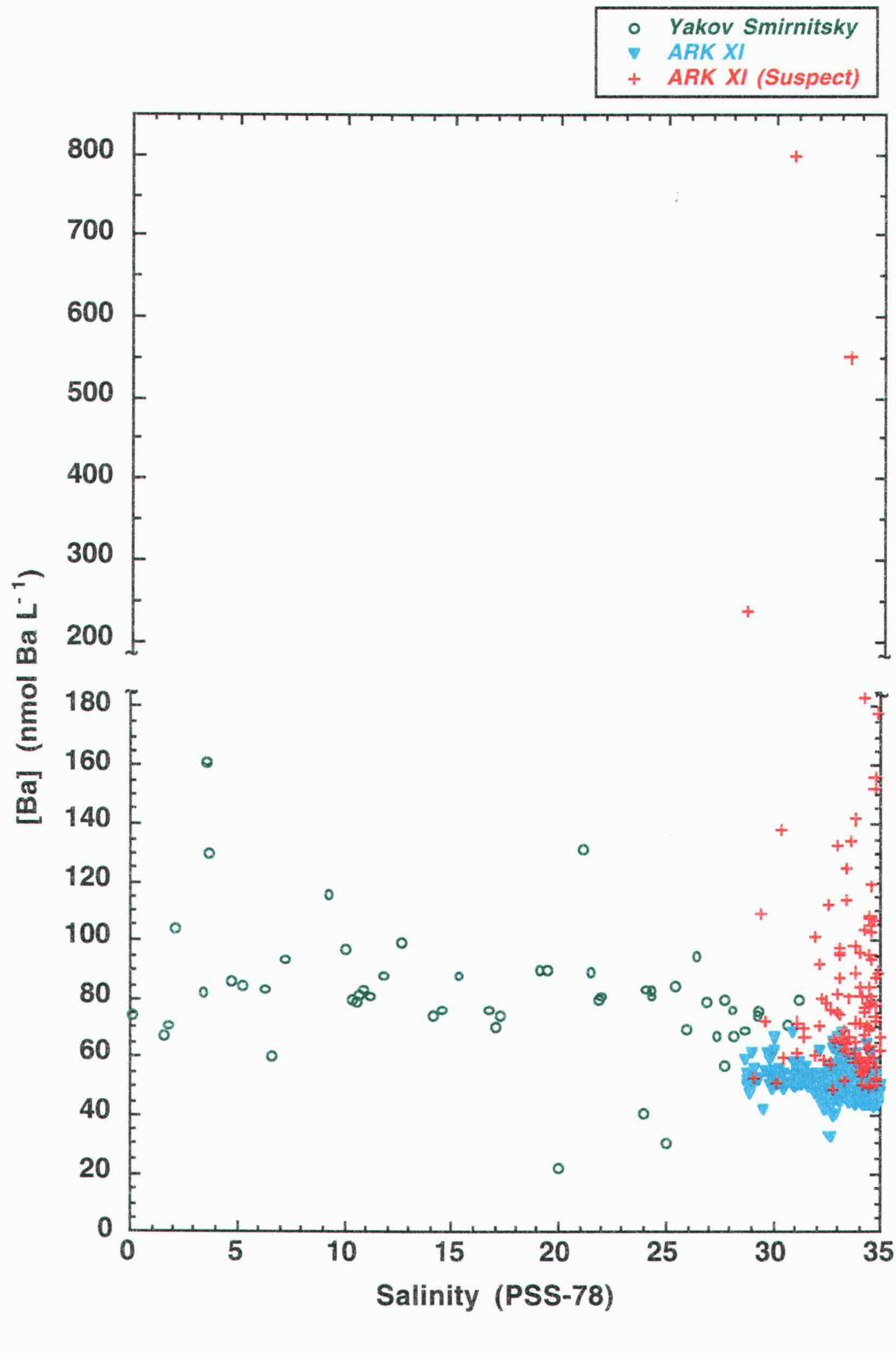

Yakov Smirnitsky
ARK XI
ARK XI (Suspect)
800
700
600
500
400
300
200
180
160
140
120
100
80
60
40
20
0
[Ba] (nmol Ba L-1)
0
5
10
15
20
25
30
35
Salinity (PSS-78)

Figure A.2

Figure A.3 Values of [Ba] for the samples collected from each of the 24 Niskin bottles deployed on the rosette during the 1995 *Polarstern* cruise. Note the different scales for the upper and lower portions of the y-axis.

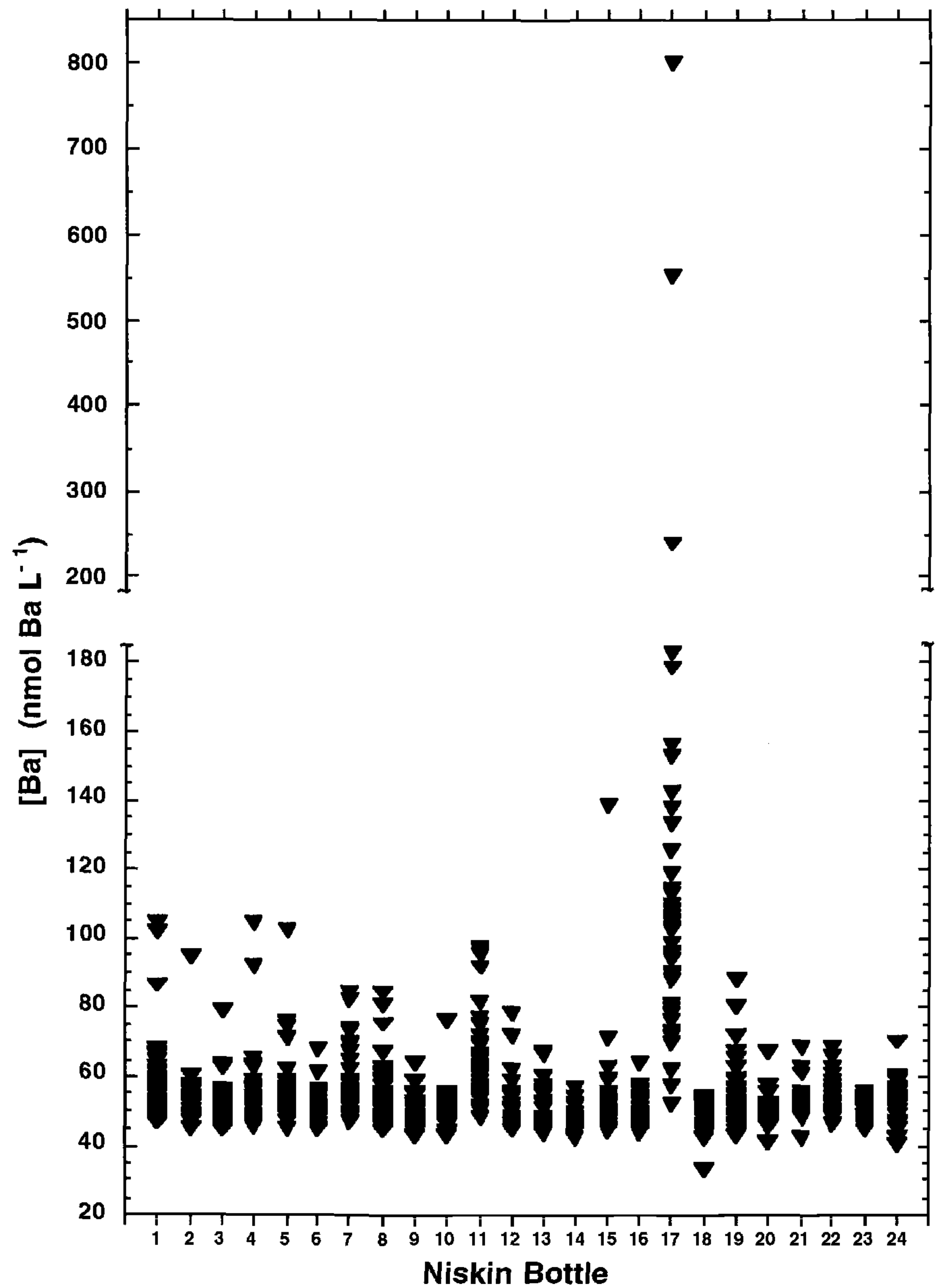
800
700
600
500
400
300
200
180
160
140
120
100
80
60
40
20
[Ba] (nmol Ba L⁻¹)
1 2 3 4 5 6 7 8 9 10 11 12 13 14 15 16 17 18 19 20 21 22 23 24
Niskin Bottle

Figure A.3.

Figure A.4 The distributions of [Ba] for the samples collected during the 1993, 1995 and 1996 *Polarstern* cruises, excluding the suspect samples from the ARK XI cruise in 1995. For each distribution, the box represents the inner quartile range (the middle 50% of the data -- i.e., the lower and upper ends of the box correspond to the 25th and 75th percentiles, respectively) and the horizontal line through the box indicates the median. The whiskers extend through all values whose distance from the box is within 1.5 times the inner quartile range. Values further than 1.5 times the inner quartile range of the box are plotted as individual symbols.

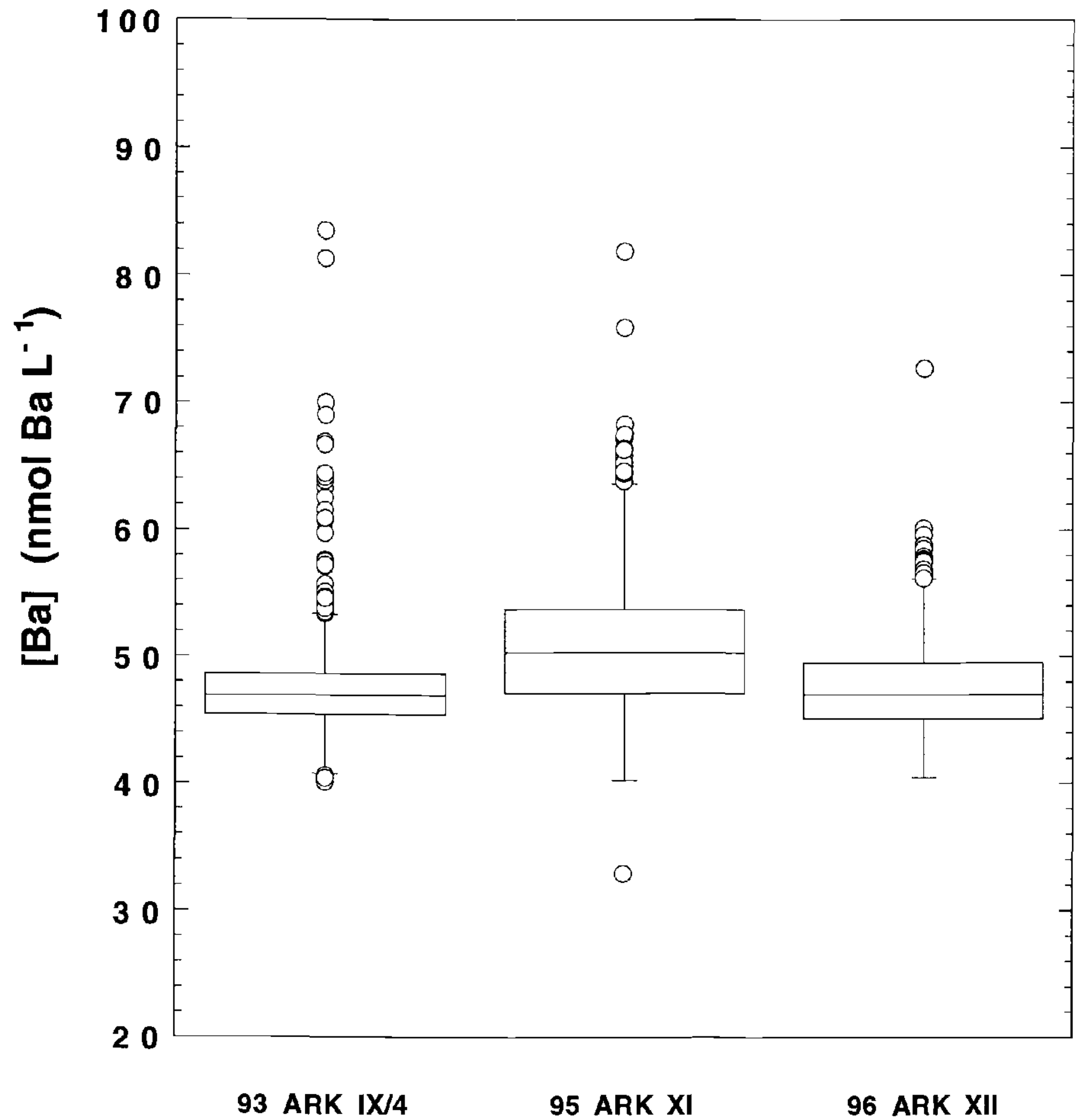

100
90
80
70
60
50
40
30
20
[Ba] (nmol Ba L-1)
93 ARK IX/4
95 ARK XI
96 ARK XII

Figure A.4

Possible sources of contamination for Ba at the sub-micromolar levels observed in these samples include the lubricants used for spigots and vent closures on Niskin bottles and the winch/rosette assembly. Even a small amount of grease inadvertently smeared on the interior of a Niskin bottle or around its spigot would potentially be enough to contaminate water samples collected from it throughout the cruise. Closure springs/tubing and o-rings that were not made of appropriate materials or cleaned adequately for trace metal work are another potential source of contamination. It is also possible that in certain instances, contamination occurred as a result of improper sampling techniques when filling the individual sample bottles with seawater from the Niskin bottles.

Although we cannot be certain that these high [Ba] values do not represent contributions from some unidentified natural source, we opted for the most conservative approach and excluded these suspect samples from the calculations of mean [Ba] for the 1995 stations. Note that [Ba] values for most of the 1995 samples are in agreement with values for the 1993 and 1996 samples having similar T-S properties, indicating that the entire 1995 Ba data set was not affected by contamination. While inferences based on the Ba data alone might still be regarded with uncertainty, our conclusions are reinforced by the combined tracer data set (i.e., temperature, salinity, Ba and oxygen isotopes).

APPENDIX B: DATA ARCHIVE SITES

The Ba data presented in this dissertation are archived at the National Snow and Ice Data Center, Campus Box 449, University of Colorado, Boulder, CO 80309-0449. Information about the archival of the other data discussed in this dissertation can be obtained from the following people:

Cruise	Type of Data	Contact
SCICEX-97	CTD	Dr. Robin Muench, John Gunn Earth and Space Research 1910 Fairview East, Suite 102 Seattle, WA 98102 e-mail: rmuench@esr.org
SCICEX-97	ZAPS	Dr. Gary Klinkhammer College of Oceanic & Atmospheric Sciences Oregon State University 104 Ocean Admin Bldg Corvallis, OR 97331 e-mail: gklinkhammer@oce.orst.edu
SCICEX-97	TOC (HTC)	Dr. Ronald Benner University of Texas Marine Science Institute 750 Channel View Drive Port Aransas, TX 78373 e-mail: benner@utmsi.utexas.edu
SCICEX-97	cholorophyll-a	Dr. Terry Whitledge School of Fisheries and Ocean Sciences University of Alaska Fairbanks, AK 99775 e-mail: whitledge@ims.uaf.edu
ARK IX/4	CTD	Dr. Ursula Schauer Alfred-Wegner-Institut für Polar- und Meeresforschung Postfach 12 01 61 D-27515 Bremerhaven, Germany e-mail: uschauer@awi-bremerhaven.de

Cruise	Type of Data	Contact
ARK IX/4	oxygen isotopes	Dr. Reinhold Bayer, Manfred Mensch Institut für Umweltphysik Ruprecht-Karls-Universität Heidelberg Im Neuenheimer Feld 366 D-69120 Heidelberg, Germany e-mail: br@uphys1.uphys.uni-heidelberg.de
ARK XI	CTD	Dr. Bert Rudels Institut für Meereskunde Universität Hamburg Troplowitzstrasse 7 D-22529 Hamburg, Germany
ARK XI	oxygen isotopes	Dr. Reinhold Bayer, Manfred Mensch
ARK XII	CTD	Dr. Ursula Schauer
ARK XII	oxygen isotopes	Dr. Reinhold Bayer, Manfred Mensch